Enhancement of the gut barrier integrity by a microbial metabolite through the Nrf2 pathway

Rajbir Singh[1], Sandeep Chandrashekharappa[2], Sobha R. Bodduluri[1], Becca V. Baby[1], Bindu Hegde[1], Niranjan G. Kotla[2], Ankita A. Hiwale[2], Taslimarif Saiyed[3], Paresh Patel[3], Matam Vijay-Kumar[4], Morgan G.I. Langille[5], Gavin M. Douglas[5], Xi Cheng [4], Eric C. Rouchka [6], Sabine J. Waigel[7], Gerald W. Dryden[7], Houda Alatassi[8], Huang-Ge Zhang[1], Bodduluri Haribabu[1], Praveen K. Vemula [2] & Venkatakrishna R. Jala[1]

The importance of gut microbiota in human health and pathophysiology is undisputable. Despite the abundance of metagenomics data, the functional dynamics of gut microbiota in human health and disease remain elusive. Urolithin A (UroA), a major microbial metabolite derived from polyphenolics of berries and pomegranate fruits displays anti-inflammatory, anti-oxidative, and anti-ageing activities. Here, we show that UroA and its potent synthetic analogue (UAS03) significantly enhance gut barrier function and inhibit unwarranted inflammation. We demonstrate that UroA and UAS03 exert their barrier functions through activation of aryl hydrocarbon receptor (AhR)- nuclear factor erythroid 2–related factor 2 (Nrf2)-dependent pathways to upregulate epithelial tight junction proteins. Importantly, treatment with these compounds attenuated colitis in pre-clinical models by remedying barrier dysfunction in addition to anti-inflammatory activities. Cumulatively, the results highlight how microbial metabolites provide two-pronged beneficial activities at gut epithelium by enhancing barrier functions and reducing inflammation to protect from colonic diseases.

[1] Department of Microbiology and Immunology, James Graham Brown Cancer Center, University of Louisville, Louisville, KY 40202, USA. [2] Institute for Stem Cell Biology and Regenerative Medicine (inStem), GKVK campus, Bangalore, Karnataka 560065, India. [3] Centre for Cellular and Molecular Platforms (C-CAMP), GKVK campus, Bangalore, Karnataka 560065, India. [4] Department of Physiology and Pharmacology, University of Toledo College of Medicine and Life Sciences, Toledo, OH 43614, USA. [5] Department of Pharmacology, Dalhousie University, Halifax, B3H 4R2 Nova Scotia, Canada. [6] Computer Engineering and Computer Science, Kentucky Biomedical Research Infrastructure Network, University of Louisville, Louisville, KY 40202, USA. [7] Department of Medicine, University of Louisville, Louisville, KY 40202, USA. [8] Department of Pathology, University of Louisville, Louisville, KY 40202, USA. Correspondence and requests for materials should be addressed to P.K.V. (email: praveenv@instem.res.in) or to V.R.J. (email: jvrao001@louisville.edu)

nflammatory bowel diseases (IBD) consisting of Crohn's and ulcerative colitis are resultant of dysregulation of the immune system leading to intestinal inflammation and microbial dysbiosis. Numerous studies in recent years highlighted the pivotal role of gut microbiota and their metabolites in host physiological processes including immune, metabolic, neurological, and nutritional homeostasis[1–4]. Thus, alterations in gut microbiota have been associated with adverse outcomes in cancer, IBD, neurological disorders, obesity, and diabetes[1,5–7]. Microbiota and their metabolites are in close proximity to the gut epithelium that constitutes a single cell-layer separating host components from the external environment. Gut barrier integrity is maintained by the tight junction proteins such as claudins (Cldn), Zona occludin -1 (ZO1), and occludin (Ocln) that are critical for epithelial cell barrier functions[8,9]. Previously, it has been reported that levels of tight junction proteins are significantly down regulated under IBD conditions leading to increased gut permeability to microbial ligands and noxious metabolites resulting in systemic inflammatory responses[8,10]. Despite the availability of large metagenomics data, the functional dynamics of microbiota and their metabolites in IBDs are unknown. Therefore, we tested the hypothesis that certain microbial metabolites will prevent gut permeability by enhancing barrier functions in addition to blocking inflammation. Treatment with such microbial metabolites will offer better therapeutic options for IBDs.

Consumption of diets containing berries and pomegranates have demonstrated significant beneficial effects on human health[11–14]. Especially, pomegranate extract or juice containing high levels of polyphenolic compounds such as ellagitannins (ETs) and ellagic acid (EA) have been suggested to prevent hypertension[15] and protect against myocardial ischemia and reperfusion injury[16]. They have been recognized as potential nontoxic chemo-preventive compounds against chronic diseases such as cancer, diabetes, cardiovascular and neurodegenerative disorders[17]. It has been suggested that further downstream metabolites of EA known as 'urolithins' generated by gut microbiota render potential health benefits, in vivo[18,19]. Among urolithins, Urolithin A (UroA) displayed potent anti-inflammatory, antioxidative and anti-ageing properties compared to other metabolites[20–23]. Due to life style variations and antibiotic/drug usage, presence of bacteria that metabolize dietary EA to urolithins have been variable among human populations. Thus, not only the consumption of diets enriched in polyphenols is required but also the presence of microbes that convert them into beneficial metabolites is critical for manifestation of their health effects. At this time, the targets or pathways through which such microbial metabolites regulate physiological processes are largely unknown.

In this study, we examined the activities of UroA and a potent synthetic structural analogue UAS03 and identified that in addition to the anti-inflammatory activities, these compounds strongly enhanced gut barrier function. We demonstrate that both UroA and UAS03 enhance barrier function by inducing tight junction proteins through activating aryl hydrocarbon receptor (AhR)-nuclear factor erythroid 2–related factor 2 (Nrf2)-dependent pathways. Further, oral treatment with UroA/UAS03 significantly mitigated systemic inflammation and colitis suggesting potential therapeutic applications for the treatment of IBD.

Results

Synthesis and anti-inflammatory activities of UroA and UAS03.
UroA (3,8-dihydroxy-6H-dibenzo[b,d]pyran-6-one) has a lactone (cyclic ester bond) that connects two mono-hydroxyl phenyl rings leading to a planar structure (Fig. 1a). Gastric pH or digestive enzymes can hydrolyze the lactone ring, which opens

the ring resulting in the loss of the planar structure and potentially its activities. To generate more stable and potent compounds, we synthesized non-hydrolyzable cyclic ether derivative, UAS03 (6H-benzo[c]chromene-3,8-diol) (Fig. 1a). The stability of both compounds was examined under conditions of gastric pH and digestive enzymes. The results showed that UAS03 indeed is stable at gastric pH and also in the presence of gastric enzymes e.g., esterases and proteases (Fig. 1a). Both UroA and UAS03-significantly decreased LPS induced IL-6 and TNF-α in mouse bone marrow derived macrophages (BMDMs) with UAS03 showing anti-inflammatory activities even at nano molar concentrations (Fig. 1b). Next, anti-inflammatory activities of UroA and UAS03 were examined in vivo in a LPS-induced peritonitis mouse model. UroA or UAS03 treatment significantly reduced the LPS-induced increase in serum IL-6 and TNF-α levels (Fig. 1c). These results suggest that UAS03 is a potent structural analogue of UroA with increased anti-inflammatory activities.

UroA/UAS03 induce tight junction proteins.
Since, microbial metabolites are in close proximity to gut epithelium; we surmise that metabolites could have a direct impact on epithelial cell function. To examine such effects, we performed RNA-Seq analysis of epithelial cell line (HT29) exposed to UroA. The analysis was performed as described in methods and to determine significance of differential gene expression, cuffdiff2 algorithm was used. Based on an uncorrected p-value cutoff of 0.05, 1960 genes were determined to be significantly differentially expressed as a result of UroA treatment in HT29 cells. Further restricting this list, 437 genes were found to be differentially expressed at FDR corrected q value <0.05 in UroA treated HT29 cells (Supplementary Fig. 1 and Supplementary Data 1). The pathway analysis using this restricted gene list was performed using Ingenuity Pathway Analysis (IPA) software (Supplementary Fig. 1). The Eukaryotic Initiation Factor 2 (eIF2), mammalian target of rapamycin (mTOR) and mitochondrial dysfunction pathways were emerged as top 3 pathways. The impact of UroA on mitochondrial dysfunction (pathways of mitophagy) have been described in previously by Ryu D et al.[22]. They demonstrated that UroA induced mitophagy and prolonged the lifespan of C. elegans and increased muscle function in rodents. The impact of UroA on mTOR and eIF2 pathways need to be established in the context of colon epithelial functions. The RNA-Seq analysis showed that cytochrome P450 1A1 (Cyp1A1) is among the top 3 UroA upregulated genes (Supplementary Data 1). The pathways analysis further indicated that the Nrf2 and AhR signaling pathways are in top 25 (Supplementary Fig. 1). We surmise that regulation of barrier function is of critical importance in mitigating IBDs. Therefore, we examined the expression of the tight junction proteins in RNA-Seq data and found that claudin 4 (Cldn4) is upregulated in UroA treated cells (Supplementary Fig. 2)[24]. In addition to Cldn4 and Cyp1A1, UroA also significantly increased the expression of heme oxygenase 1 (HMOX1 or HO1) (Supplementary Fig. 2). HO1 is well known Nrf2-dependent gene, which exerts wide variety of beneficial activities including removal of toxic heme, protection against oxidative stress, regulation of apoptosis, and inflammation[25]. Based on these observations, we hypothesized that UroA and UAS03 will induce tight junction proteins and enhance barrier function through AhR and Nrf2 pathways

Ingenuity Pathway Analysis (IPA) revealed significant enrichment of Nrf2 and AhR signaling pathways (Supplementary Fig. 1), supporting a role for these pathways in UroA signaling. A potential therapeutic avenue in IBD is the ability to increase barrier function. It was therefore of interest that we observed a
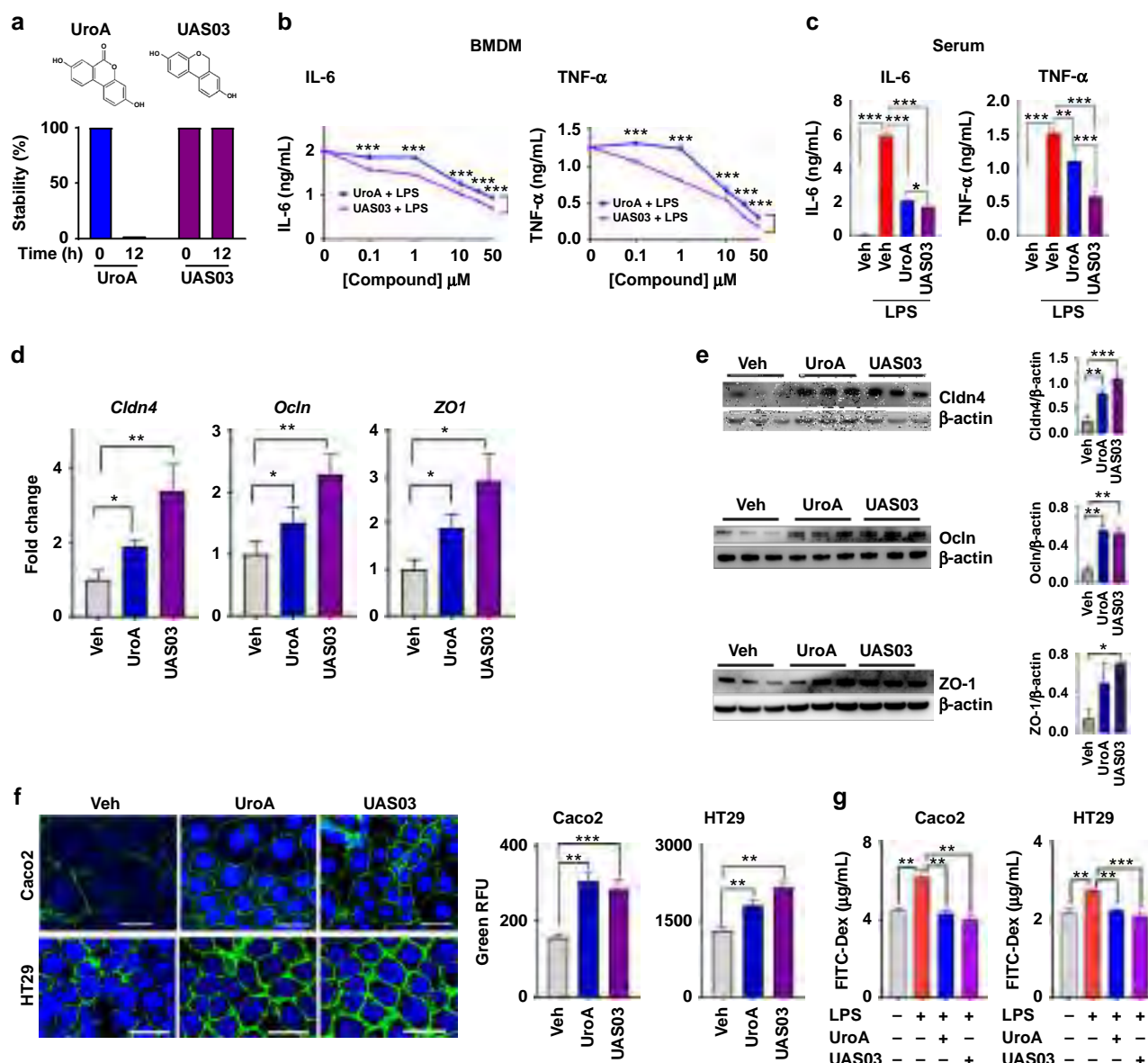
Fig. 1 UAS03 is a potent anti-inflammatory structural analogue of UroA and induces tight junction proteins. **a** Chemical structures of UroA, UAS03. UroA/ UAS03 stability was examined in the presence of gastric pH 2.0 and digestive enzymes. UroA and UAS03 (0.2 mg/ml) were incubated with digestive enzymes (esterases and proteases, 100 U/ml) for 12 h at 37 °C and compound levels were quantified. **b** BMDMs were stimulated with LPS (50 ng/ml) without or with UroA (blue line)/UAS03 (purple line) (0.1, 1, 10, 25, and 50 μM) for 6 h. IL-6 and TNF-α levels in supernatants were measured. **c** C57BL/6 mice (n = 3–4) were pretreated with UroA (20 mg/kg) and UAS03 (20 mg/kg). After 4 h, LPS (2 mg/kg) was injected intraperitoneally. Post 4 h of LPS administration, serum levels of IL-6 and TNF-α was measured. **d–f** HT29 or Caco2 cells were treated with vehicle (DMSO-0.01%) or UroA/UAS03 (50 μM) for 24 h. **d** The fold changes in mRNA levels of claudin 4 (*Cldn4*), occludin (*Ocln*), and Zona occludens 1 (*ZO1*) in HT29 cells were determined by RT PCR method. **e** UroA/UAS03 induced protein expression of Cldn4, Ocln, and ZO1 in HT29 cells were determined by immunoblots and quantified by Image J software. **f** Caco2 or HT29 cells were grown on coverslip bottom FluroDish and treated with Vehicle, UroA/UAS03 for 24 h. The cells were stained with anti-Cldn4 followed by secondary antibody tagged with Alexa-488. Nucleus was stained using DAPI. The confocal images were captured. The green intensity (n = 15–20 cell membrane regions) was measured. Scale bars for Caco2 and HT29 cells indicate 50 and 25 μm respectively. **g** Monolayer HT29 or Caco2 cells on transmembranes were treated with vehicle or UroA/UAS03 (50 μM) for 24 h followed by treatment with LPS (50 ng/ml) for 2 h. FITC-dextran was added to these cells (top of the membrane) and incubated for 2 h and FITC-dextran levels in bottom chamber well was measured. Results are representative of three independent experiments with triplicates for each concentration. *p < 0.05, **p < 0.01, ***p < 0.001, unpaired t-test between Veh, UroA, or UAS03. Error bars, ±SEM. Source Data are provided as a Source Data File

significant increase in expression of the tight junction protein Cldn4 in UroA treated cells. Although not statistically significant in our RNA-seq dataset, we further observed an increase in expression of additional tight junction proteins ZO-1 and Ocln1 using real-time PCR (Fig. 1d). The increased levels of these proteins by UroA or UAS03 was confirmed by western blots (Fig. 1e) and Cldn4 by confocal imaging (Fig. 1f) in both HT29

and another colon epithelial cell line, Caco2. Further, we observed elevated expression of Cldn4 in the colons of mice treated with UroA/UAS03 (Supplementary Fig. 3a). The functional consequence of increased tight junction proteins was examined using in vitro FITC-dextran permeability assay in transwell plates. As shown in Fig. 1g, pretreatment of Caco2 or HT29 cells with UAS03 or UroA significantly inhibited LPS induced leakage of

FITC-dextran into bottom chambers. Overall, these results suggest that treatment with UroA/UAS03 increased the expression of tight junction proteins potentially enhancing the gut barrier integrity.

AhR mediates the activities of UroA/UAS03. RNA-Seq data and real-time PCR data suggested that UroA significantly upregulated *Cyp1A1* (Supplementary Data 1, Supplementary Fig. 2, Fig. 2a, b). The P450-Glo Cyp1A1 assay (Fig. 2c) as well as 7-ethoxyresorufin-*O*-deethylase (EROD) assay (Supplementary Fig. 4) were performed to determine, whether the Cyp1A1 enzyme activity was similarly affected. UroA/UAS03 significantly induced Cyp1A1 activity in colon epithelial cells (Fig. 2c and Supplementary Fig. 4). Since Cyp1A1 is a well-known downstream target of AhR signaling[26], we examined whether UroA/UAS03 mediate their actions through AhR. In these assays, we utilized well established potent AhR ligands [2,3,7,8-tetrachlorodibenzo-p-dioxin (TCDD) or 6-Formylindolo[3,2-b]carbazole (FICZ) and low affinity AhR ligand (beta-naphthoflavone (BNF)] to compare the Cyp1A1 activities with UroA/UAS03. UroA/UAS03 activated Cyp1A1 similar to low affinity AhR ligand BNF at 50 μM. As expected, the high affinity ligands such as FICZ and TCDD showed increased Cyp1A1 activity even at nano molar concentrations compared to UroA/UAS03/BNF (Fig. 2c and Supplementary Fig. 4). More importantly, we tested whether UroA/UAS03 induce the Cyp1A1 activities in vivo using wild type and AhR$^{-/-}$ mice. As shown in Fig. 2d, UroA/UAS03 significantly activated Cyp1A1 activity in colon and liver of wild type but not in AhR$^{-/-}$ mice. Moreover, UroA/UAS03 treated wild type mice showed relatively more Cyp1A1 activity in colon tissues compared to BNF and FICZ treated mice (Supplementary Fig. 5a, b). Interestingly, FICZ and BNF that are delivered through intra peritoneum (i.p) showed more Cyp1A1 activity in liver compared to UroA/UAS03 that are delivered through oral route (Supplementary Fig. 5a, b). It could be attributed to first pass effect. To directly compare the administration route, we delivered UroA or UAS03 or FICZ through i.p. and determined Cyp1A1 enzyme activities. As expected, high affinity AhR ligand, FICZ, induced Cyp1A1 activity ~30 fold in liver compared to 5–6 fold by UroA/UAS03 (Supplementary Fig. 5c). In colons, FICZ only increased Cyp1A1 activity up to ~5 fold, whereas UroA/USA03 increased by only ~3 fold. In summary, these results suggest that UroA/UAS03 upregulate expression of Cyp1A1 and enhances the enzyme activity through AhR albeit at low levels in vivo.

The direct activation of AhR by UroA/UAS03 was examined in HT29 cells by XRE-luciferase reporter assay as well as nuclear translocation of AhR. The data showed that UroA/UAS03 treatment resulted in 2–4 fold induction of luciferase activity (Fig. 2e) compared to the high affinity ligand MeBio that caused higher levels (~15 fold) of AhR activation. Both UroA and UAS03 induced the nuclear translocation of AhR (Fig. 2f, g). AhR was upregulated in mice treated with UroA or UAS03 (Supplementary Fig. 3b). Next, we asked whether AhR or Cyp1A1 are required for UroA/UAS03 mediated upregulation of tight junction protein, Cldn4. For this purpose, *AhR* or *Cyp1A1* expression was suppressed using siRNA knockdown and Cldn4 expression was examined. As shown in Fig. 2h, i and Supplementary Fig. 6, UroA/UAS03 failed to induce Cldn4 both in AhR or Cyp1A1 knockdown cells. In addition, we also deleted Cyp1A1 in HT29 cells using CRISPR/Cas9 methods and examined UroA/UAS03 mediated activities. Deletion of Cyp1A1 did not show effect on basal levels of Cldn4 compared to parental HT29 cells (Supplementary Fig. 7a). As shown in Supplementary Fig. 7b–d, UroA/UAS03 failed to upregulate Cldn4 or NQO1 in Cyp1A1

deleted cells. These results suggest that UroA/US03 induce the expression of tight junction proteins through activation of AhR-Cyp1A1-dependent pathway.

UroA/UAS03 enhance gut barrier function through Nrf2. Since AhR is required for UroA mediated activities, we analyzed existing AhR-ligand Chip analysis using ChIP-Atlas (http://chip-atlas.org/target_genes) that were performed on breast cancer cell line MCF-7 (http://dbarchive.biosciencedbc.jp/kyushu-u/hg19/target/AHR.1.html). The analysis suggested that Nrf2 is a target of AhR signaling cascade (Supplementary Fig. 8a). Similarly, AhR also has influence on tight junction proteins such as Ocln, TJP3, Cldn2, 3 and 5 (Supplementary Fig. 8b). Furthermore, the pathway analysis of our RNA seq data (Ingenuity) also revealed that AhR and Nrf2 pathways are listed in top 25 (Supplementary Fig. 1). Previously, it was shown that TCDD mediates some of its activities through Nrf2 pathways[27,28]. Therefore, we hypothesized that UroA/UAS03 induce tight junction proteins through activating AhR-Nrf2 dependent pathways. We tested this hypothesis in colon epithelial cells as well as in mice deficient in AhR and Nrf2. Treatment with UroA/UAS03 significantly upregulated *Nrf2* both at mRNA and protein levels (Supplementary Fig. 9a and Fig. 3a) and induced its nuclear translocation in HT29 cells (Fig. 3b, c). Nrf2-promoter activities were validated utilizing ARE-luciferase assays, where UroA/UAS03 significantly enhanced luminescence upon treatment (Supplementary Fig. 9b) similar to known Nrf2 activator sulforaphane (SFN) albeit at lower levels. Nrf2 and its target gene HO1 are upregulated in the colons of wild type mice treated with UroA/ UAS03 (Supplementary Fig. 3) as well as in HT29 cells (Supplementary Fig. 9c). To examine the precise function and interdependency of AhR-Nrf2 pathways in UroA/UAS03 induced Cldn4 upregulation, we utilized colon explants from C57BL/6 (wild type, WT), AhR$^{-/-}$ and Nrf2$^{-/-}$ mice. NAD(P)H:quinone oxidoreductase (NQO1) encodes cytoplasmic 2-electron reductase and the induction is shared by both AhR and Nrf2 pathways[27]. We examined whether UroA/UAS03 upregulate expression of NQO1 in colon explants of these mice. Treatment with UroA/UAS03 induced the expression of both Nrf2, NQO1, and Cldn4 in WT colon explants (Fig. 3d, e and Supplementary Fig. 10). But these compounds failed to induce Cldn4 and NQO1 in both Nrf2$^{-/-}$ and AhR$^{-/-}$ colon explants as well as Nrf2 in AhR$^{-/-}$ mice colon explants (Fig. 3d, e, Supplementary Fig. 10) suggesting requirement of AhR and Nrf2 expression for UroA/UAS03 mediated activities. The basal level comparison of expression of Cldn4 and NQO1 in WT, AhR$^{-/-}$, and Nrf2$^{-/-}$ mice colon explants suggests that lack of AhR and Nrf2 reduced the expression of NQO1 and Cldn4 (Supplementary Fig. 10a). The data suggest that expression of Clnd4 is reduced in AhR$^{-/-}$ and Nrf2$^{-/-}$ but not in Cyp1A1 knock down cells.

To define the in vivo requirement of AhR and Nrf2 for UroA/UAS03 mediated upregulation of tight junction proteins, we utilized WT, Nrf2$^{-/-}$, and AhR$^{-/-}$ mice. Examination of basal level expression of Cldn4, NQO1 in the colon tissues of these mice suggests that lack of AhR or Nrf2 have reduced significantly NQO1 levels, but did not show statistical significance for reduction of Cldn4 albeit there was a trend towards reduced expression. (Supplementary Fig. 11c). The mice were treated daily with UroA/UAS03 (orally, 20 mg/kg bodyweight) for 7 days and barrier functions were analyzed. Treatment with UroA/UAS03 significantly upregulated Nrf2 and tight junction proteins (Cldn4, NQO1, Ocln, ZO1, and TJP3) in WT mice (Fig. 3f and Supplementary Fig. 11). In contrast, UroA/UAS03 failed to induce these proteins in Nrf2$^{-/-}$ and AhR$^{-/-}$ mice (Fig. 3f and Supplementary Fig. 11).
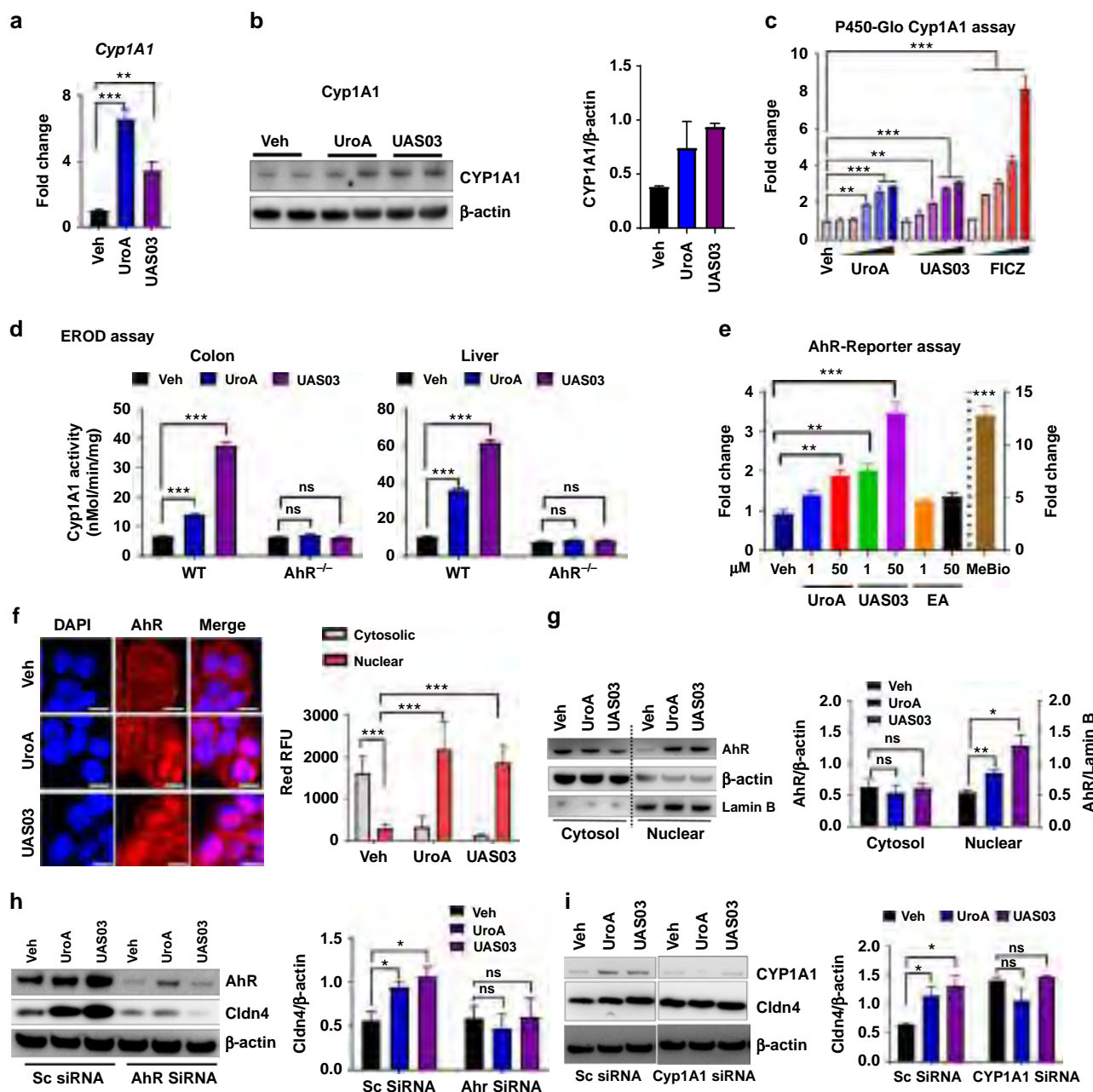
Fig. 2 UroA/UAS03 enhance tight junction proteins in AhR-dependent manner. **a** HT29 cells were treated with vehicle (DMSO-0.01%)/UroA/UAS03 (50 μM) for 24 h. mRNA levels of Cytochrome P450 1A1 (*Cyp1A1*) was measured by RT PCR. **b** Cyp1A1 protein levels were measured using immunoblots and quantified band intensities by Image J software. **c** Cyp1A1 enzyme activity was measured by P450-Glo Cyp1A1 assay. HT29 cells were treated with UroA or UAS03 (0.1, 1, 10, 25, 50 μM) or FICZ (0.1, 1, 10, 25, 50 nM) for 24 h and enzyme Cyp1A1 activity was measured. **d** C57BL/6 and AhR$^{-/-}$ ($n = 3$) mice were treated orally with Vehicle (0.25% CMC), UroA or UAS03 (20 mg/kg) for 1 week and Cyp1A1 activity was measured in colons and livers by ethoxyresorufin-O-deethylase (EROD) assay. **e** The cells expressing AhR-reporter (luciferase) were treated with Veh or UroA/UAS03 or ellagic acid (EA) or MeBio (AhR high affinity ligand) for 6 h and fold change of luminescence over vehicle treatment was measured. **f** Immunofluorescence confocal images of HT29 cells treated with vehicle/UroA/UAS03 (50 μM) for 6 h. The cells were stained with anti-AhR antibody (red) and DAPI (blue). Relative fluorescence ($n = $~20 cells) in the cytosol and nucleus was measured. The scale bar indicates 10 μm. **g** AhR levels in cytosol and nuclear fractions of HT29 cells treated for 2 h with Veh or UroA/UAS03 (50 μM). **h** AhR or **i** Cyp1A1 was knocked down using siRNA in HT29 cells and the cells were treated with vehicle/UroA/UAS03 (50 μM) for 24 h and immnunoblots were performed to detect expression of AhR, Cyp1A1, and Cldn4. Scrambled (Sc) siRNA transfections were used as controls. Immunoblots were quantified using Image J software. The data is representative of two independent repeats with triplicate wells for each treatment. Statistics performed using unpaired *t*-test using Graphpad Prism software. All in vitro studies were performed in triplicates. Error bars, ±SEM; ***$p < 0.001$; **$p < 0.01$; **$p < 0.05$. Source Data are provided as a Source Data File
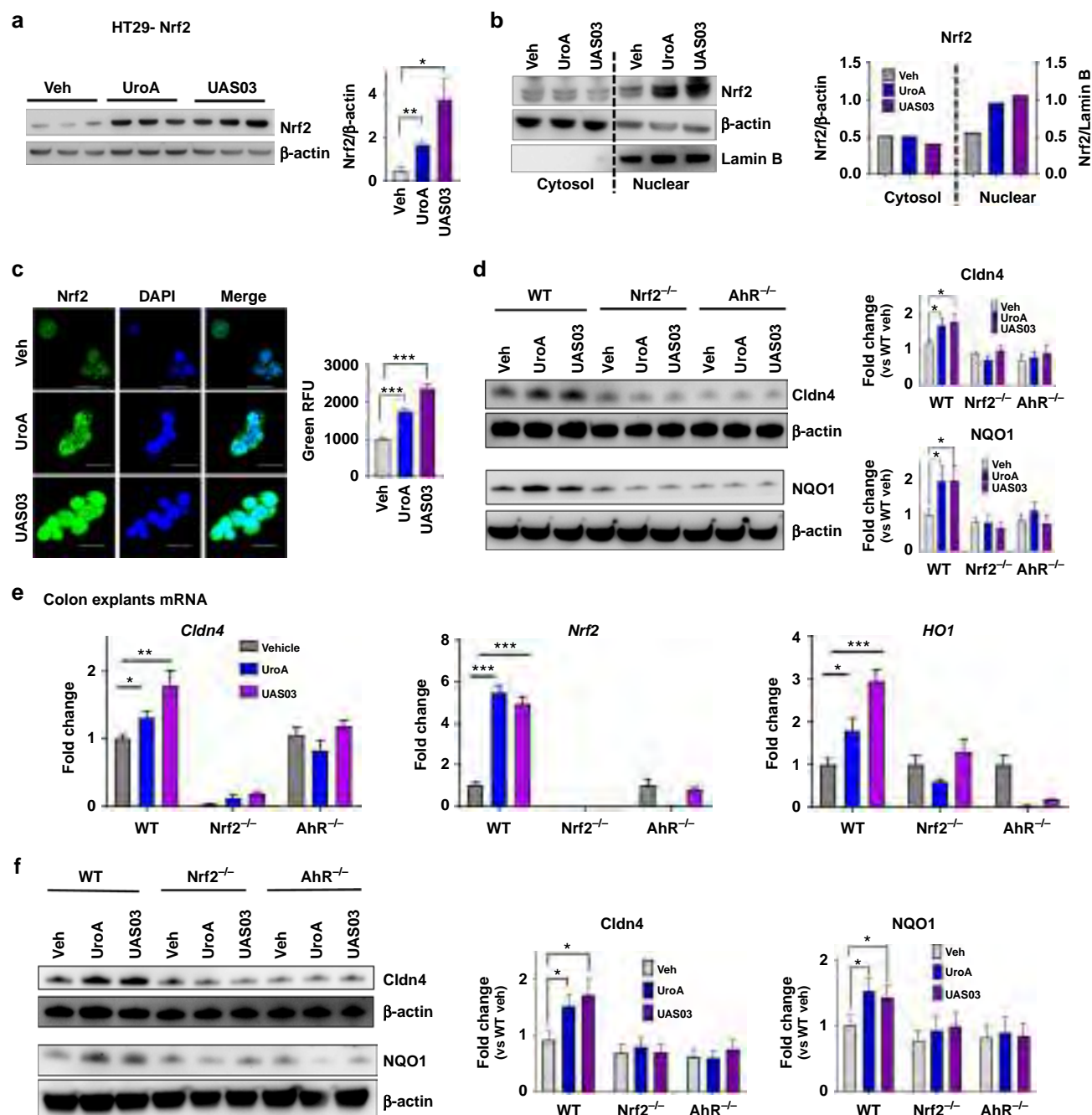
Fig. 3 Nrf2 is required for UroA/UAS03 mediated upregulation of tight junction proteins. **a** Nrf2 levels were determined by immunoblots in HT29 cells treated with vehicle/UroA/UAS03 (50 μM) for 24 h. **b** Nrf2 expression in cytosolic and nuclear fractions of HT29 cells treated with Veh/UroA/UAS03 (50 μM) for 6 h. **c** Immunofluorescence confocal images of HT29 cells treated with vehicle/UroA/UAS03 (50 μM) for 6 h. The cells were stained with anti-Nrf2 antibody and DAPI. Relative green fluorescence (n = ~20 cells) intensity was measured. Scale bars indicate 25 μm. **d** Expression of Cldn4 and NQO1 in colon explants from WT, Nrf2$^{-/-}$, and AhR$^{-/-}$ mice treated with vehicle/UroA/UAS03 (50 μM) for 24 h. Immunoblots were quantified using Image J software. **e** mRNA levels of *Cldn4, Nrf2*, and *HO1* from colon explant cultures was measured by real-time PCR using SyBr green method. **f** C57BL/6, Nrf2$^{-/-}$, and AhR$^{-/-}$ mice (n = 3) treated orally daily with veh or UroA/UAS03 (20 mg/kg) for 1 week. Cldn4 and NQO1 protein levels in colons were measured by immunoblots and quantified by Image J software. All in vitro studies were performed in triplicates. The immunoblots of colon explants and colon tissues were quantified from at least 6 independent runs. The levels of proteins were normalized to β-actin and Wild type vehicle treatment was set to 1 and calculated the fold changes. Statistics performed using unpaired *t*-test using Graphpad Prism software. Error bars, ±SEM; *p < 0.05; **p < 0.01; ***p < 0.001. Source Data are provided as a Source Data File

UroA/UAS03 induced NQO1 expression was also confirmed in HT29 cells (Supplementary Fig. 9d). Overall these results suggest that both AhR and Nrf2 are required for UroA/UAS03 mediated upregulation of tight junction proteins and NQO1.

Treatment with UroA/UAS03 mitigates colitis. The physiological relevance of UroA/UAS03 regulated barrier function was examined in the 2,4,6-Trinitrobenzenesulfonic acid (TNBS)-induced colitis model[29]. Oral treatment with UroA/UAS03 (20 mg/kg at 12 h intervals) significantly protected from TNBS-
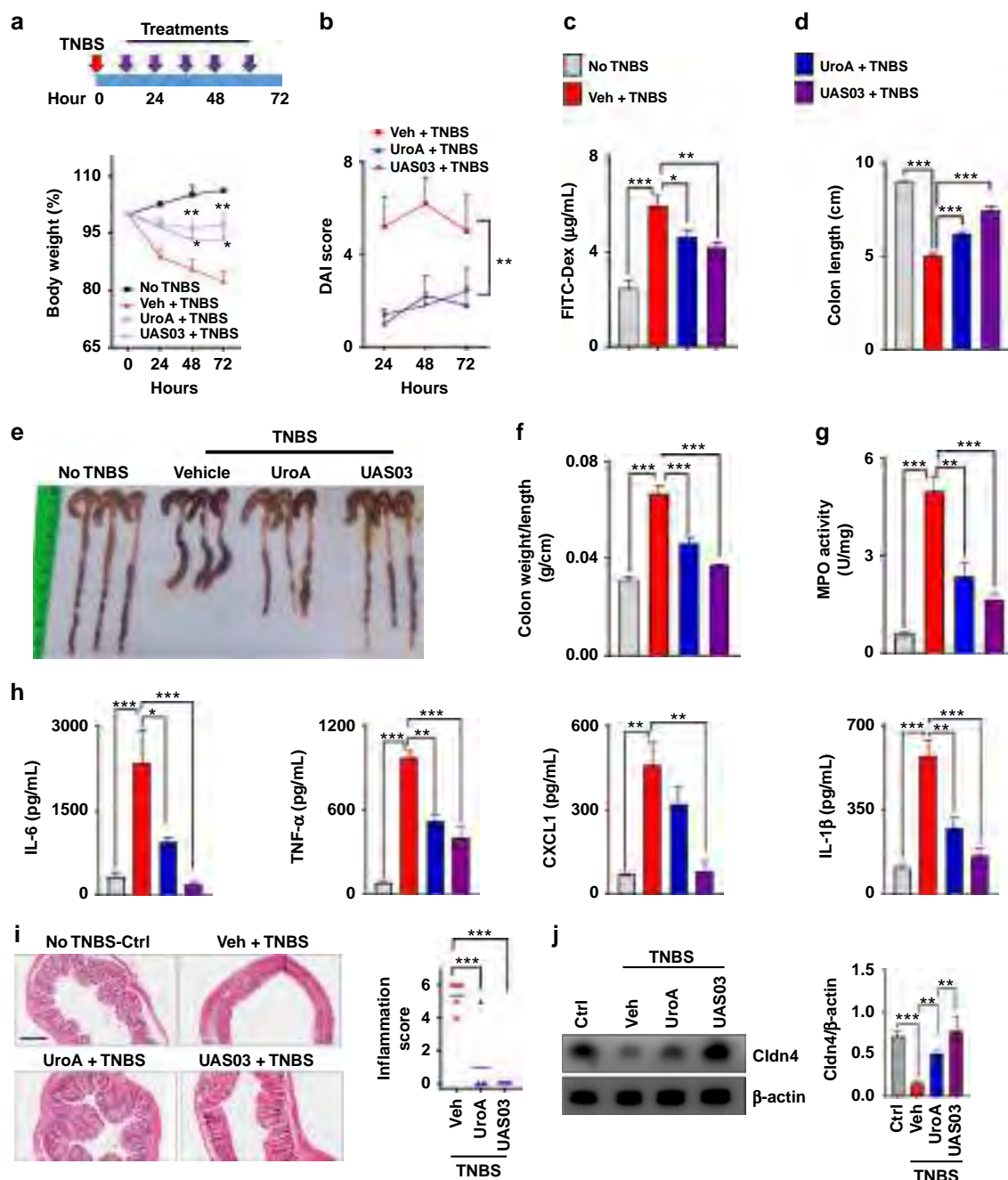
Fig. 4 UroA/UAS03 treatment attenuates TNBS-induced colitis in mice. Colitis was induced by intrarectal administration of TNBS (2.5 mg/mouse) in C57BL/6 (8 week age old, $n = 5$/group) mice. Mice were orally treated with vehicle or UroA (20 mg/kg) or UAS03 (20 mg/kg body weight) every 12 h post-TNBS instillation for 60 h and the experiment terminated at 72 h. Representative data from one of three independent experiments is shown. **a** Percent body weight loss (No TNBS- Solid black line; Veh + TNBS- Solid red line; UroA + TNBS- Solid blue line; UAS03 + TNBS- Solid purple line). **b** disease activity index, **c** intestinal permeability, **d** colon lengths were measured. **e** Gross morphological changes of colon, **f** ratio of colon weight/length, **g** colonic myeloperoxidase (MPO) levels, **h** serum IL-6, TNF-α, CXCL1, and IL-1β levels, **i** microphotographs of hematoxylin and eosin (H&E) stained sections of colons and inflammation scores are shown. Scale bar indicates 300 μm. **j** Cldn4 expression in the colons of these mice ($n = 3$) was measured by immunoblots and quantified. Statistical analysis was performed (unpaired t-test) using Graphpad Prism software. Error bars, ±SEM ***$p < 0.001$; **$p < 0.01$ *$p < 0.05$. Source Data are provided as a Source Data File

induced body weight loss (Fig. 4a), reduced disease activity index (DAI) score (Fig. 4b) and intestinal permeability (Fig. 4c). UroA/UAS03 treatment significantly protected from TNBS-induced colon shortening (Fig. 4d, e) and reduced weight to length ratio (Fig. 4f) suggesting decreased colonic inflammation. UroA/UAS03 treatment also reduced neutrophil infiltration as evident from myeloperoxidase (MPO) activity (Fig. 4g) as well as serum

inflammatory markers such as IL-6, TNF-α, CXCL1, and IL-1β (Fig. 4h) that are hallmarks of ulcerative colitis. Consistent with these findings, H&E analysis of colon sections showed significantly less tissue damage and inflammation scores (Fig. 4i). Furthermore, UroA/UAS03 also protected from TNBS-induced downregulation of Cldn4 in the colons of these mice (Fig. 4j). We further examined the effects of dose and frequency of UroA/

UAS03 treatments as well as their preventive efficacy in mitigating colitis. As shown in Supplementary Fig. 12, UroA/UAS03 mitigated TNBS-induced colitis with a single treatment at 4 or 20 mg/kg body weight. The comparisons bodyweights at each time points suggest that TNBS treatment in all the groups led to decrease in body weight and treatment seems to decrease the loss of body weight, but did not reach significance (Supplementary Fig. 13). However, treatments significantly showed impact on other parameters such as protecting from shortening of colons, blocking inflammatory mediators. Supplementing wild type mice with UroA or UAS03 did not exhibit any signs of toxicity as evident from no observed changes in their body weights, CBC counts as well as serum ALT and AST levels (Supplementary Fig. 14).

Since UroA/UAS03 exhibited strong barrier protective activities by upregulating tight junction proteins, we investigated whether regular exposure to these metabolites would have sustained beneficial effects in preventing colitis. The prophylactic activity profile of UroA/UAS03 was examined in the TNBS-induced colitis model. WT mice were orally fed daily with vehicle or UroA/UAS03 for 1 week followed by TNBS administration to induce colitis. These mice did not receive any further UroA/

UAS03. The treatment regimen and percent bodyweights are shown in Fig. 5a and Supplementary Fig. 15. The pre-treated mice were significantly protected from TNBS-induced colon shortening and colonic inflammation (colon length/weight) similar to a therapeutic regimen (Fig. 5b–d). Pre-treatment also significantly enhanced barrier function and decreased TNBS-induced inflammation (Fig. 5e, f). These results suggest that UroA/UAS03 mediated enhanced gut barrier function will likely have long-term beneficial effects in preventing colitis. In therapeutic regimen, mice were treated with UroA or UAS03 24 h post-TNBS, where mice develop severe colitis. In this setting, treatment with UroA/UAS03 also significantly reversed the colitis phenotype by reducing shortening of colons, gut permeability and inflammation compared to vehicle treatment.

The therapeutic applications of UroA/UAS03 were also examined in the dextran sodium sulfate (DSS)-induced colitis model. DSS chemically disrupts the epithelial cell barrier and leads to increased penetration of bacteria resulting in inflammation and colonic tissue damage. As shown in Supplementary Fig. 16, the mice treated with UroA/UAS03 were significantly protected from 3% DSS induced acute colitis. UroA/UAS03 treatment mice displayed overall decreased DAI scores during the
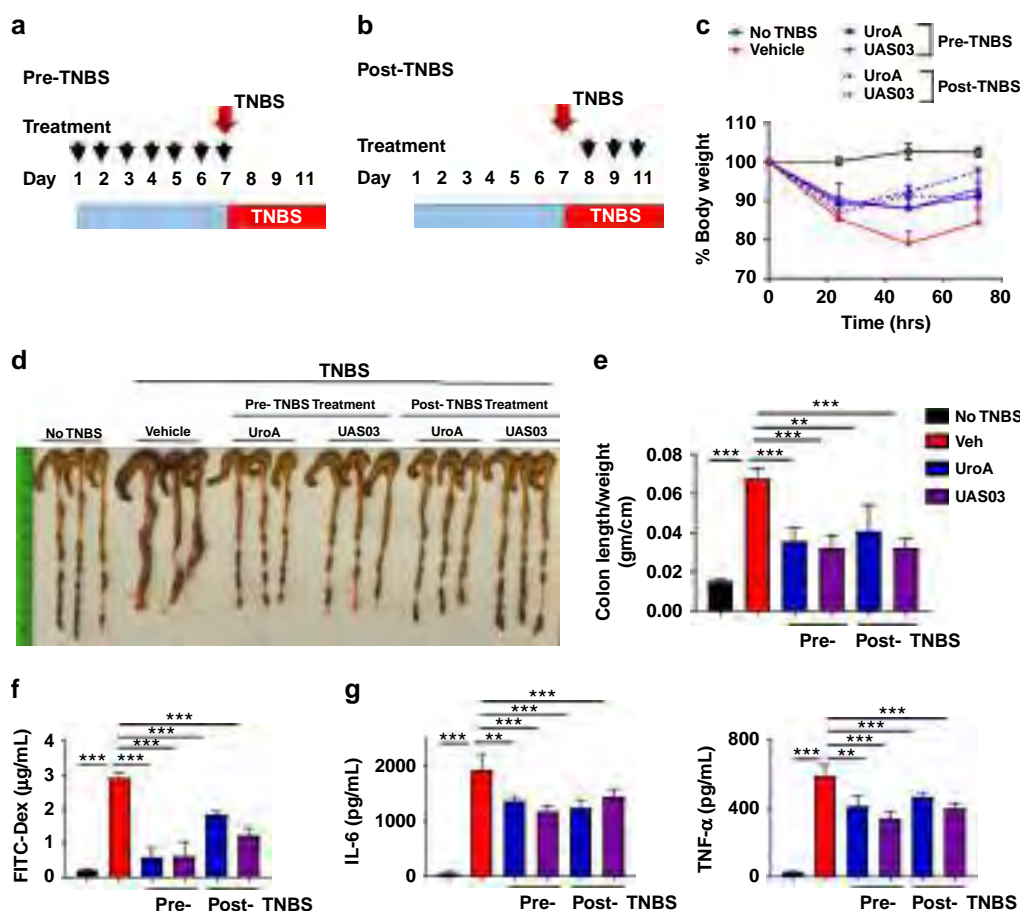

Fig. 5 UroA/UAS03 prevent TNBS-induced colitis and sustain beneficial barrier activities. **a** Pre-TNBS treatment. Male C57BL/6 mice (n = 5 per group at 7–8 week old age) were given orally vehicle (Veh; 0.25% sodium carboxymethylcellulose) or UroA or UAS03 (20 mg/kg/bodyweight) daily for one week followed by rectal administration of TNBS to induce colitis. These mice did not receive any treatment post-TNBS administration. Mice were euthanized 72 h post-TNBS administration and characterized. **b** Post-TNBS treatment. Another set group of C57BL/6 mice (n = 5 per group at 7–8 week old age) received Veh or UroA or UAS03 (20 mg/kg) 24, 48, and 72 h post-TNBS. **c** Percent body weight loss was recorded after TNBS-administration. (No TNBS- Solid black line; Veh + TNBS- Solid red line; Pre-TNBS + UroA- Solid blue line; Pre-TNBS + UAS03- solid purple line; Post-TNBS + UroA- dashed blue line; Post-TNBS + UAS03- dashed purple line). **d** Representative colon images of control (no TNBS) along with vehicle/UroA/UAS03 treated mice from pre- and post-treatment groups. **e** Ratio of colon weight/length, **f** intestinal permeability was evaluated using FITC-dextran leakage assay. **g** Serum levels of IL-6 and TNF-α were measured using standard ELISA methods. Statistical analysis was performed (unpaired t-test) using Graphpad Prism software. Error bars, ±SEM ***p < 0.001. Source Data are provided as a Source Data File

disease progression. Importantly, UroA/UAS03 treatments protected from shortening of colons, decreased gut permeability and reduced inflammation compared to vehicle treatment (Supplementary Fig. 16) at the end of experiment on day 15. Further, the therapeutic efficacies of UroA/UAS03 were also examined in a chronic DSS model, where mice were given 4 cycles of 2% DSS in drinking water for 7 days with an interval of 14 days in each cycle on regular water (Fig. 6a). Treatment with UroA/UAS03 significantly protected from DSS-induced colitis as evident from decreased gut permeability (Fig. 6b), reduced shortening of colons (Fig. 6c, d), increased colon weight/length ratio (Fig. 6e), reduced inflammation (serum IL-6, IL-1β, TNF-α as well as colonic tissue MPO levels) (Fig. 6f, g). Analysis of tight junction proteins in these mice also suggest that treatment with UroA/UAS03 enhanced the expression of Cldn4 (Fig. 6h). These results highlight the model independent beneficial activities of UroA/UAS03 in preserving the barrier integrity and mitigating colonic inflammation.

UAS03/UroA mediated protection against colitis requires AhR-Nrf2 pathways. The studies described above indicated the importance of AhR-Nrf2 pathway in UroA/UAS03 enhanced barrier function. To examine the relevance of these pathways in colitis, we tested the in vivo requirement for Nrf2 (Fig. 7) and AhR (Fig. 8). Treatment of Nrf2−/− mice with UroA/UAS03 failed to restore body weight loss caused by TNBS-induced colitis (Fig. 7a, b and Supplementary Fig. 17) or protect from shortening

of colons (Fig. 7c). UroA/UAS03 treatment did not enhance barrier function in Nrf2−/− mice as evident from similar FITC-dextran leakage in UroA/UAS03 treated mice compared to vehicle treatment (Fig. 7d). These results demonstrated that UroA/UAS03 enhanced gut barrier integrity requires the expression of Nrf2. Interestingly, UroA/UAS03 partially reduced serum inflammatory mediators such as IL-6 and TNF-α levels in Nrf2−/− mice (Fig. 7e), suggesting that UroA/UAS03 could mediate some of the anti-inflammatory activities in Nrf2-independent manner. To define the role of AhR in UroA/UAS03 mediated protective activities, the TNBS-induced colitis model was executed in AhR−/− mice along with wild type mice (Fig. 8a). As expected AhR−/− mice were more susceptible to TNBS-induced colitis model as evident from rapid loss of body weight (Fig. 8b and Supplementary Fig. 18). Therefore, we terminated the experiment at post 60 h TNBS administration (Fig. 8a). Treatment with UroA/UAS03 failed to protect from shortening of colon lengths in AhR−/− mice compared to wild type mice (Fig. 8c, d). Additionally, UroA/UAS03 failed to correct the barrier dysfunction in AhR−/− mice as evident from in vivo permeability assays (Fig. 8e). Analysis of serum inflammatory mediators suggest that UroA/UAS03 failed to reduce IL-6 and slightly reduced the TNF-α in AhR−/− mice, whereas UroA/UAS03 treatments significantly reduced IL-6 and TNF-α in wild-type mice as observed above (Fig. 8f). Based on these results we propose that UroA/UAS03 exert protective barrier functional activities through AhR-Nrf2-dependent pathways by inducing tight junction proteins (Fig. 8g).
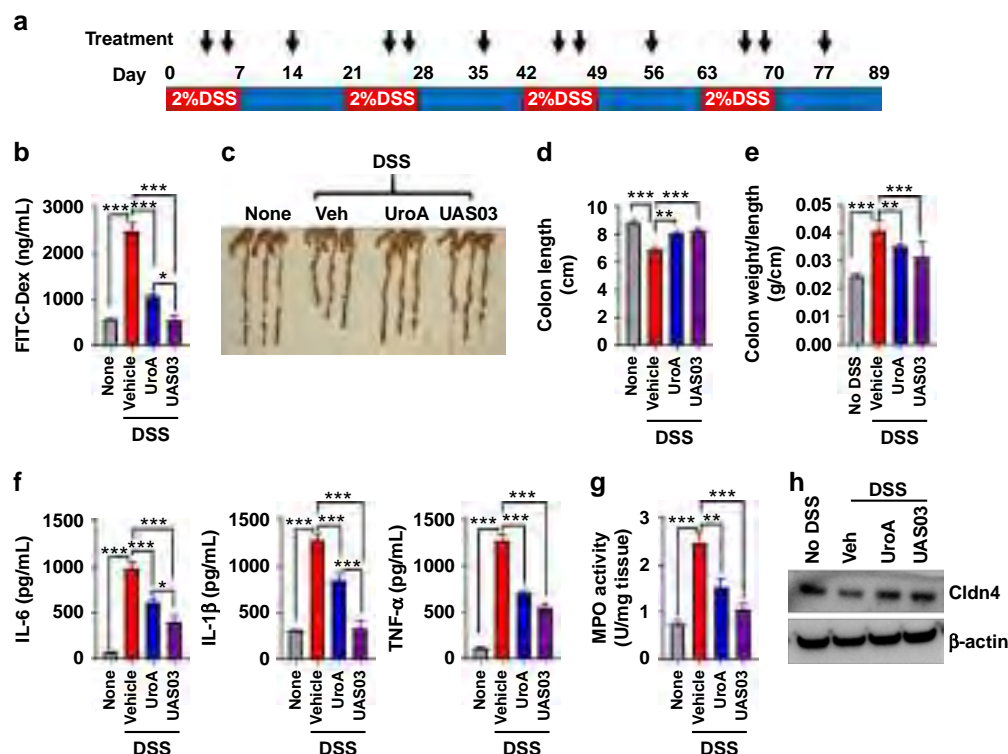
Fig. 6 Treatment with UroA/UAS03 mitigate DSS-induced chronic colitis. **a** C57BL/6 mice (7–8 week age old) were treated with four cycles of DSS (2%) with 7 days/cycle with an interval of 14 days with regular water. Control group of mice (n = 5) received the regular water without DSS. UroA/UAS03 (20 mg/kg/day/body weight) that was resuspended in 0.25% sodium carboxymethylcellulose (CMC) solution (n = 9) or vehicle (CMC) (n = 9) was administered on 4th and 6th day of each DSS cycle and one treatment while on regular water. n = 5/control; n = 9/veh and UroA; n = 8/UAS03 group) Mice were euthanized at day 89 and the colitis phenotype was characterized. **b** Intestinal permeability using FITC-dextran was evaluated. **c** Representative colon images **d** colon lengths, **e** ratios of colon weight/length are shown. **f** Serum levels of IL-6, IL-1β, and TNF-α were measured using ELISA methods. **g** MPO levels were determined in colon tissues. **h** Cldn4 expression in the colons of these mice (n = 3) was measured by immunoblots. Statistics performed using unpaired t-test using Graphpad Prism software. Error bars, ±SEM ***p < 0.001; **p < 0.01; *p < 0.05. Source Data are provided as a Source Data File
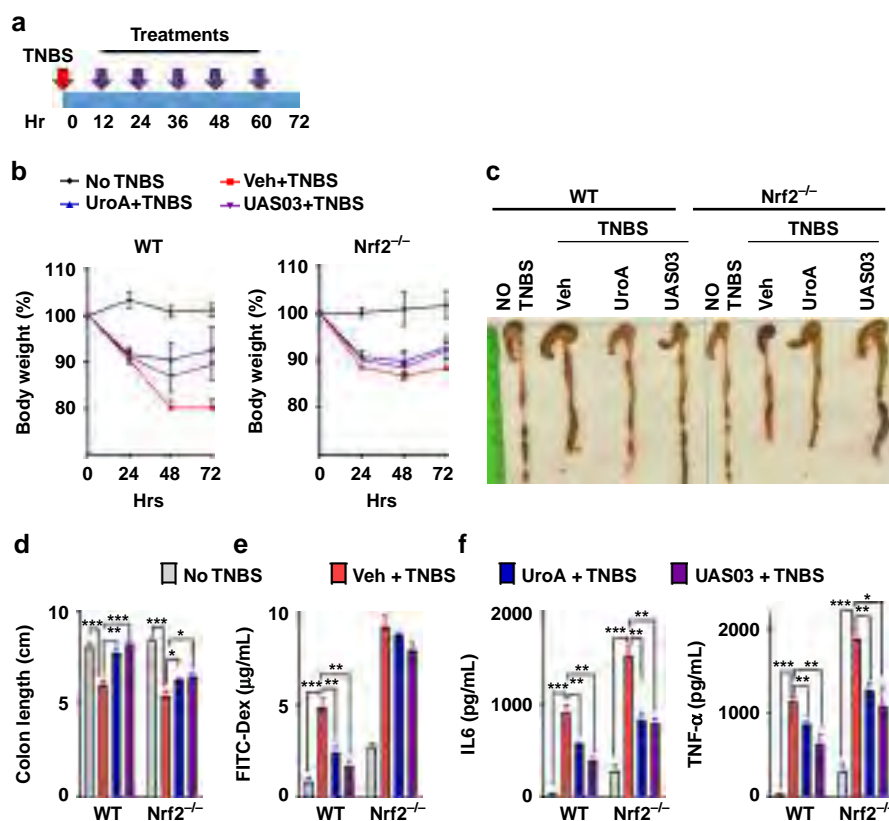
Fig. 7 UroA/UAS03 utilize Nrf2 pathways to mitigate colitis. **a–e** Colitis was induced using TNBS in C57BL/6 (WT) and Nrf2$^{-/-}$ mice ($n = 4$–5/group 7–8 week old age). Mice were treated with Veh or UroA/UAS03 (20 mg/kg bodyweight) every 12 h post TNBS administration ending at 72 h. Representative data from two independent experiments is shown. **a** TNBS-induced colitis experimental design and treatment regimen. **b** Percent body weight loss (No TNBS- Solid black line; Veh + TNBS- Solid red line; UroA + TNBS- Solid blue line; UAS03 + TNBS- Solid purple line), **c** representative colon images, **d** colon lengths, **e** gut permeability, **f** serum levels of IL-6 and TNF-α were determined. Statistical analysis was performed (unpaired t-test) using Graphpad Prism software. Error bars, ±SEM ***$p < 0.001$; **$p < 0.01$ *$p < 0.05$. Source Data are provided as a Source Data File

Since the macrophages are critical mediators of colonic inflammation in IBDs[30,31], we determined if UroA/UAS03 mediated anti-inflammatory activities require the AhR-Nrf2 pathways in macrophages. First, we examined whether UroA/UAS03 activates Nrf2-dependent pathways in macrophages. The results showed that treatment with UroA/UAS03 significantly upregulated Nrf2 expression and induced its nuclear translocation, as well as upregulation of Nrf2-target genes such as HO1 expression in macrophages (Supplementary Fig. 19a–e). Further, analysis of UroA/UAS03 mediated down regulation of LPS-induced IL-6 production in macrophages from WT, Nrf2$^{-/-}$ and AhR$^{-/-}$ mice showed that LPS-induces much higher levels of IL-6 in Nrf2$^{-/-}$ and AhR$^{-/-}$ macrophages relative to WT (Fig. 8h). UroA/UAS03 also reduced the NF-κB activation in an AhR-dependent manner in macrophages (Supplementary Fig. 19f). AhR$^{-/-}$ BMDM are hyper responsive to LPS stimulation as evident from increased NF-κB activation as well as increased levels of IL-6 compared to wild type (Fig. 8h and Supplementary Fig. 19g). Despite significant lowering of IL-6 levels by UroA/UAS03 in Nrf2$^{-/-}$ macrophages, these reduced levels are still higher compared to LPS-induced IL-6 in WT macrophages. When compared, the fold reduction upon treatments (Supplementary Fig. 20), UroA/UAS03 reduced IL-6 in Nrf2$^{-/-}$ similar to WT indicating Nrf2-independent anti-inflammatory activities both in vivo (TNBS model) and in vitro BMDM (LPS-induced IL-6). In contrast, UroA/UAS03 did not block LPS-induced IL-6 production in AhR$^{-/-}$ macrophages up to 30 μM as well as in AhR$^{-/-}$ mice in TNBS-induced colitis model suggesting that

UroA/UAS03 mediate anti-inflammatory activities through AhR-dependent manner. AhR$^{-/-}$ BMDM slight decrease in IL-6 levels at 50 μM dose may suggest some of unknown AhR-independent anti-inflammatory activities. The results presented here highlight that single microbial metabolite regulates the barrier function in epithelial cells via the activating AhR-Nrf2 signaling pathways and also anti-inflammatory activities in AhR dependent pathways.

Discussion

In this study, we identified that microbial metabolite UroA, and its analogue UAS03, increases overall gut health by enhancing barrier function in addition to their anti-inflammatory activities. UroA/UAS03 activate the phase I (AhR-Cyp1A1) and phase II (Nrf2-anti-oxidative pathways) metabolic pathways to enhance expression of tight junction proteins and inhibit inflammation. We further demonstrate that treatment with these compounds significantly mitigated colitis both in preventive and therapeutic settings.

A key physiological function of gut microbiota is to catabolize dietary components into absorbable metabolites. Despite the identification of numerous microbial metabolites, the molecular targets and mechanisms of action for many metabolites is unknown. Urolithins, derived from dietary polyphenols such as ETs, EA by microbiota are linked to the beneficial effects associated with high consumption of fruits and vegetables in humans[11,18,19]. It was reported that the *Bifidobacterium pseudo-catenulatum INIA P815* strain was able to metabolize EA to
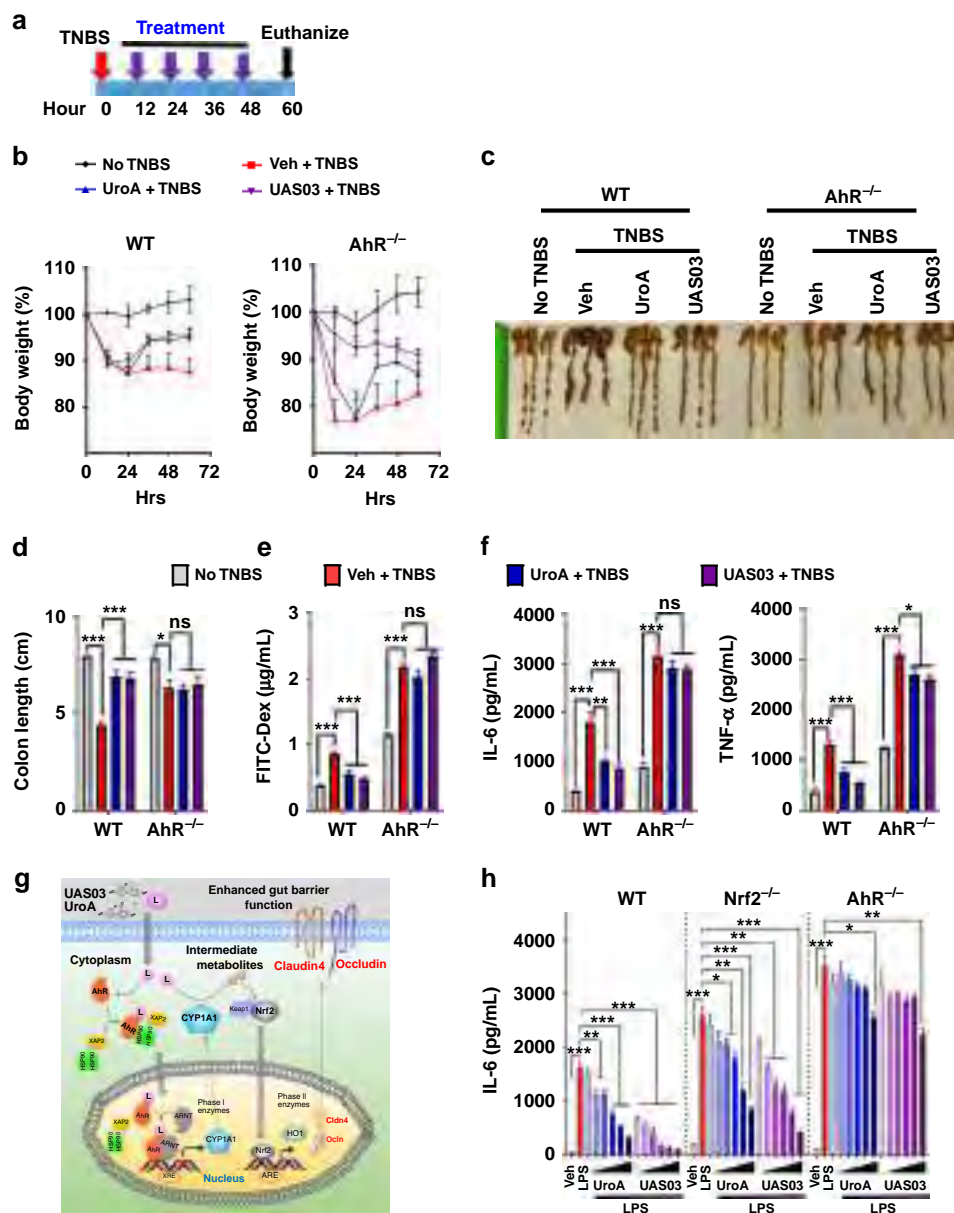
Fig. 8 UroA/UAS03 exert beneficial activities through AhR-dependent pathways. **a–e** Colitis was induced using TNBS in C57BL/6 (WT) and AhR$^{-/-}$ mice ($n = 4$/group 7–8 week old age). Mice were treated with Veh or UroA/UAS03 (20 mg/kg bodyweight) every 12 h post TNBS administration and mice were euthanized at post 60 h TNBS administration. **a** TNBS-induced colitis experimental design and treatment regimen. **b** Percent body weight loss (No TNBS- Solid black line; Veh + TNBS- Solid red line; UroA + TNBS- Solid blue line; UAS03 + TNBS- Solid purple line), **c** representative colon images, **d** colon lengths, **e** gut permeability, **f** serum levels of IL-6 and TNF-α were determined. Statistical analysis was performed (unpaired t-test) using Graphpad Prism software. Error bars, ± SEM ***$p < 0.001$; **$p < 0.01$; *$p < 0.05$. **g** AhR-Nrf2 dependent tight junction protein regulation by UroA/UAS03. UroA/UAS03 (L: ligands) bind to AhR and activate its nuclear translocation to induce expression of Cyp1A1 and Nrf2. Further, UroA/UAS03 causes Nrf2-dependent upregulation of tight junction proteins and enhanced barrier function. **h** LPS (50 ng/ml)-induced IL-6 levels were measured in the presence of Vehicle or UroA or UAS03 (0.1, 1, 10, 20, 30, and 50 μM) in bone marrow derived macrophages (BMDM) from wild type (WT), Nrf2$^{-/-}$ and AhR$^{-/-}$ mice. The data is representative of two independent experiments with triplicates. Statistical analysis was performed (unpaired t-test) using Graphpad Prism software. Error bars, ±SEM ***$p < 0.001$; **$p < 0.01$ *$p < 0.05$. Source Data are provided as a Source Data File

produce UroA and UroB[32]. Large inter-individual variability in UroA levels[18] suggests that bacteria responsible for UroA production may also be highly variable in humans. Urolithin levels can reach up to micro molar concentrations in human serum depending on their microbiota composition[18]. The premise of this study is that direct supplementation of UroA will overcome the intrinsic variation in microbiota among populations and offer health benefits. In this regard, we also successfully developed UAS03, a more stable and potent structural analogue of UroA

that displayed increased gut barrier protection and anti-inflammatory activities.

Previous studies demonstrated inhibitory activities of urolithins in inflammation, proliferation, and aging in various models[20,22,33]. However, the molecular targets or mechanisms of action of these metabolites on pathophysiological processes are unknown. Our approach of searching for an epithelial cell function for these metabolites by RNA-Seq analysis revealed several important clues for their function and potential mechanisms.

UroA/UAS03 mediated up regulation of tight junction proteins (e.g., Cldn4, Ocln, and ZO1) and protection from LPS induced leakage in epithelial monolayers showed that these metabolites clearly play an important role in the regulation of barrier function. Tight junctions consist of both transmembrane proteins (e.g., occludin, claudins, junctional adhesion molecules, and tricellulin) as well as peripheral membrane proteins (e.g., ZO-1 and cingulin) to regulate paracellular permeability and maintain gut barrier function. The disruption of tight junctions leads to barrier dysfunction and is implicated in IBDs and other disorders[34]. In particular, gut barrier dysfunction leads to bacterial invasion and excessive inflammation[35,36]. The inflammatory cytokines and growth factors such as TNF-α, IFNγ, IL-1β, TGF-α, and platelet derived growth factors as well as bacterial endotoxins (LPS) are known to increase permeability by disrupting tight junctions[37]. Thus, barrier dysfunction and inflammation form a self-perpetuating loop in IBDs and blocking one of these is often insufficient for mitigating the disease process.

Our RNA-seq studies and expression analysis showed that in addition to upregulation of Cldn4, UroA also induced the expression of Cyp1A1 and HO1 in colon epithelial cells. Since Cyp1A1 and HO1 represent the activation of phase I and phase II drug metabolic pathways, these results suggested the potential involvement of AhR and Nrf-2 in mediating UroA/UAS03 functions. AhR is a nuclear transcription factor that responds to both xenobiotic and endogenous ligands leading to cell-specific gene regulation and cellular functions. AhR activation is responsible for the induction of multiple Phase I and Phase II xenobiotic chemical metabolizing enzymes such as Cyp1A1[38]. AhR can be activated by many chemicals including environmental polycyclic aromatic hydrocarbons, coal tar, phytochemicals, and products from commensal bacteria and tryptophan metabolism[39]. Historically, human exposure to high affinity AhR ligand, TCDD (which is not metabolized by Cyp1A1) displayed severe adverse events such as appearance of cysts, eruptions, pustules, and erythema as well as life threatening manifestations including liver, renal failures, myocardial degeneration[39]. However, AhR activation by FICZ ligand (amenable to Cyp1A1 drug metabolism) has been implicated in controlling the immune system and protection from colitis[40,41]. Our studies revealed that UroA/UAS03 treatments induced the expression and nuclear translocation of AhR and enhanced transcription of XRE-target genes as well as induced Cyp1A1 enzyme activities without exhibiting toxicity.

Interestingly, UroA/UAS03 failed to induce Cldn4/NQO1 in Cyp1A1 knockdown cells. Previously, it was reported that overexpression of Cyp1A1 in mice resulted in depletion of natural AhR ligands and deletion of Cyp1-enzymes in mice (Cyp1A1, Cyp1A2, Cyp1B1 triple knockout mice) led to increase in availability of AhR ligands and increased their activities[42]. Similarly, we also anticipated that deletion of drug metabolizing and detoxifying enzyme, Cyp1A1, would enhance the availability of UroA/UAS03 and enhance their activities. However, we did not observe increased activities upon deletion of Cyp1A1 in colon epithelial cells. We still do not understand the complete mechanisms for these observations. It may be necessary to delete all Cyp enzymes to avoid compensation mechanisms to detect increased activities. It also is possible that UroA/UAS03 undergo Cyp1A1 drug metabolism and generates unknown active phase I metabolites, which could activate Nrf2 pathways. It was reported by Gimenez-Bastida et al.[43] that UroA-glucuronide (UroA-Gluc) forms displayed beneficial activities, where treatment with UroA-Gluc ameliorated the TNF-α induced inflammation and associated molecular markers in human aortic endothelial cells. UroA is known to circulate as glucuronide and sulfate conjugates as well as parent form (UroA) in plasma[20]. Therefore, it is possible that

products from UroA drug metabolism Phase I and II intermediates could also exert certain beneficial activities. Alternatively, UroA/UAS03 could induce basal ROS that is dependent on expression of Cyp1A1 and leading to activation of Nrf2-pathways. Additional studies are required to support these possibilities and to define precise role of Cyp1A1 in UroA/UAS03 mediated activities using Cyp1-enzyme whole body and intestinal epithelial cells (villin) specific knock out mice.

UroA/USA03 failed to exert their activities in cells lacking AhR or in AhR−/− colon explants as well as in AhR−/− mice suggesting a critical role for the AhR pathway in mediating UroA/UAS03 activities. While the regulation of immune cell function by AhR has been previously demonstrated[41,44], our current studies highlight the importance of this pathway in epithelial cells to regulate tight junction proteins and barrier function.

Previous studies suggested that interdependency of AhR and Nrf2 pathways[28,45,46]. Nrf2, a basic region-leucine zipper transcription factor, protects cells and tissues from oxidative stress by inducing the expression of antioxidant and phase II-enzymes such as glutathione S-transferase and NQO1[47] as well as controlling LPS-induced inflammation[48]. Our studies both in vitro and in vivo suggest that UroA/UAS03 significantly induced the expression of Nrf2 as well as its target genes such as HO1 and NQO1 in colon epithelium. Furthermore, our results also showed that AhR-Cyp1A1-Nrf2 pathways are essential for UroA/UAS03 mediated upregulation of tight junction proteins (Figs. 2 and 3).

Our extensive studies in colitis models revealed that treatment with UroA/UAS03 significantly enhanced tight junction proteins, decreased gut permeability, and reduced local and systemic inflammation leading to attenuation of colitis (Figs. 4–8). Even a single dose of UroA/UAS03 exhibited therapeutic efficacies against TNBS-induced colitis. Importantly, prophylactic benefits of UroA/UAS03 on gut barrier function and prevention of colitis development was observed (Fig. 5). The mice pre-treated with UroA/UAS03 prior to TNBS administration significantly reduced gut permeability (Fig. 5e), which is consistent with increased expression of tight junction proteins. Despite not receiving further treatments post-TNBS administration, these mice were protected from disease development suggesting prophylactic effects of these compounds through enhanced barrier function. Moreover, UroA/UAS03 supplementing daily for 7 days induced expression of AhR, Nrf2, and Cldn4 in the colons of wild-type mice without observable toxicity (Fig. 3f, Supplementary Figs. 3, 11 and 14) suggesting potential translational applications for these compounds. Further, treatment with UroA/UAS03 also mitigated both chronic and acute DSS-induced colitis indicating model independent beneficial activities of these metabolites Fig. 6 and Supplementary Fig. 16). Previously, it was shown that mice lacking AhR or Nrf2 are more susceptible to colitis compared to wild type[40,49]. In contrast to the toxicity associated with the high affinity AhR ligands such as TCDD, UroA/UAS03 are low affinity non-toxic AhR ligand (partial agonist) like BNF that suppressed the pathogenesis of DSS-induced colitis[40].

It was suggested that Nrf2 protects from colitis through regulation of pro-inflammatory cytokines and induction of phase II detoxifying enzymes. Kobayashi et al.[50] demonstrated that Nrf2 suppresses inflammation through redox control, by opposing the transcriptional upregulation of proinflammatory cytokine genes and identified Nrf2 as the upstream regulator of cytokine production. Previously, it was also demonstrated that ablation of Nrf2 leads to enhancement of NF-κB activation resulting in increased inflammatory cytokines production[51] and severe colitis[49]. We also observed increased basal level of inflammatory mediators in Nrf2−/− mice compared to wild-type mice as well as in Nrf2−/− BMDM. Further, addition of LPS significantly upregulated IL-6 in Nrf2−/− BMDM compared to wild-type BMDM

as well as in TNBS-induced colitis model. UroA/UAS03 failed to repair TNBS-induced barrier dysfunction and colitis in Nrf2$^{-/-}$ mice (Fig. 7).

The role of AhR in UroA/UAS03 mediated upregulation of tight junction proteins was demonstrated using AhR siRNA, colon explants from AhR$^{-/-}$ mice as well as in vivo treatments in AhR$^{-/-}$ mice. Additionally, UroA/UAS03 failed to mitigate TNBS-induced colitis in mice lacking AhR (Fig. 8). Interestingly, UAS03 seems to have some protective role against rapid body weight loss in AhR$^{-/-}$ mice that are treated with TNBS. It is not clear at this time, why UAS03 exhibits these beneficial effects. However, it did not protect against other parameters such as shortening colon lengths, increased permeability, and increased inflammatory mediators. We acknowledge the inherent problems of AhR$^{-/-}$ mice. AhR$^{-/-}$ mice inherently suffer from variety of organ disorders including a decline in the efficacy of their immune system and high sensitivity to inflammatory stimuli[52]. Previously, it was demonstrated that activation of AhR protects against colitis[41,53] and AhR$^{-/-}$ mice develop severe colitis compared to wild type mice and display increased inflammatory mediators[54]. Similarly, our studies also showed that increased susceptibility to TNBS-induced colitis in AhR$^{-/-}$ mice compared to wild type. AhR$^{-/-}$ mice exhibited rapid body weight loss leading to termination of the experiment at 60 h. Generally, the endogenous ligands of AhR regulate multiple functions in the body via AhR and maintains the homeostasis in wild type mice. In AhR$^{-/-}$ mice, the endogenous ligands cannot act as bioregulatory molecules due to lack of AhR potentially leading to severe colitis phenotype compared to wild type mice. It is therefore possible that failure of UroA/UAS03 mediated protective activities against colitis in AhR$^{-/-}$ mice may not provide conclusive evidence for AhR role. Further studies are warranted using Villin Cre AhR floxed mice, to tease out involvement of AhR in UroA/UAS03 mediated protective activities in colitis models. Despite plethora effects in AhR$^{-/-}$ mice, studies involving colon epithelial cells, siRNA knockdown, AhR$^{-/-}$ colon explant studies as well as BMDM studies reinforces the involvement of AhR pathways in mediating UroA/UAS03 barrier and anti-inflammatory activities. Recent study from Dr. Brigitta Stockinger's group[55] also suggests AhR protects from inflammatory damage by maintaining intestinal stem cell homeostasis and barrier integrity supporting our observations that activation of AhR enhances the barrier integrity. In this paper, they demonstrated that AhR promotes barrier function through direct activity on intestinal epithelial cells (IEC) by using mice that lack AhR in IEC (Villin^{Cre}Ahr$^{fl/fl}$). These mice exhibit decreased expression of Muc2 and increased levels of IL-6 suggesting that AhR role in barrier integrity and inflammation[55].

The current studies highlight the critical requirement for AhR-Nrf2 in protecting from barrier dysfunction. It is possible that UroA/UAS03 are exerting colitis protective activities by two pronged mechanisms of action. These compounds directly act on immune cells (e.g., macrophages) to prevent LPS/bacterial induced inflammation as well as exhibit anti-oxidative activities through AhR-Nrf2 pathways. Most importantly, these metabolites have direct impact on gut epithelium and gut barrier function by upregulating tight junction proteins. Enhanced barrier function reduces the bacterial leakage in the gut leading to significant reduction in systemic inflammation. To delineate the effects on immune cells versus epithelial cells, further in depth studies involving cell specific deletion of AhR and Nrf2 in transgenic mice using Cre/lox methodologies are required. RNA-Seq pathway analysis as well as studies by Ryu et al.[22] suggest that UroA plays an important role in regulating mitochondria functions through inducing mitophagy. Several evidences suggest that mitochondrial dysfunction is a major contributor in the

pathophysiology of IBD[56]. It was shown that isolated enterocytes from IBD patients have swollen mitochondria with irregular cristae[57]. The intestinal epithelial cells isolated from experimental colitis mice models also exhibited abnormal mitochondrial structures[58]. Therefore, we speculate that in addition to anti-inflammatory and barrier protective activities, UroA/UAS03 may potentially reduce IBD through regulating mitochondrial dysfunction.

Evolutionarily, human-microbiota developed indigenous mechanisms to protect from external challenges. It is possible that excess use of antibiotics and modern dietary trends led to microbial dysbiosis resulting in the elimination of some bacterial populations that are capable of producing beneficial metabolites. More rigorous and systematic studies are required to assess the beneficial advantages of direct consumption of metabolites in humans both in healthy and disease conditions, whether supplementation of metabolites could overcome the dysbiosis. The current study summarizes one such metabolite, UroA and its analogue, UAS03 with activities in mitigating IBDs by enhancing gut barrier function and reducing inflammation. Existing IBD treatments include utilizing anti-TNF-α antibodies to reduce inflammation; here we suggest that enhancing gut barrier functions in addition to inhibiting inflammation might provide better therapeutic options for control of IBDs. Overall, UroA/UAS03 will not only be efficacious in IBD-related diseases but may also have significant translational implications in other disorders involving barrier dysfunction and inflammation such as alcohol liver diseases, neurological disorders, and colon cancers.

Methods

Materials. General laboratory chemicals and reagent solutions were purchased from Sigma-Aldrich (St. Louis, MO). ELISA kits for IL-6 and TNF-α were purchased from Bio-legend. ELISA kit for CXCL1 was purchased from R&D systems. All antibodies were purchased from Santacruz unless otherwise specified. LPS was purchased from Sigma Aldrich. Colitis grade DSS (36,000–50,000 M.W) was purchased from MP Bio. UroA was custom synthesized as previously described[23].

Mice. C57BL/6 mice were either bred in our animal facility or purchased from Jackson Laboratories. Breeding pairs of Nrf2$^{-/-}$ mice (B6.129x1-Nfe2/2^{tm1Ywk}/J, stock # 0170009) were purchased from Jackson Laboratories and bred at U of L animal facility to generate experimental animals. AhR$^{-/-}$ mice (Model# 9166) were purchased from Taconic Laboratories. We utilized the mice at the ages of between 7–9 weeks age old for colitis experiments. Mice were kept in specific pathogen-free (SPF) barrier conditions with temperature-controlled room with alternate 12 h cycles of dark and light. Animals were allowed free excess to feed and water ad libitum. All studies were performed under approved protocols from Institutional Animal Care and Use Committee (IACUC), University of Louisville, Louisville, KY, USA. Source Data for all the bar graphs are provided as a Source Data File.

Synthetic procedure for synthesis of UAS03. Chemically UroA (3,8-dihydroxy-6H-dibenzo[b,d]pyran-6-one) structure has a bridge ester, lactone, and two hydroxyl on two phenyl rings. UroA has a lactone (cyclic ester) bond that connects two phenyl rings and leads to the planar structure. Gastric pH or digestive enzymes can hydrolyze the lactone bond leading to opening of the ring. This will result in losing the planar structure, becomes propeller structure, and potentially loses its activities. To generate more stable and potent compounds, we have synthesized non-hydrolyzable cyclic ether derivative, UAS03 by the following procedure (Supplementary Fig. 21).

Sodium borohydride (0.165 g, 4.38 mmol) was added to dry THF (10 ml), and the mixture was cooled 10 °C before borontrifluoride etherate (0.80 g, 5.7 mmol) was added drop wise over a period of 1 h. Then 3,8-dihydroxy-6H-benzo[c] chromen-6-one (Uro-A) (0.5 g, 2.19 mmol) in THF (5 ml) was added over a period of 10 min. The mixture was allowed to stir for 5 h at 50 °C. The completion of reaction was monitored by thin layer chromatography (TLC). The reaction was quenched with methanol. 3 N aqueous HCl solution (10 ml) was added, and the mixture was gently heated to 50 °C for 30 min. The reaction mixture was adjusted to neutral with 10% NaOH solution, and the volatiles were evaporated under reduced pressure. The crude product was purified by column chromatography using 50% ethylacetae in Hexane with 60–120 mesh silica gel to get pure 6H-benzo [c]chromene-3,8-diol product.

MS (M+1) = 215.2. ^{1}H-NMR (DMSO-d$_6$): δ: 9.49 (2H, s), 7.51–7.50 (1H, d, J = 6.6 Hz), 7.48–7.47 (1H, d, J = 6.6 Hz), 6.75–6.73 (1H, m), 6.61 (1H, s), 6.48–6.46

(1H, m), 6.32 (1H, s), 4.96 (2H, s). ^{13}C-NMR (DMSO-d$_6$): δ: 158.10, 156.71, 154.93, 131.88, 123.86, 122.79, 121.66, 115.72, 114.89, 111.84, 110.07,103.95, 68.18.

Cell cultures. Human colon epithelil carcinoma cell lines, HT29 (ATCC # HTB-38^{TM}) and Caco2 cells (ATCC # HTB-37^{TM}) were maintained in DMEM-high glucose and EMEM-high glucose (Cornings; 10-009CV) respectively, supplemented with 10% fetal bovine serum, 1X penicillin-streptomycin solution (100 U/ml penicillin, and 100 μg/ml streptomycin; Sigma Aldrich) in a humidified atmosphere (5% CO_2, 95% air, 37 °C). Mouse bone marrow derived macrophages (BMDMs) were isolated and cultured using the following procedure[59]. Briefly, mice were killed by CO_2 anesthesia, rinsed in 70% ethanol and bone marrow was isolated from tibias and femurs. Bone marrow cells were plated (2×10^6 cell/ml) in DMEM-high glucose (HyClone) supplemented with 10% FBS, 1% glutamine, 1X penicillin-streptomycin solution and 50 ng/mL mouse M-CSF (R&D Systems Inc., Minneapolis, MN) for 7 days for differentiation.

Measurements of IL-6 and TNF-α levels in BMDM. BMDM were plated in 96 (10,000 cells/well) and 12 wells (0.1×10^6 cells/well) plate for ELISA and RNA isolation. To evaluate the anti-inflammatory properties, BMDMs were stimulated with *E. coli*-derived lipopolysaccharides (LPS; O55:B5; Sigma) at 50 ng/mL concentration for six hours alone or in combination with UroA or UAS03 at indicated concentrations (0.01, 0.1, 1, 10, 25, and 50 μM) in quadruplicates. For cytokine production via ELISA, the supernatant was collected and centrifuged at $10,000 \times g$ for 10 min at 4 °C to pellet down any cell and cytokines were quantified using IL-6 and TNF-α specific ELISA kit (Biolegend) following manufacturer's instruction.

LPS-induced peritonitis. Male mice (C57BL/6J; 6–8 weeks old) were randomly divided in 3 groups *viz.* vehicle (0.25% sodium carboxymethylcellulose (CMC)), UroA and UAS03. UroA and UAS03 groups received oral gavage of respective compounds (20 mg/kg in 100 μl of volume) at 0, 6, 12, 18, and 24 h. Vehicle group received same volume of CMC at same time. After 24 h, mice were injected intraperitoneally with LPS (2 mg/kg; Sigma-Aldrich). Post 4 h LPS challenge, mice were killed and blood was collected. The serum was prepared using BD Microtainer separator tubes. The serum samples were analyzed for IL-6 and TNF-α using respective ELISA assay kit (Biolegend).

Real-time PCR. Total RNA was isolated from cells/tissue using Maxwell® 16 LEV simplyRNA tissue kit (Promega) and reverse transcribed with TaqMan™ Reverse transcription Kit (Applied Biosystems, CA, USA). The transcribed cDNA (after dilution) was mixed with 100 nM gene specific primers (Real time primers LLC) and 1X SYBR green reaction mix (Power SYBR® Green PCR Master Mix; Applied Biosystems, CA, USA). Changes in gene expression was analyzed using CFX96^{TM} Real-Time System (Bio Rad) and fold change in expression was calculated using $2^{-\Delta\Delta CT}$ method using GAPDH/β-actin as house keeping gene and normalized with untreated control.

In vitro permeability study. For in vitro cellular permeability studies, Caco2 cells or HT29 cells (2×10^4 cells/cm^2) were seeded in 24-well Transwell® plates (Cornings; USA), on polyester membrane filters (pore size 0.4 μm, surface area 1.12 cm^2)[60]. Culture medium was added to both apical and basal chamber and the medium was changed every other day up to 21 days for Caco2 cells or 5–7 days for HT29 cells. For Caco2 cells, transepethelial electrical resistance (TEER) was calculated using EMD Millipore Millicell-ERS2 Volt-Ohm Meter (Millipore). Filters (with cell monolayer) showing more than 600 Ω.cm^2 were used for permeability study. After cells reach desired confluence (monolayered cells), cells were pre-treated with vehicle (0.01% DMSO) UroA (50 μM) and UAS03 (50 μM) for 24 h. After treatment, monolayer was washed with PBS to remove any residual drug and 200 μL of LPS (50 ng/ml in HBSS) was added to each well and incubated for 2 h. After LPS treatment, the monolayer was washed with PBS twice and 200 μL of FITC-Dextran (FD-4; Sigma Aldrich, USA) solution (1 mg/mL in HBSS) was added. After 2 h, a sample from the basal chamber was withdrawn and FD4 concentration was determined using fluorescence 96-wells plate reader at excitation and emission wavelengths were 480 and 525 nm, respectively.

RNA sequencing. Total RNA was isolated from HT29 cells treated with vehicle and UroA (50 μM) ($n = 3$) for 24 h and RNA was isolated using Trizol based lysis followed by Qiagen RNeasy kits. The isolated RNA was checked for integrity (RIN>9.5) using the Agilent Bioanalyzer 2100 system (Agilent Technologies, Santa Clara, CA) and quantified using a Qubit fluorometric assay (Thermo Fisher Scientific, Waltham, MA). Poly-A enriched mRNASeq libraries were prepared following Illumina's TruSeq Stranded mRNA LT library preparation protocol (Illumina Inc., San Diego, CA) using 1 μg of total RNA. All 15 samples were individually barcoded and quantitated with the KAPA Library Quantitation Kit for Illumina Platforms (Kapa Biosystems, Wilmington, MA) in conjunction with an Agilent Bioanalyzer DNA 1000 analysis (Agilent Technologies, Santa Clara, CA) for fragment size determination. The average fragment size was approximately 300 bp. 1.8 pM of the pooled libraries with 1% PhiX spike-in was loaded on one NextSeq 500/550 75 cycle High Output Kit v2 sequencing flow cell and sequenced

on the Illumina NextSeq 500 sequencer. The quality of the 1×75 bp sequences was checked using FASTQC (version 0.10.1)[61]. Trimming was not necessary with the median quality score above 30 (error probability = 0.001 or 1 base call in 1000 is predicted to be incorrect) across the entire length of the read and the lower quantile above a score of 20 (error probability = 0.01) at the end of the read where there is an expected decrease in quality. The raw reads for each sample were directly aligned to the *Homo sapiens* (hg38) reference genome assembly (hg38.fa) using tophat2 (version 2.0.13)[62], generating alignment files in bam format. Optional parameters include –no-coverage-search and –library-type fr-firststrand. The human ENSEMBL[63] transcriptome gtf v82 was used for transcript identification, resulting in 60,903 total genes. Supplementary Table 1 indicates the number of raw reads successfully aligned for each of the samples. On average, 26 million reads were aligned per sample with a mean alignment rate of 97%. Following sequence mapping, differentially expressed genes were determined using tuxedo suite of programs including cuffdiff2 (version 2.2.1)[64,65] with the optional parameter –library-type fr-firststrand. The RNA-seq data was deposited in gene data base (GEO # GSE113581).

Immunoblots (western blots). The total protein lysates were collected either from colon tissue/cells using radioimmunoprecipitation assay (RIPA) buffer (Sigma-Aldrich, USA) and quantified using BCA protein quantification kit (Thermo Scientific) as per instructional manual. Total protein (20–50 μg) of was resolved on NuPAGE^{TM} 4–12% Bis-Tris gel (Novex Life technologies) and transferred to polyvinylidene difluoride membrane (0.22 μm pore; Millipore, USA). After blocking with 5% (w/v) skim milk powder (containing 1X TBS) for 1 h, the membrane was then incubated with respective antibodies at 4 °C overnight (dilutions of respective antibodies is given in Table 1). Next day, respective secondary antibody conjugated with Horseradish peroxidase were probed and the chemiluminescent substrate was used to detect the protein bands (ImageQuant LAS 4000). Densitometry analysis of bands were done using ImageJ software. Anti-bodies for Cldn4, Ocln, Cldn1, Cyp1A1, AhR, HO1, NQO1, Keap1, β-actin, and Lamin B were purchased from Santa Cruz Biotechnologies (USA) and Nrf2 from Novus Biologicals (USA). Source and list of antibodies are provided in Table 1. The uncropped images of important immunoblots are shown in Supplementary Fig. 22.

Confocal imaging. HT29 or CaCo2 or BMDM cells (50,000 cells/well) were plated on to 8-well chambered slides (154534PK; ThermoFisher Scientific) allowed them to grow overnight. The cells were induced with vehicle (0.01% DMSO) or UroA (50 μM) or UAS03 (50 μM) for desired time points and fixed with cold methonol. The AhR or Nrf2 or Cldn4 stained with respective anti-bodies (1:200 dilution) followed by fluorecently labeled (Alexa flour 594 for AhR and Alexa flour 488 for Nrf2 and Cldn4) secondary ab (1:500 dilution; ThermoFisher Scientific). The nucleus was stained with DAPI (Sigma Aldrich). The confocal images were captured using Nikon A1R confocal microscope using ×60 magnification lense with appropriate laser channels.

AhR-reporter assay. AhR-reported assay was performed using AhR Reporter Assay system (Indigo Biosciences). The AhR Reporter cells (expressing luciferase under AhR promoter) as well as positive control MeBio (AhR ligand) compound were provided in the kit. The cells were treated with Vehicle or UroA or UAS03 or ellagic acid or MeBio for 6 h and luminoscence was measured according to manufacture's instructions.

Nrf2-reporter assay. ARE-luciferase plasmid vector was obtained from Cayman Chemicals. HT29 cells were transfected at 50% confluency using lipofectamine 3000 reagent (ThermoFisher Scientific). Briefly, cells were seeded in 6-well plates (0.5×10^6 cells) and grown for 24 h. The transfection complex containing 1 μg of plasmid DNA and transfection reagent was added to each well in absence of FBS. After 6 h medium containing 10% FBS was added and cells were incubated for another 16–18 h. These cells were treated with vehicle (0.01% DMSO) or UroA (50 μM) or UAS03 (50 μM) or sulforaphane (10 μM) for 24 h. After incubation with inducers, cells were lysed and firefly luciferase activities (luminescence) were measured with Luciferase Assay System (Promega) using mutiwell plate luminometer (BMG, LABTECH).

Measurements of Cyp1A1 enzyme activty (ex vivo). Mice were treated with Vehicle or UroA or UAS03, BNF, or FICZ daily for 1 week at indicated concentration either through oral or i.p. route. After 1 week, mice were euthanized and the colon and liver tissues were dissected. Microsomes from these tissues were prepared using the following procedure[66]. For hepatic microsomes, liver was first perfused with 0.9% sodium chloride solution and excised out. Adhering blood and saline was removed by blotting on tissue paper and tissue was homogenized in tissue homogenization buffer (50 mM Tris-HCl, pH 7.4 with 250 mM sucrose). Homogenate was centrifuged at $10,000 \times g$ for 30 min at 4 °C. supernatant obtained was further centrifuged at $105,000 \times g$ for 60 min at 4 °C. The pellet was washed with homogenization buffer and centrifuged again at $105,000 \times g$ for 60 min at 4 °C. The pellet was suspended in homogenization buffer and used for protein and CYP assay. For intestinal microsome preparation, intestine was removed and washed with 0.9% sodium chloride. The intestine was longitudinally cut open to expose

Table 1 List of antibodies used for western blots

Sr no	Antibody	Source	Dilution
1	Nrf2 (NBP1-32822)	Novus Biologicals	1:1000
2	HO-1 (sc-10789)	Santa Cruz Biotechnology	1:500
3	Cldn4 (sc-376643)	Santa Cruz Biotechnology	1:1000
4	ZO-1 (5406)	Cell Signaling Technology	1:2000
5	Ocln (sc-133256)	Santa Cruz Biotechnology	1:1000
6	NQO1 (sc32793)	Santa Cruz Biotechnology	1:1000
7	β-actin (Sc-47778 HRP)	Santa Cruz Biotechnology	1:5000
8	Lamin B (sc-6216)	Santa Cruz Biotechnology	1:100
9	AhR (sc-133088)	Santa Cruz Biotechnology	1:1000
10	Cyp1A1 (H00001543-D01P)	Novus Biologicals	1:100

mucosal layer and mucosa was scrapped with help of glass slide. The scraped tissue was collected in homogenization buffer (50 mM Tris-HCl buffer containing glycerol (20% v/v), protease inhibitor (1%) and heparin (3 U/ml)). This suspended mucosa was homogenized and centrifuged at $10,000 \times g$ for 20 min at 4 °C. Supernatant obtained was further centrifuged at $105,000 \times g$ for 60 min at 4 °C. The pellet was washed with buffer and centrifuged again at $105,000 \times g$ for 60 min at 4 °C. The pellet was suspended homogenization buffer and used for protein and CYP enzymes assays.

Ethoxyresorufin-O-deethylase (EROD) assay. The microsomal proteins (0.5 mg) were mixed with 200 μL Tris buffer (0.1 M, pH 7.4) containing ethoxyresorufin (0.01 mM). To start reaction, NADPH (0.1 mM) was added and incubated at 37 °C for 10 min. After 10 min, reaction was terminated by adding equal volume of acetonitrile and reaction mixture was centrifuged at $13,000 \times g$ for 10 min at 4 °C. Supernatant was used to determine resorufin by measuring fluorescence (Ex. 530 nm, Em. 580 nm). Pure resorufin (Sigma Aldrich) was used to generate standard curve.

P450-Glo Cyp1A1 luminescence assay. The above microsomes (20 μg) were used for P450-Glo Cyp1A1 luminescence assays as per manufacturer's instructions.

Measurement of Cyp1A1 enzyme activities in vitro. EROD assay: HT-29 cells (15,000 cells/well) treated with vehicle, UroA and UAS03 (24 h), were rinsed with HBSS buffer, and then fresh HBSS buffer was added along with 5 μM of 7-ethoxyresorufin. Cells were further incubated at 37 °C for 1 h. After the incubation time, fluorescence (Exc. 530 nm, Em. 580 nm) was measured and product (resorufin) formed was calculated from calibration standard and normalized with protein concentration.

P450-Glo Cyp1A1 luminescence assay: HT29 cells (25,000 cells/well) were plated in 48 well plate. Cell were then treated with UroA (0.1, 1, 10, 25, and 50 μM) or UAS03 (0.1, 1, 10, 25, and 50 μM) or FICZ (0.1, 1, 10, 25, and 50 nM) for 24 h. After treatment, cells were washed to remove any residual drugs, and fresh medium containing Cyp1A1 substrate (as per protocol provided with kit Cat.# V8751; Promega) for 3 h. After incubation, 25 μl of culture medium was removed from each well and transferred to a 96-well white opaque plate and 25 μl of luciferin detection reagent was added to initiate the luminescence reaction and plate was incubated at room temperature for 20 min. After incubation, luminescence was recorded in luminometer. The data reported as fold change over vehicle treatment.

Small interfering RNA (siRNA) mediated knockdown experiment. The AhR siRNA (SR300136) and Cyp1A1 siRNA (SR301093) was purchased from Origene. For knockdown experiments, HT29 cells (0.5×10^6 cells/well) were plated in 6 well plate and grown for 24 h. The AhR, Cyp1A1 and control-siRNA was transfected into HT29 cells using Lipofectamine ® RNAiMAX reagent (ThermoFisher Scientific) as per intruction given. After 24 h of transfections, cell were induced with vehicle (0.01% DMSO), UroA (50 μM), and UAS03 (50 μM) for 24 h. After treatment with inducers, cells were lysed using RIPA buffer and total protein was used to analyse the expression of AhR, Cyp1A1 and Cldn4 by western blot.

Cyp1A1 deletion by CRISPR/Cas9 method. HT29 cells (1.5×10^5) were plated in 6-well in antibiotic free standard growth medium 24 h prior to transfection. At 60% confluency cells, cells were co-transfected with 2 μg each of CRISPR/Cas9 KO Plasmid (sc-400511-KO-2; Santa cruz) and HDR Plasmid (sc-400511-HDR-2; Santa cruz) using UltraCruz® Transfection Reagent (sc-395739; Santa Cruz). Medium was replaced with selective medium (containing 4 μg/mL puromycin) 96 h post transfection. Transfection was confirmed with fluorescence microscopy and western blot (CYP1A1). The double postive cells for GFP and RFP were sorted using MoFlo XDP sorting instrument (Beckman Coulter). The deletion of Cyp1A1 in these sorted was confirmed by western blots. These cells were then plated in 6-well plate for in standard medium for evaluating the effect of UroA/UAS03 on

Cldn4 expression. After 24 h of UroA/UAS03 treatment cells were harvested for protein and Cldn4 expression was investigated along with normal HT29 cells.

NF-κB EMSA assay. RAW 264.7 cells or BMDM were plated in 100 mm dishes (1×10^6) in DMEM supplemented with 10% fetal bovine serum (FBS), 100 U/ml penicillin, and 100 U/ml streptomycin. Cells were allowed to grow for 24 h and after incubation, cells were treated with LPS (50 ng/mL) with and without UroA (50 μM) and UAS03 (50 μM) for 6 h. After treatments, culture medium was removed and washed with PBS. Cells were scraped and pelleted down in PBS. Supernatant was discarded and pellet was used for isolation of nuclear and cytosolic protein using NE-PER Nuclear and Cytoplasmic kit (Thermo Scientific; Cat #78833). Later nuclear protein (2 μg) was used for EMSA using Non-Radioactive EMSA Kits with IR Fluo-Probes for Nuclear factor kappa B p65 (Viagene Biotech Inc Cat # IRTF282 60).

Colon explant culture. Colon tissue pieces (0.5–1 cm length) from wild type (C57BL/6) or Nrf2$^{-/-}$ or AhR$^{-/-}$ mice were cultured in triplicates for 24 h in complete DMEM-high glucose medium (supplemented with 10% fetal bovine serum, 1X penicillin-streptomycin solution) in a humidified atmosphere in the presence of vehicle (0.01% DMSO), UroA (50 μM) or UAS03 (50 μM). The tissues were processed for protein preparation (tissue lysates with RIPA plus buffer) or total RNA isolation. These tissue lysates or RNA were used to determine the expression of Nrf2, Cldn4 and AhR.

Tissue processing for RNA and protein analysis. Mice were treated with as described in results section. Mice were euthanized with CO_2 asphyxiation followed by cervical dislocation. Colon was dissected out and luminal contents were flushed out with cold PBS (containing PMSF and Sodium orthvandate). Small portion of colon was snap frozen in liquid nitrogen and stored at −80 °C for RNA analysis. For preparation of protein samples, colon was opened longitudinally and mucosa was scraped in ice-cold 1X PBS using pre-chilled glass slide and centrifuged at $300 \times g$ for 10 min at 4 °C. Supernatant was discarded and pellet was suspended in RIPA buffer (containing 1X protease inhibitor) and vortexed at high speed. After 30 min incubation on ice, samples were centrifuged at $13,000 \times g$ for 20 min at 4 °C. Supernatant was collected and protein was quantified using BCA protein quantification kit. The lysates were used appropriately for western blots.

28-day repeated dose toxicity study. To evaluate toxicity of UroA and UAS03, we performed 28-days repeated dose toxicity study. Mice were fed (oral gavage) with UroA (20 and 40 mg/kg/day) and UAS03 (20 and 40 mg/kg/day) daily for 28 days. Body weight, food, and water intake were assessed weekly. After 28 days, mice were killed and gross examination of all major organs were performed. Blood was collected to obtain serum. Serum alanine aminotransferase (ALT) and asparate aminotransferase (AST) were analyzed using ALT/ AST kit (BioVision) as per instructional manual.

2,4,6-Trinitrobenzenesulfonic acid (TNBS)-induced colitis. Male C57BL/6 or Nrf2$^{-/-}$ mice (6–8 week old age mice) were anesthetized with ketamine/xylazine (100 mg/12.5 mg/kg IP) mixture and administered with single dose of TNBS (2.5 mg/mice; Sigma Aldrich, USA) in 50% ethanol. After administration of TNBS, mice were held upside down for 30–60 s to ensure proper distribution of TNBS in the colon. Control group received 50% ethanol without TNBS. Mice with TNBS were randomly divided into three groups, viz. vehicle (0.25% sodium carboxymethylcellulose (CMC), UroA and UAS03. UroA or UAS03 was resuspended in 0.25% sodium-CMC at desired concentrations. The mice were given orally Veh or UroA or UAS03 in 100 μl at desired concentrations (4 or 20 mg/kg/body weight). The treatment started after 12 h of TNBS administration and every 12 h thereafter up to 72 h. The experiment was terminated post 60 h TNBS, where AhR$^{-/-}$ mice were involved. In some experiments, we treated only once at post 12 h TNBS administration. TNBS administered and control mice were euthanized for tissue

and plasma collection after 80 h of TNBS/ethanol treatment. Mice were examined for colitis phenotype.

DSS-induced colitis. Acute experimental colitis in mice was induced by giving 3% (w/v) colitis grade DSS (MP Biomedicals) in drinking water for 7 days. Control animal received drinking water without DSS. All colitis group mice were randomly divided into three groups viz. vehicle treated (0.25% Na-CMC), UroA (20 mg/kg/day) and UAS03 (20 mg/kg/day) on the 4th and 6th day of DSS treatment. After 7 days, animals were put back on regular water for a period of 7 days. For chronic DSS colitis model, we used three cycles of 2.0% (w/v) DSS and each DSS cycle consisted or 7 days followed by 10 days of regular water and mice were treated with UroA (20 mg/kg/day) on every 4th and 6th day of DSS cycle.

Assessment of colitis severity and tissue collection. Mice were evaluated daily for change in body weight, stool consistency, and rectal bleeding and score was given and combined to obtained disease activity index[67]. After euthanasia, the colon was removed and flushed with PBS containing (1 mM PMSF and 0.2 mM sodium orthovanadate). Colon length and colon weight were measured and small parts of colon were excised for myeloperoxidase (MPO) activity and RNA isolation. Tissues for MPO and RNA extraction were snap frozen in liquid nitrogen and stored in −80 °C until further analysis. Tissue for histological examination was stored in 10% phosphate buffered saline formalin. Blood was collected and serum was separated by centrifugation at $3500 \times g$ for 15 min. Serum cytokines (IL-6, TNF-α; Biolegend) and chemokines (CXCL1; R&D Systems) levels were measured by ELISA according to manufacturer's instructions.

In vivo intestinal permeability assay. The gut barrier function was evaluated by in vivo intestinal permeability using FITC-Dextran (MW 4000; FD4, Sigma-Aldrich, USA)[68]. Briefly, mice were orally administered with FITC-dextran (60 mg/100 gm body weight). Mice were fasted for 4 h prior to euthanization. The FITC-dextran concentration in serum was determined using the standard curve of FITC-dextran in serum (excitation, 485 nm; emission, 525 nm; BMG LABTECH).

Myeloperoxidase (MPO) activity. The MPO activity in the colons was determined using the following procedure[69]. Briefly, colon tissue was homogenized in 0.5% (w/v) hexadecyltrimethylammonium bromide (H6269; Sigma-aldrich, USA) in 50 mM PBS, pH 6.0. This homogenate underwent 3 freeze-thaw cycles and 10–15 s sonication to obtain homogenous suspension. The supernatant from this suspension was collected after centrifugation at $13000 \times g$ for 20 min at 4 °C. The supernatant (10 μl) was then added to 50 mM potassium phosphate buffer (pH 6.0) containing 0.167 mg/ml o-dianisidine (Sigma-Aldrich, USA) and 0.0005% H_2O_2 (Sigma-Aldrich USA) and absorbance was taken at 450 nm (BMG, LABTECH) at 2 min interval. Units of MPO in each sample was determined by considering that one unit (U) of MPO = 1 μmol of H_2O_2 split with molar extinction coefficient of 1.13×10^{-2} nm/min and MPO in each sample calculated by using $[\Delta A(t_2 − t_1)]/\Delta min \times (1.13 \times 10^{-2})$ formula and MPO units were normalized with per mg tissue.

Histopathology. Collected colon tissue were fixed in 10% buffered formaldehyde solution overnight and fixed tissue underwent standard histopathological processing. Briefly, after fixation tissue underwent dehydration and cleaning with xylene before paraffin embedding. The paraffin section of 5 μm were cut (Leica microtome) and stained for H&E staining. The H&E images were captured using Aperio Scanscope. H&E sections were scored blindly using index scoring described by Erben et al.[70].

Data availability

The RNA-seq data described in this MS is deposited with GEO # GSE113581. The hyperlink for RNA seq as follows: https://urldefense.proofpoint.com/v2/url?u=https-3A__www.ncbi.nlm.nih.gov_geo_query_acc.cgi-3Facc-3DGSE113581&d=DwIBAg&c=OAG1LQNACBDguGVBeNj18Swhr9TMTjS-x4O_KuapPgY&r=gYAe1Rux-xOAaWAT6YX2N_noYeYJBx7FLRBVFljZPt0&m=aQROwFtABYMDtrIp4k7mNRkL77nfCBUH4EqXd2nQLK0&s=RH4q-x-nZSE8JU035mWKJs4mmznYY-E3Nvx9CkS_QKs&e=. The full raw data that support the findings of this study are available from the corresponding author upon reasonable request. The Source Data underlying all the bar graphs in the Figures are provided in the Source Data File.

References

1. Lynch, S. V. & Pedersen, O. The human intestinal microbiome in health and disease. N. Engl. J. Med. **375**, 2369–2379 (2016).
2. Levy, M., Kolodziejczyk, A. A., Thaiss, C. A. & Elinav, E. Dysbiosis and the immune system. Nat. Rev. Immunol. **17**, 219–232 (2017).
3. Sonnenburg, J. L. & Backhed, F. Diet-microbiota interactions as moderators of human metabolism. Nature **535**, 56–64 (2016).
4. Belkaid, Y. & Hand, T. W. Role of the microbiota in immunity and inflammation. Cell **157**, 121–141 (2014).
5. Dzutsev, A. et al. Microbes and cancer. Annu. Rev. Immunol. **35**, 199–228 (2017).
6. Tamboli, C. P., Neut, C., Desreumaux, P. & Colombel, J. F. Dysbiosis in inflammatory bowel disease. Gut **53**, 1–4 (2004).
7. Gopalakrishnan, V., Helmink, B. A., Spencer, C. N., Reuben, A. & Wargo, J. A. The Influence of the gut microbiome on cancer, immunity, and cancer immunotherapy. Cancer Cell **33**, 570–580 (2018).
8. Landy, J. et al. Tight junctions in inflammatory bowel diseases and inflammatory bowel disease associated colorectal cancer. World J. Gastroenterol. **22**, 3117–3126 (2016).
9. Schulzke, J. D. et al. Epithelial tight junctions in intestinal inflammation. Ann. N. Y. Acad. Sci. **1165**, 294–300 (2009).
10. Vindigni, S. M., Zisman, T. L., Suskind, D. L. & Damman, C. J. The intestinal microbiome, barrier function, and immune system in inflammatory bowel disease: a tripartite pathophysiological circuit with implications for new therapeutic directions. Ther. Adv. Gastroenterol. **9**, 606–625 (2016).
11. Heber, D. Multitargeted therapy of cancer by ellagitannins. Cancer Lett. **269**, 262–268 (2008).
12. Sak, K. Cytotoxicity of dietary flavonoids on different human cancer types. Pharmacogn. Rev. **8**, 122–146 (2014).
13. Habauzit, V. & Morand, C. Evidence for a protective effect of polyphenols-containing foods on cardiovascular health: an update for clinicians. Ther. Adv. Chronic Dis. **3**, 87–106 (2012).
14. Gbinigie, O. A., Onakpoya, I. J. & Spencer, E. A. Evidence for the effectiveness of pomegranate supplementation for blood pressure management is weak: a systematic review of randomized clinical trials. Nutr. Res. **46**, 38–48 (2017).
15. Stockton, A., Farhat, G., McDougall, G. J. & Al-Dujaili, E. A. S. Effect of pomegranate extract on blood pressure and anthropometry in adults: a double-blind placebo-controlled randomised clinical trial. J. Nutr. Sci. **6**, e39 (2017).
16. Razani, Z., Dastani, M. & Kazerani, H. R. Cardioprotective effects of pomegranate (Punica granatum) juice in patients with ischemic heart disease. Phytother. Res. **31**, 1731–1738 (2017).
17. Derosa, G. & Maffioli, P., . & Sahebkar, A. Ellagic acid and its role in chronic diseases. Adv. Exp. Med. Biol. **928**, 473–479 (2016).
18. Cerda, B., Periago, P., Espin, J. C. & Tomas-Barberan, F. A. Identification of urolithin a as a metabolite produced by human colon microflora from ellagic acid and related compounds. J. Agric. Food Chem. **53**, 5571–5576 (2005).
19. Selma, M. V., Beltran, D., Garcia-Villalba, R., Espin, J. C. & Tomas-Barberan, F. A. Description of urolithin production capacity from ellagic acid of two human intestinal Gordonibacter species. Food Funct. **5**, 1779–1784 (2014).
20. Espin, J. C., Larrosa, M., Garcia-Conesa, M. T. & Tomas-Barberan, F. Biological significance of urolithins, the gut microbial ellagic acid-derived metabolites: the evidence so far. Evid.-Based Complement. Alternat. Med. **2013**, 270418 (2013).
21. Tomas-Barberan, F. A. et al. Urolithins, the rescue of 'old' metabolites to understand a 'new' concept: metabotypes as a nexus between phenolic metabolism, microbiota dysbiosis and host health status. Mol. Nutr. Food Res. **61**, 1–35 (2016).
22. Ryu, D. et al. Urolithin A induces mitophagy and prolongs lifespan in C. elegans and increases muscle function in rodents. Nat. Med. **22**, 879–888 (2016).
23. Saha, P. et al. Gut Microbiota conversion of dietary ellagic acid into bioactive phytoceutical urolithin a inhibits heme peroxidases. PLoS One **11**, e0156811 (2016).
24. Tsukita, S. & Furuse, M. Claudin-based barrier in simple and stratified cellular sheets. Curr. Opin. Cell Biol. **14**, 531–536 (2002).
25. Loboda, A., Damulewicz, M., Pyza, E., Jozkowicz, A. & Dulak, J. Role of Nrf2/HO-1 system in development, oxidative stress response and diseases: an evolutionarily conserved mechanism. Cell. Mol. Life Sci. **73**, 3221–3247 (2016).
26. Beischlag, T. V., Luis Morales, J., Hollingshead, B. D. & Perdew, G. H. The aryl hydrocarbon receptor complex and the control of gene expression. Crit. Rev. Eukaryot. Gene Expr. **18**, 207–250 (2008).
27. Yeager, R. L., Reisman, S. A., Aleksunes, L. M. & Klaassen, C. D. Introducing the "TCDD-inducible AhR-Nrf2 gene battery". Toxicol. Sci. **111**, 238–246 (2009).
28. Miao, W., Hu, L., Scrivens, P. J. & Batist, G. Transcriptional regulation of NF-E2 p45-related factor (NRF2) expression by the aryl hydrocarbon receptor-xenobiotic response element signaling pathway: direct cross-talk between

phase I and II drug-metabolizing enzymes. *J. Biol. Chem.* **280**, 20340–20348 (2005).

29. Antoniou, E. et al. The TNBS-induced colitis animal model: an overview. *Ann. Med. Surg.* **11**, 9–15 (2016).

30. Smith, P. D. et al. Intestinal macrophages and response to microbial encroachment. *Mucosal Immunol.* **4**, 31–42 (2011).

31. Bain, C. C. & Mowat, A. M. Macrophages in intestinal homeostasis and inflammation. *Immunol. Rev.* **260**, 102–117 (2014).

32. Gaya, P., Peiroténa, A., Medinaa, M., Álvarezb, I. & Landete, J. M. Bifidobacterium pseudocatenulatum INIA P815: The first bacterium abl e to produce urolithins A and B from ellagic acid. *J. Funct. Foods* **45**, 95–99 (2018).

33. Larrosa, M. et al. Anti-inflammatory properties of a pomegranate extract and its metabolite urolithin-A in a colitis rat model and the effect of colon inflammation on phenolic metabolism. *J. Nutr. Biochem.* **21**, 717–725 (2010).

34. Forster, C. Tight junctions and the modulation of barrier function in disease. *Histochem. Cell Biol.* **130**, 55–70 (2008).

35. Arrieta, M. C., Bistritz, L. & Meddings, J. B. Alterations in intestinal permeability. *Gut* **55**, 1512–1520 (2006).

36. Konig, J. et al. Human intestinal barrier function in health and disease. *Clin. Transl. Gastroenterol.* **7**, e196 (2016).

37. Capaldo, C. T. & Nusrat, A. Cytokine regulation of tight junctions. *Biochim. Biophys. Acta* **1788**, 864–871 (2009).

38. Esser, C. & Rannug, A. The aryl hydrocarbon receptor in barrier organ physiology, immunology, and toxicology. *Pharmacol. Rev.* **67**, 259–279 (2015).

39. Stockinger, B., Di Meglio, P., Gialitakis, M. & Duarte, J. H. The aryl hydrocarbon receptor: multitasking in the immune system. *Annu. Rev. Immunol.* **32**, 403–432 (2014).

40. Furumatsu, K. et al. A role of the aryl hydrocarbon receptor in attenuation of colitis. *Dig. Dis. Sci.* **56**, 2532–2544 (2011).

41. Goettel, J. A. et al. AHR activation is protective against colitis driven by T cells in humanized mice. *Cell Rep.* **17**, 1318–1329 (2016).

42. Schiering, C. et al. Feedback control of AHR signalling regulates intestinal immunity. *Nature* **542**, 242–245 (2017).

43. Gimenez-Bastida, J. A. et al. Ellagitannin metabolites, urolithin A glucuronide and its aglycone urolithin A, ameliorate TNF-alpha-induced inflammation and associated molecular markers in human aortic endothelial cells. *Mol. Nutr. Food Res.* **56**, 784–796 (2012).

44. Monteleone, I. et al. Aryl hydrocarbon receptor-induced signals up-regulate IL-22 production and inhibit inflammation in the gastrointestinal tract. *Gastroenterology* **141**, 237–248 (2011). 248 e231.

45. Shin, S. et al. NRF2 modulates aryl hydrocarbon receptor signaling: influence on adipogenesis. *Mol. Cell. Biol.* **27**, 7188–7197 (2007).

46. Hayes, J. D., Dinkova-Kostova, A. T. & McMahon, M. Cross-talk between transcription factors AhR and Nrf2: lessons for cancer chemoprevention from dioxin. *Toxicol. Sci.* **111**, 199–201 (2009).

47. Mitsuishi, Y., Motohashi, H. & Yamamoto, M. The Keap1-Nrf2 system in cancers: stress response and anabolic metabolism. *Front. Oncol.* **2**, 200 (2012).

48. Al-Sawaf, O. et al. Nrf2 in health and disease: current and future clinical implications. *Clin. Sci.* **129**, 989–999 (2015).

49. Khor, T. O. et al. Nrf2-deficient mice have an increased susceptibility to dextran sulfate sodium-induced colitis. *Cancer Res.* **66**, 11580–11584 (2006).

50. Kobayashi, E. H. et al. Nrf2 suppresses macrophage inflammatory response by blocking proinflammatory cytokine transcription. *Nat. Commun.* **7**, 11624 (2016).

51. Wardyn, J. D., Ponsford, A. H. & Sanderson, C. M. Dissecting molecular cross-talk between Nrf2 and NF-kappaB response pathways. *Biochem. Soc. Trans.* **43**, 621–626 (2015).

52. Sekine, H. et al. Hypersensitivity of aryl hydrocarbon receptor-deficient mice to lipopolysaccharide-induced septic shock. *Mol. Cell. Biol.* **29**, 6391–6400 (2009).

53. Benson, J. M. & Shepherd, D. M. Aryl hydrocarbon receptor activation by TCDD reduces inflammation associated with Crohn's disease. *Toxicol. Sci.* **120**, 68–78 (2011).

54. Fukumoto, S. et al. Identification of a probiotic bacteria-derived activator of the aryl hydrocarbon receptor that inhibits colitis. *Immunol. Cell Biol.* **92**, 460–465 (2014).

55. Metidji, A. et al. The environmental sensor AHR protects from inflammatory damage by maintaining intestinal stem cell homeostasis and barrier integrity. *Immunity* **49**, 353–362 e355 (2018).

56. Novak, E. A. & Mollen, K. P. Mitochondrial dysfunction in inflammatory bowel disease. *Front. Cell Dev. Biol.* **3**, 62 (2015).

57. Delpre, G., Avidor, I., Steinherz, R., Kadish, U. & Ben-Bassat, M. Ultrastructural abnormalities in endoscopically and histologically normal and involved colon in ulcerative colitis. *Am. J. Gastroenterol.* **84**, 1038–1046 (1989).

58. Rodenburg, W. et al. Impaired barrier function by dietary fructo-oligosaccharides (FOS) in rats is accompanied by increased colonic mitochondrial gene expression. *BMC Genomics* **9**, 144 (2008).

59. Kurowska-Stolarska, M. et al. IL-33 amplifies the polarization of alternatively activated macrophages that contribute to airway inflammation. *J. Immunol.* **183**, 6469–6477 (2009).

60. Kowapradit, J. et al. In vitro permeability enhancement in intestinal epithelial cells (Caco-2) monolayer of water soluble quaternary ammonium chitosan derivatives. *AAPS PharmSciTech* **11**, 497–508 (2010).

61. Andrews S. FastQC: A Quality Control Tool for High Throughput Sequence Data. (2014).

62. Kim, D. et al. TopHat2: accurate alignment of transcriptomes in the presence of insertions, deletions and gene fusions. *Genome Biol.* **14**, R36 (2013).

63. Flicek, P. et al. Ensembl 2014. *Nucleic Acids Res.* **42**, D749–D755 (2014).

64. Trapnell, C. et al. Differential analysis of gene regulation at transcript resolution with RNA-seq. *Nat. Biotechnol.* **31**, 46–53 (2013).

65. Trapnell, C. et al. Differential gene and transcript expression analysis of RNA-seq experiments with TopHat and Cufflinks. *Nat. Protoc.* **7**, 562–578 (2012).

66. Singh, R. et al. Evaluation of memory enhancing clinically available standardized extract of Bacopa monniera on P-glycoprotein and cytochrome P450 3A in Sprague-Dawley rats. *PLoS ONE* **8**, e72517 (2013).

67. Murthy, S. N. et al. Treatment of dextran sulfate sodium-induced murine colitis by intracolonic cyclosporin. *Dig. Dis. Sci.* **38**, 1722–1734 (1993).

68. Furuta, G. T. et al. Hypoxia-inducible factor 1-dependent induction of intestinal trefoil factor protects barrier function during hypoxia. *J. Exp. Med.* **193**, 1027–1034 (2001).

69. Kim J. J., Shajib M. S., Manocha M. M., Khan W. I. Investigating intestinal inflammation in DSS-induced model of IBD. *J. Vis. Exp.* **60**, 3678 (2012).

70. Erben, U. et al. A guide to histomorphological evaluation of intestinal inflammation in mouse models. *Int. J. Clin. Exp. Pathol.* **7**, 4557–4576 (2014).

Acknowledgements

Author contributions

V.R.J. and P.K.V. conceived, designed the experiments, and analyzed the data. R.S., S.C., S.R.B., B.B., B.H., N.G.K., A.A.H., T.S., and P.P. designed, performed the experiments, and analyzed the data. M.V.-K., M.G.I.L., G.M.D., G.W.D., H.-G.Z., and B.H. contributed through invaluable discussions. X.C., E.C.R., and S.J.W. assisted in analyzing RNA-Seq data. A.H. scored the inflammation of colons. R.S., B.H., P.K.V., and V.R.J. wrote the paper, all authors discussed the results. P.K.V. and V.R.J. supervised the project.

Additional information

Oxime-functionalized anti-insecticide fabric reduces insecticide exposure through dermal and nasal routes, and prevents insecticide-induced neuromuscular-dysfunction and mortality

Mahendra K. Mohan [1], Ketan Thorat [1], Theja Parassini Puthiyapurayil [1], Omprakash Sunnapu [2], Sandeep Chandrashekharappa [1], Venkatesh Ravula [1], Rajamohammed Khader [1], Aravind Sankaranarayanan [1,3], Hadi Muhammad [1] & Praveen Kumar Vemula [1] ✉

Farmers from South Asian countries spray insecticides without protective gear, which leads to insecticide exposure through dermal and nasal routes. Acetylcholinesterase plays a crucial role in controlling neuromuscular function. Organophosphate and carbamate insecticides inhibit acetylcholinesterase, which leads to severe neuronal/cognitive dysfunction, breathing disorders, loss of endurance, and death. To address this issue, an Oxime-fabric is developed by covalently attaching silyl-pralidoxime to the cellulose of the fabric. The Oxime-fabric, when stitched as a bodysuit and facemask, efficiently deactivates insecticides (organophosphates and carbamates) upon contact, preventing exposure. The Oxime-fabric prevents insecticide-induced neuronal damage, neuro-muscular dysfunction, and loss of endurance. Furthermore, we observe a 100% survival rate in rats when repeatedly exposed to organophosphate-insecticide through the Oxime-fabric, while no survival is seen when organophosphate-insecticide applied directly or through normal fabric. The Oxime-fabric is washable and reusable for at least 50 cycles, providing an affordable solution to prevent insecticide-induced toxicity and lethality among farmers.

Farmers from agrarian countries, specifically South Asian countries, spray insecticides without using protective gear. Acute insecticide poisoning affects more than 300 millions farmers each year, while intentional self-poisoning kills ~150,000 people each year[1-3]. Enzyme acetylcholinesterase (AChE) plays a pivotal role in both central and peripheral nervous system[4,5]. Organophosphate (OP) and carbamate insecticides inhibit the enzyme AChE, resulting in excessive acetylcholine accumulation, which affects muscarinic and nicotinic

[1]Institute for Stem Cell Science and Regenerative Medicine (DBT-inStem), GKVK Post, Bellary Road, Bangalore 560065 Karnataka, India. [2]Sepio Health Private Limited, Bangalore 560065 Karnataka, India. [3]Tata Institute for Genetics and Society (TIGS), inStem, GKVK Post, Bellary Road, Bangalore 560065, India. ✉e-mail: praveenv@instem.res.in

receptors at synapses. Therefore, inhibition of AChE due to insecticide exposure causes neurological dysfunction, breathing disorder, paralysis, and death in severe cases[6–8]. India is one of the major countries in the world that heavily uses insecticides, and farmers from the Asian-Pacific region are repeatedly exposed to insecticides during farming[8–11]. Electroencephalograms of OP-exposed humans and monkeys revealed that in addition to their acute toxic effects, OPs have also been reported to have long-term effects[12]. Additionally, agricultural workers have reported neuro-behavioral changes even two years after a single exposure to OPs[13,14]. Based on the reported studies, it is known that pre- and postnatal exposures to OPs hinder neurodevelopment in children from agricultural communities, and they are vulnerable to neuropsychiatric disorders[15,16]. Typically used insecticides include OPs (methyl parathion, methamidophos, oxydemeton-methyl, chlorpyrifos, malathion, and primifos-methyl), and carbamates (carbaryl, aldicarb, carbofuran, and ferbam).

While spraying, insecticide exposure primarily occurs through dermal contact and inhalation. Tropical conditions prevent agriculture workers from wearing polythene or non-breathable fabric-based personal protective equipment (PPE), while regular cotton/semi-cotton cloths do not prevent insecticide exposure. Therefore, developing efficient prophylactic technologies to minimize dermal and inhalation exposure to reduce insecticide-induced hazardous effects is a critical unmet clinical need. Currently available headgear, facemasks, gloves, and suits are seldom used, owing to high cost and enormous discomfort under tropical conditions in low and middle income countries[17–19]. Additionally, physical barrier creams were developed to minimize exposure to OPs[20–22]. However, these systems showed limited success as they do not deactivate insecticides, and they physically trap OPs on the surface, which can still enter the system over a longer duration and through hand-to-mouth contact. Hence, physical barrier creams are not adequate to prevent exposure. Therefore, to overcome this limitation, a couple of non-physical barrier dermal systems that can chemically deactivate OPs upon contact were developed by others[23,24] and our group[25]. Due to potential DNA damage caused by metal (CeO$_2$) nanoparticle-based systems in dermal fibroblasts, using these systems as dermal protectants to prevent insecticide exposure is considerably restricted[26,27].

Although earlier we have developed a prophylactic topical gel that can chemically deactivate OPs and limit insecticide-induced toxicity[25], before commercial development of such topical gel for human applications, we wanted to engage with agriculture workers to get their feedback on willingness to adopt this technology. As a community engagement, we interacted with over 200 farmers from 60 rural villages in India, who are suffering from insecticide-induced acute toxicity due to exposure while spraying to see whether they are willing to adopt such prophylactic dermal cream. Although they are thrilled to know about this technology, one critical feedback was received. The need to apply the dermal cream on the entire body every time they spray will be challenging, and compliance might go down over time. This critical feedback inspired us to develop a user-friendly, efficient fabric-based prophylactic technology to prevent exposure while spraying insecticides in the agricultural field. At present, due to comfort, farmers wear regular cotton cloths while farming, which cannot prevent insecticide exposure. Therefore, an ideal solution will be developing an active fabric that can be stitched into a bodysuit and a facemask that can chemically deactivate insecticides upon contact, hence can prevent insecticide exposure through dermal and inhalation routes, respectively (Fig. 1). Additionally, an affordable bodysuit which is wash-resistant, reusable, and low-cost will increase the compliance and have a significant impact on the healthcare of agricultural workers whose purchase power is low.

Herein, we have developed an active fabric by covalently attaching a silyl-oxime-based nucleophile to cellulose that can hydrolyze insecticides upon contact before they enter the body, either in a solution or aerosol form. Earlier, we demonstrated that pralidoxime can hydrolytically deactivate a wide range of OPs and carbamates[25] in addition to their better-known effect of reactivating OP-inhibited acetylcholinesterase[28]. Here, we developed an oxime fabric by covalently connecting silyl-pralidoxime to cellulose fabric. Oxime-fabric, when stitched as a bodysuit and a facemask, can catalytically deactivate a wide range of insecticides (OPs and carbamates), prevent exposure through dermal and inhalation routes, and thereby limit insecticide-induced toxicity and mortality. These results are remarkable, and we aim to develop reusable protective bodysuits and facemasks, which may have an enormous impact on protecting agricultural workers from insecticide-induced toxicity.

Results
Preparation of Oxime-fabric and deactivation of insecticides, ex vivo

Commonly used insecticides are from organophosphorus and carbamates classes. The use of insecticides in India is different from that for the different parts of the world. In India OP-based insecticides are 76% of the total pesticides, as compared to 44% globally[29]. On the contrary, herbicides and fungicides are used less compared to insecticides[29,30]. We hypothesized that nucleophile-mediated hydrolysis may deactivate insecticides. Since N-hydroxy α-nucleophiles, such as oximes are efficient nucleophiles[31–35], we envisaged that covalent conjugation of pralidoxime based α-nucleophile to the cellulose of fabric would generate an anti-insecticide fabric, Oxime-fabric, which may hydrolyze insecticides upon contact (Fig. 1). Pralidoxime was quaternized with (3-chloropropyl)triethoxysilane, and resulted silyl-oxime was conjugated to cellulose of fabric (Fig. 1 and Methods). A detailed characterization of compounds is given in Supplementary Figs. S1 and S2. To provide further evidence for covalent functionalization of silyl-oxime on the fabric, solid state Cross Polarization Magic Angle Spinning (CP/MAS) ^{13}C-NMR studies were performed. Pyridinium ring carbons in silyl-pralidoxime compound give peaks between 141–148 δ ppm (Supplementary Fig. S2). Therefore, to find the presence of silyl-pralidoxime upon covalent functionalization on the fabric, ^{13}C-NMR was recorded for Normal fabric, Oxime-fabric and Oxime-fabric after extensive washing to remove non-covalent bound silyl-pralidoxime. Spectra in Supplementary Figs. S3 and S4 show the presence of silyl-pralidoxime on the fabric. The peaks corresponding to pyridinium group are completely absent in spectra of normal fabric, whereas these peaks were found in spectra of Oxime fabric. Subsequently, Oxime fabric was extensively washed with both detergent and methanol in which silyl-oxime is soluble. However, despite of extensive washing, it did not remove pyridinium peaks, suggesting that silyl-oxime has been covalently attached to the fabric.

Furthermore, we used a bromophenol blue assay to quantify the amount of silyl-pralidoxime attached to the fabric. An acidic dye, Bromophenol Blue (BPB), has been used to quantify the concentration of quaternary ammonium salts on fabric[36,37]. Due to the presence of the pyridinium group, the BPB assay gave the quantitative oxime presence on the fabric (Fig. 2a–c). Post-functionalization of pyridinium-oxime on the fabric, extensive washes were done to remove unfunctionalized oxime. Subsequently, the calculated concentration of pyridinium-oxime on normal fabric and Oxime-fabric was 0.26 ± 0.14 and $125 \pm 6\ \mu g/cm^2$, respectively (Fig. 2c), which confirmed the presence of pyridinium-oxime on Oxime-fabric.

The ability of Oxime-fabric to deactivate insecticides and prevent insecticide-induced AChE inhibition was tested using the Franz diffusion apparatus, which is generally used to mimic transdermal penetration (Fig. 2d). OPs are known to inhibit AChE in the blood[38]. An ex vivo assay was performed using rat blood in a Franz diffusion cell to test the ability of Oxime-fabric to reduce MPT-induced AChE inhibition (Fig. 2e). Either normal fabric or Oxime-fabric was placed over a 3.5 kDa dialysis membrane between donor and acceptor
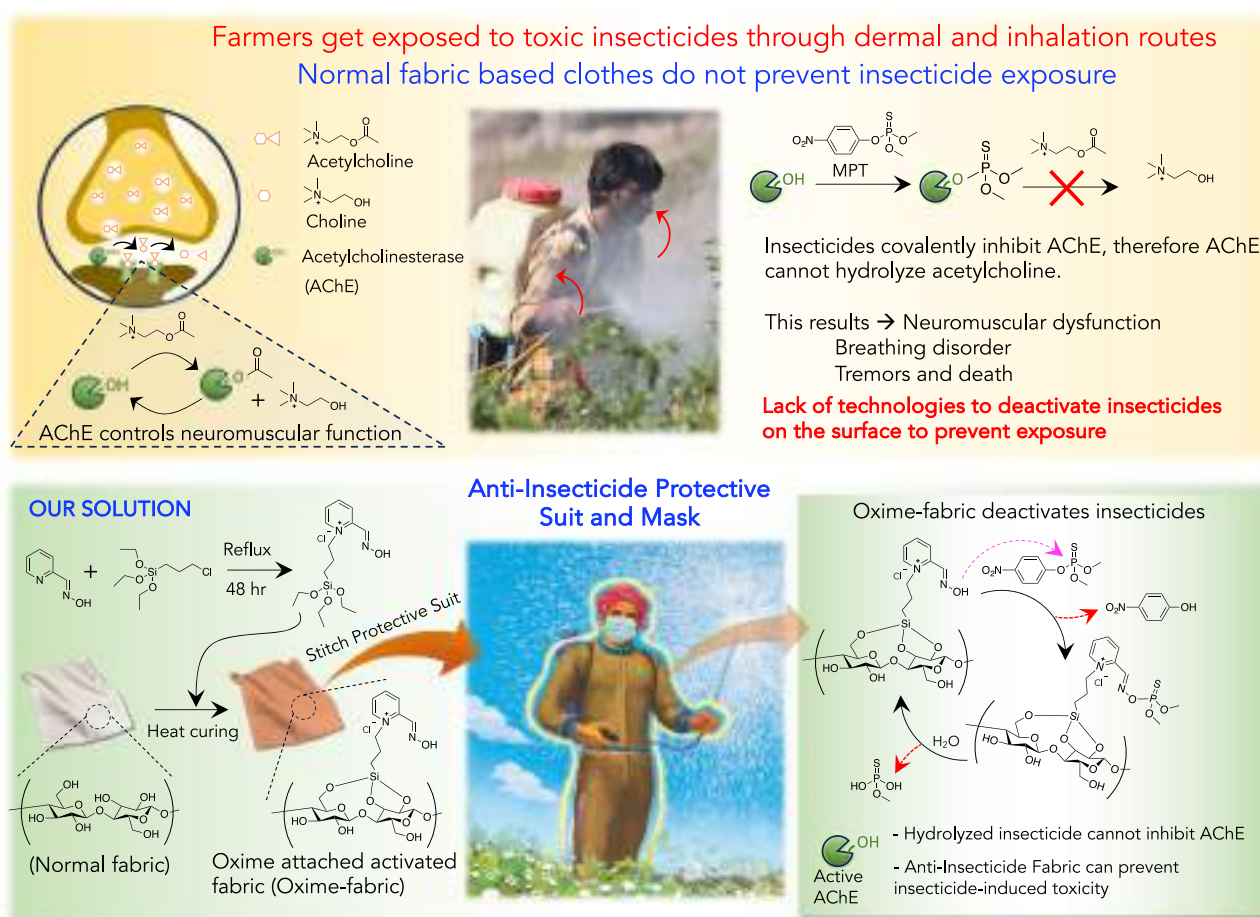
Fig. 1 | Developing an oxime-fabric that can hydrolyze insecticides to prevent insecticide-induced toxicity. Top, acetylcholinesterase (AChE) enzyme controls neuromuscular function by hydrolyzing acetylcholine, a neurotransmitter at synapses. While spraying, agriculture workers get exposed to insecticides (methyl parathion, MPT), through dermal and inhalation routes. Upon exposure, organophosphates covalently inhibit AChE, which causes severe toxicity and mortality. bottom, In our approach, α-nucleophile, oxime-based silyl-pralidoxime is covalently attached to the cellulose of fabric to generate Oxime-fabric. Oxime-fabric can be stitched as a bodysuit and a facemask, which, upon contact, can hydrolyze organophosphates into phosphoric acid that cannot inhibit AChE. Therefore, Oxime-fabric could prevent exposure to insecticides, thereby preventing insecticide-induced toxicity and mortality.

chambers. Subsequently, methyl parathion (MPT) was added into the donor chamber, and the acceptor chamber was filled with 1000× diluted rat blood that contains AChE. As one of the controls, only dialysis membrane was used and no fabric was placed between chambers. The chamber's temperature was maintained at 37 °C. The percentage of the AChE activity was quantified using a modified colorimetric Ellman's assay[39] (Methods). In the absence of MPT, no change was observed in the activity of AChE after 3 h (Fig. 2e). The addition of MPT (2.5 μM) in the donor chamber significantly inhibited AChE activity in blood. Direct exposure or the presence of normal fabric did not prevent MPT-induced AChE inhibition (Fig. 2e). On the other hand, Oxime-fabric deactivated MPT before entering into the acceptor chamber, thereby completely reduced MPT-induced inhibition of blood AChE activity.

To test the reusability of Oxime-fabric, after covalent functionalization, Oxime-fabric was subjected to delicate washing cycles mimicking the laundry and washing machine using 0.1% of detergent (Fig. 2f and Methods). After completion of 10, 25, and 50 wash cycles, the concentration of pyridinium-oxime present on the fabric was quantified using BPB assay. Data in Fig. 2g reveal that repeated wash cycles did not reduce the amount of pyridinium-oxime present on the fabric, suggesting that pyridinium-oxime is covalently attached to the fabric and does not leach while washing with the detergent. Subsequently, after different wash cycles (10, 25, and

50), Oxime-fabric was tested for its ability to deactivate MPT to prevent MPT-induced AChE inhibition using Franz diffusion assay. Even after 50 cycles of detergent washes, Oxime-fabric effectively deactivated MPT and prevented AChE inhibition (Fig. 2h). Typically, farmers dry their cloths under the sun. Therefore, to test the stability of Oxime fabric under sunlight, Oxime fabric was exposed to sunlight for 3 days, and subsequently investigated its efficacy to deactivate insecticides. The data in Supplementary Fig. S5 suggest that even after exposed to the sunlight Oxime fabric retained its activity and prevented MPT-induced AChE inhibition.

To test the robustness of Oxime-fabric to deactivate a wide range of insecticides, a similar assay was performed using commercial formulations that contain carbamates and OPs. These formulations are carbaryl (carbamate), Macacid-50 (MPT 50%), Aalphos (Monocrotophos 36%), Raise-505 (Chlorpyrifos 50% + Cypermethrin 5%), and Profex Super (Profenofos 40% + Cypermethrin 4%). In the Franz diffusion assay (Supplementary Fig. S6), Oxime-fabric could hydrolytically cleave all commercial OP formulations to prevent insecticide-induced AChE inhibition. As controls, we have used normal fabric that was not functionalized with silyl-oxime, and commercially available physical barrier Hazmat suits. The data in Supplementary Fig. S6e–h suggest that normal fabric and Hazmat suit fabrics could not prevent insecticide-induced AChE inhibition, while Oxime-fabric could prevent AChE inhibition suggesting that α-nucleophile oxime is essential for
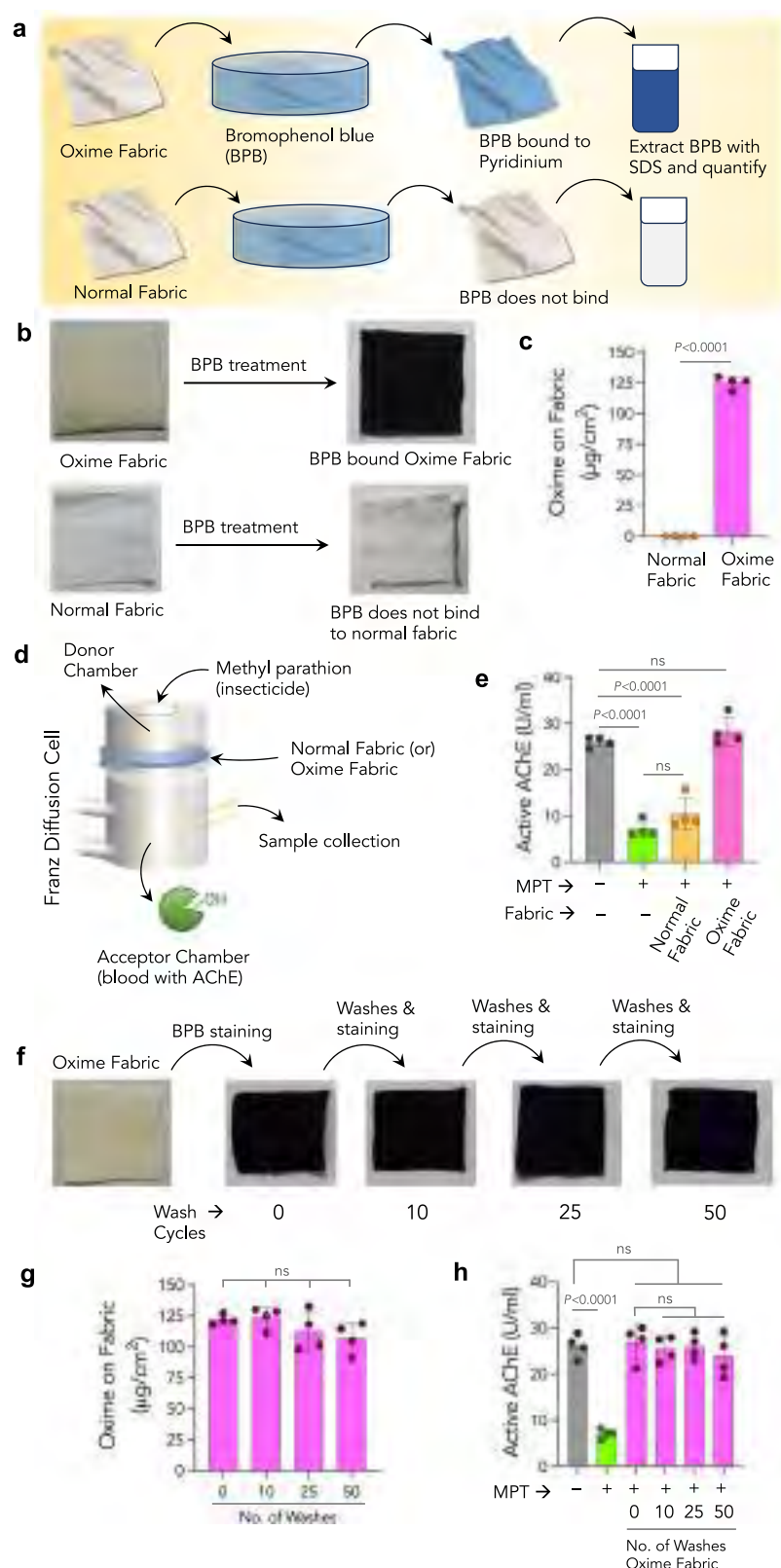
the activity. These results suggest that Oxime-fabric could reduce OP or carbamate insecticide-induced AChE inhibition by chemically deactivating insecticides.

To unambiguously demonstrate that Oxime-fabric does not act like physical barrier cloth, and characterize oxime-mediated hydrolytic cleavage of MPT, normal fabric or Hazmat suit fabric or Oxime-fabric was placed between donor and acceptor chambers that were filled with phosphate-buffered saline (PBS). Subsequently, MPT was added to the donor chamber, and the concentrations of MPT and its hydrolytically degraded product p-nitrophenol were quantified in both chambers at 1 and 180 mins after MPT addition (Methods and Supplementary Fig. S7a, b). In the presence of normal fabric, MPT was quantitatively diffused into the acceptor chamber within 3 h (Supplementary Fig. S7c), whereas Oxime-fabric prevented MPT diffusion

Fig. 2 | Washable and reusable Oxime-fabric deactivates MPT to prevent MPT-mediated AChE inhibition, ex vivo. a–c Schematic of bromophenol blue (BPB) assay to quantify the amount of silyl-pralidoxime attached to the fabric (**a**); **b** photographs of Oxime-fabric and normal fabric before and after treating BPB dye, and **c** quantification of silyl-pralidoxime present on fabric, suggested that silyl-pralidoxime (125 µg/cm²) was present on Oxime-fabric, while it was not detectable on normal fabric ($P < 0.0001$; unpaired two-tailed t test). **d** Schematic of Franz diffusion cell. **e** The efficacy of Oxime-fabric to prevent methyl parathion (MPT)-induced AChE inhibition, an ex vivo assay was performed using rat blood. Active AChE was measured in unexposed native blood and 3 hr post addition of MPT. The normal fabric could not prevent MPT diffusion into the acceptor chamber, which resulted in significant inhibition of AChE activity ($P < 0.0001$; ordinary one-way ANOVA with Tukey's post hoc analysis). On the contrary, Oxime-fabric could hydrolyze MPT before it diffuses, preventing the MPT-induced inhibition of AChE ($P = 0.6161$; ordinary one-way ANOVA with Tukey's post hoc analysis). **f–h** Oxime-fabric was subjected to delicate washing cycles in a washing machine using a mild non-ionic detergent (0.1%). Photographs of Oxime-fabric after 10, 25, and 50 cycles of washing and stained with BPB dye (**f**), and quantification of silyl-pralidoxime after 10, 25, and 50 cycles of washing (**g**). **h** Franz diffusion assay to investigate the efficacy of multiple cycles of washed Oxime-fabric to hydrolyze MPT to prevent MPT-induced inhibition of AChE activity. Direct exposure to MPT significantly inhibited AChE activity ($P < 0.0001$; ordinary one-way ANOVA with Tukey's post hoc analysis). On the contrary, multiple washing cycles did not cause the leaching of active compound from the fabric and retained its activity. Data are mean ± s.d. ($n = 4$, from independent experiment*s*). **c** P values were determined by two-tailed Student's t test with Welch's correction, and for **e, h**, by ordinary one-way ANOVA with Tukey's post hoc analysis, and for **g**, by repeated measures one-way ANOVA by GraphPad PRISM 9, and exact P values are indicated. ns not significant. Source data are provided as a Source Data file.

(Supplementary Fig. S7d). It suggests that normal fabric is not a physical barrier, and MPT can easily pass through it. Interestingly, commercial Hazmat suit fabric, to some extent, prevented the diffusion of MPT, but not quantitatively. Approximately 30% of MPT penetrated and entered into the acceptor chamber (Supplementary Fig. S7e). Data in Supplementary Fig. S7g show that Oxime-fabric was able to hydrolyze MPT into *p*-nitrophenol, which was quantified in both donor and acceptor chambers. Additionally, due to the lack of an Oxime-functional group, either normal fabric (Supplementary Fig. S7f) or Hazmat suit fabric (Supplementary Fig. S7h) could not hydrolyze MPT, therefore, *p*-nitrophenol was not generated in the absence of Oxime-fabric. These results suggest that Oxime-fabric prevents the penetration of MPT, not as a physical barrier but via chemically hydrolyzing MPT.

Oxime-fabric prevents dermal exposure to insecticides, and reduces insecticide-induced AChE inhibition in blood and tissue, in vivo

To assess the ability of Oxime-fabric to prevent dermal exposure of MPT, and reduce MPT-induced AChE inhibition, 15 Sprague-Dawley rats (10–12 weeks) were randomly divided into three groups ($n = 5$ per group). The dorsal coat was clipped, and was exposed to a single dose of MPT (150 mg/kg) either directly or in the presence of normal fabric (10×8 cm²) or through Oxime-fabric (10×8 cm²) (Fig. 3a and Methods). MPT is an insecticide categorized as "highly hazardous" (class Ib) by the World Health Organization, as its median lethal dose (LD$_{50}$) falls within 10–100 mg/kg of body weight in rats when exposed via dermal route[40,41]. Therefore, when Sprague-Dawley (SD) rats are exposed to 150 mg/kg of MPT via the dermal route, it is known to cause significant AChE inhibition and toxicity[25]. To investigate the efficiency of Oxime-fabric, the active AChE in the blood at pre-exposure (before) and post-exposure (after three days) was quantified. The data revealed that dermal exposure to MPT either directly or through normal fabric significantly decreased the active AChE in blood. However, in the presence of Oxime-fabric, no such decrease was observed (Fig. 3b). Additionally, after three days, animals were sacrificed, and tissues such as brain, lung, liver, kidney, and heart were isolated, and active AChE was quantified and compared with the active AChE in tissues collected from unexposed naive rats (Fig. 3c–g). Data shown in Fig. 3c–g suggest that dermal exposure of MPT either directly or through normal fabric caused a significant decrease in active AChE levels. However, on the contrary, the same dose of MPT exposure through Oxime-fabric did not decrease the active AChE levels in the studied organs. Therefore, this data corroborates that Oxime-fabric does not act like a physical barrier, but it hydrolytically deactivates OP insecticides, causing prevention of insecticide-induced AChE inhibition, in vivo.

Oxime-fabric prevents insecticide-induced neuronal damage and perturbed signaling at neuromuscular junctions, in vivo

OP and carbamate insecticides disrupt the functioning of the cholinergic nervous system by inhibiting AChE, which hydrolyses acetylcholine at the synapse. Hence, inhibition of AChE leads to overstimulation of cholinergic receptors, resulting in neuronal excitotoxicity, dysfunction, and disrupted signaling at the neuromuscular junctions. Quantifying the sciatic nerve function is a surrogate method to quantify neuronal damage. Gait analysis is a widely accepted non-invasive method to study sciatic nerve function[42–45]. The analysis of a walking pattern is decided by the posture of the foot, the force exerted, and the angle formed with the ground. These parameters combined will establish a particular print length, toe spread, and intertoe spread of an animal, and these parameters alter significantly when function of the sciatic nerve is impaired[46,47] (Fig. 4a, b). The sciatic functional index (SFI) is an empirically derived formula to evaluate nerve function[44,45] (Methods). Typically, a healthy and unimpaired sciatic nerve function provides SFI values between +11 to −11, whereas SFI values below −20 indicate partial impairment of sciatic nerve function. Gait analysis was performed on 15 animals (SD rats, 10–13 weeks) to evaluate their walking pattern. Before MPT exposure, all animals were trained for 4 days to walk through an alley (Fig. 4a and Methods) and collected the prints of paws (Fig. 4b). Post-training, animals were randomly divided into three groups ($n = 5$ per group), and their SFI was measured. They were subsequently exposed to a single dose of MPT (150 mg/kg) through the dermal route either directly or through normal fabric or Oxime-fabric. Post MPT exposure, the direct exposure and normal fabric groups showed SFI values significantly decreasing to −60 and −36, respectively, which indicate impairment of sciatic nerve function (Fig. 4c). On the contrary, Oxime-fabric protected animals did not show any significant reduction in SFI (+6, Fig. 4c), suggesting complete prevention of impairment in the sciatic nerve function.

OP-insecticide-induced AChE inhibition causes the accumulation of the neurotransmitter acetylcholine at the synapse, leading to perturbed signaling at neuromuscular junctions and overstimulation of muscles. Electromyograms (EMG) were used to monitor if there is signaling impairment at neuromuscular junctions. Upon exposure to MPT (150 mg/kg) through the dermal route either directly or through normal fabric, visible muscular spasms were observed in the animals. For all animals across three groups, we recorded EMG between *spinotrapezius* and *Gluteus maximus* when the animal was awake. EMG of animals exposed to MPT either directly or through normal fabric showed high frequent muscle activity, compared to unexposed animals (Fig. 4d), which suggests the involuntary muscle activity due to accumulation of acetylcholine at synapse. On the contrary, this involuntary muscle activity was completely absent in the animals that were exposed to MPT through Oxime-fabric akin to unexposed animals
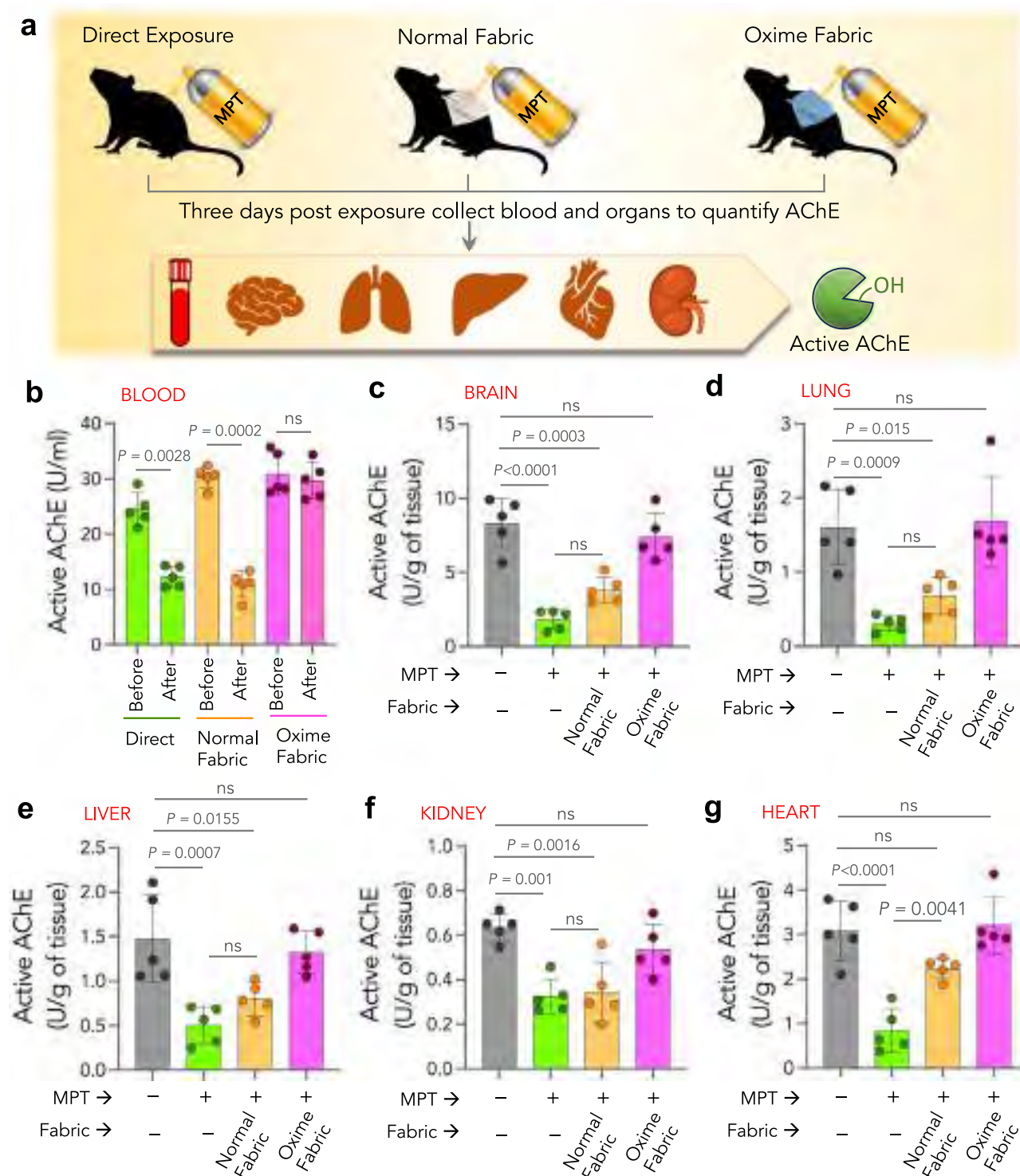
Fig. 3 | Oxime-fabric prevents acute exposure to a lethal dose of MPT, and reduces AChE inhibition, in vivo. a Schematic of experimental design: The dorsal coat of Sprague-Dawley (SD) rats was clipped using a hair clipper one day prior to exposure. Organophosphate, methyl parathion (MPT, 150 mg/kg) was applied on the skin either directly or in the presence of normal fabric or Oxime-fabric. **b–g** Before and after 72 h of exposure to MPT, active AChE in the blood (**b**) and internal organs such as brain (**c**), lung (**d**), liver (**e**), kidney (**f**), and heart (**g**) was quantified. Three days post-exposure to MPT, animals were sacrificed, tissues were collected, and the amount of active AChE was quantified using modified Ellman's assay. Dermal exposure of MPT directly or through normal fabric significantly reduced the active AChE in blood and tissues. On the contrary, Oxime-fabric deactivated MPT and prevented MPT-induced inhibition of AChE. Data are mean ± s.d. ($n = 5$ rats per group). **b** P values were determined by two-tailed Student's t test with Welch's correction, and for **c–g** by ordinary one-way ANOVA with Tukey's post hoc analysis by GraphPad PRISM 9, and exact P values are indicated. ns not significant. Source data are provided as a Source Data file.
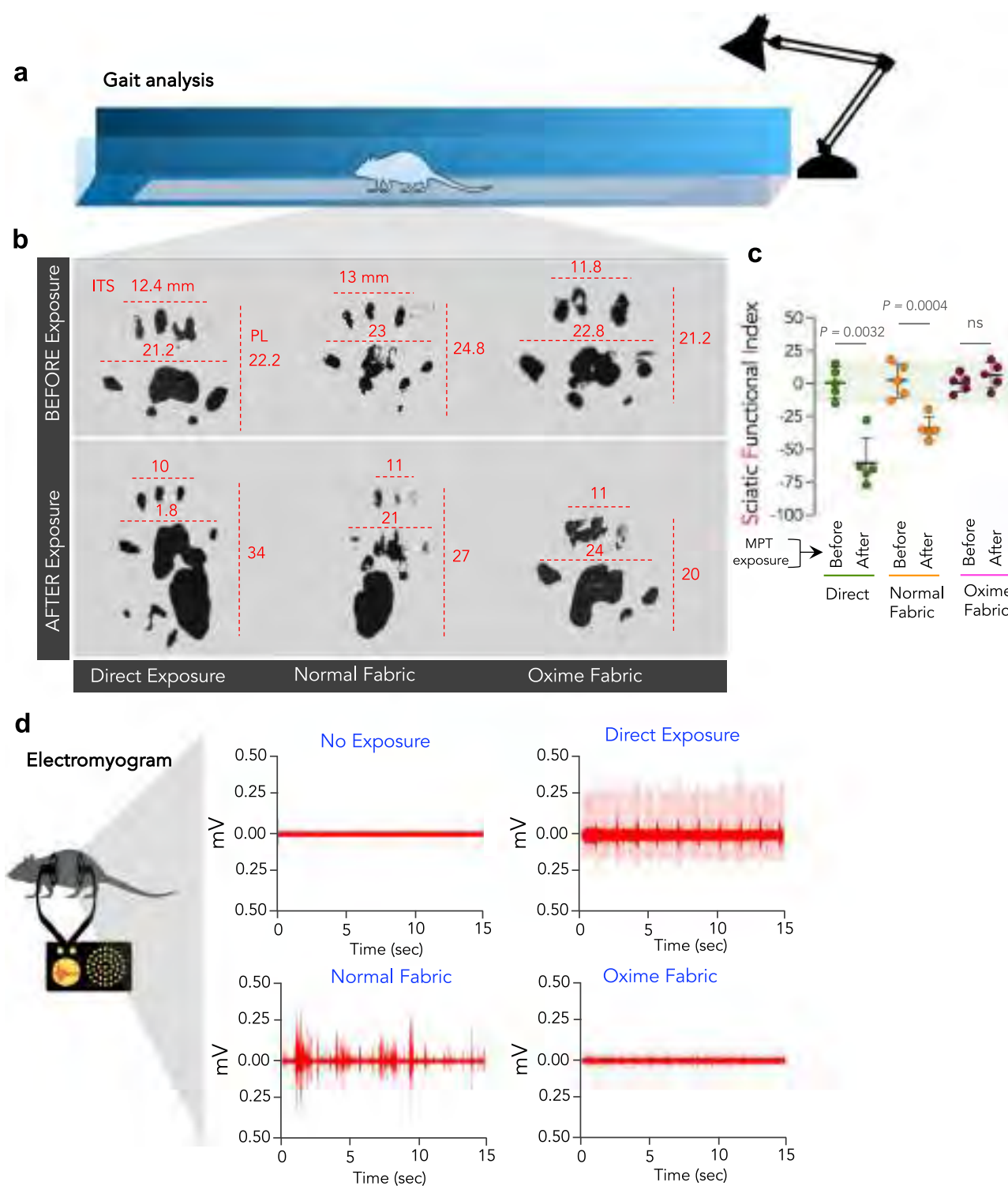
Fig. 4 | Oxime-fabric prevented sciatic nerve function impairment and involuntary muscle activity, in vivo. Schematic of an alley in which rats were walked to collect the footprints (a). Fifteen Sprague-Dawley rats were randomly divided into three groups (*n* = 5 per group). All paws of the animal were colored with different non-toxic water colors, and trained to walk through an ally (8 cm width, 120 cm length and 10 cm height) leading to its cage. Before exposure to methyl parathion (MPT), footprints of animals in all groups were collected (b), and analyzed manually, and the Sciatic function index (SFI) was calculated using the formula reported elsewhere[41,42]. **c** A single dose of MPT (150 mg/kg) was exposed dermally either directly or through normal fabric or Oxime-fabric, and 72 h post-exposure SFI was calculated. Dermal exposure of MPT directly or through normal fabric significantly reduced SFI values, which represents severe impairment of sciatic nerve function, whereas Oxime-fabric prevented such impairment. **d** Electromyograms (EMGs) were recorded before and 72 h post-exposure to MPT for all animals in three groups. Representative graphs are given here. MPT exposure directly and through normal fabric caused overstimulation of neuromuscular signaling and muscle spasms, while Oxime-fabric showed complete prevention of muscle spasms. Data are mean ± s.d. (*n* = 5 rats per group). **c** *P* values were determined by a two-tailed Student's *t* test with Welch's correction by GraphPad PRISM 9, and exact *P* values are indicated. ns not significant. Source data are provided as a Source Data file.
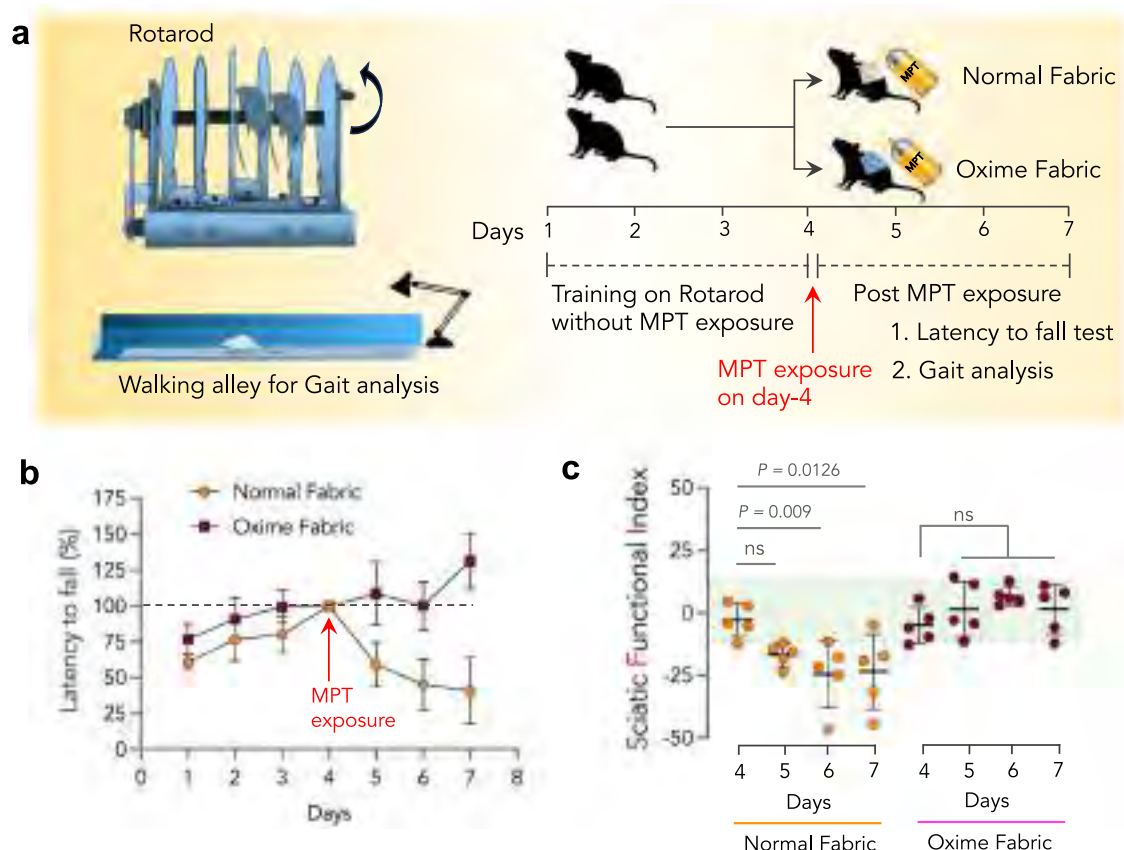
Fig. 5 | Oxime-fabric prevented insecticide-induced muscular dysfunction and neuronal damage, in vivo. a Schematic of rotarod and Gait analysis done over time post-exposure to methyl parathion (MPT). Rotarod was used to study muscle function endurance in animals that were exposed to MPT (150 mg/kg) through normal fabric or Oxime fabric. **b** 10 Sprague-Dawley rats were trained on a rotarod for four days, and latency to fall was measured by measuring the time the animal stayed on the rotarod at a constant speed of 20 rpm. The latency to fall obtained on day 4 was considered as 100%, and ten rats were randomly divided into two groups and exposed to MPT through either normal fabric or Oxime-fabric. Post-exposure to MPT, latency to fall has significantly dropped in the normal fabric group, indicating muscle dysfunction and loss of endurance, whereas Oxime-fabric prevented loss of endurance. **c** On day 4, before MPT exposure, the sciatic functional index (SFI) was measured for animals in both groups. Subsequently, after exposing to MPT (150 mg/kg) through either normal fabric or Oxime-fabric, SFI was measured as a function of time. A significant drop in SFI values when exposed to MPT through the normal fabric was observed, indicating neuronal damage, which Oxime-fabric prevented. Data are mean ± s.d. ($n = 5$ rats per group). **c** P values were determined by Repeated Measures one-way ANOVA by GraphPad PRISM 9, and exact P values are indicated. ns = not significant. Source data are provided as a Source Data file.

(Fig. 4d), suggesting that Oxime-fabric could prevent insecticide-induced perturbation in neuronal signaling.

Oxime-fabric prevents insecticide-induced loss of endurance and motor coordination, in vivo

OP insecticide-induced AChE inhibition impairs signaling at motor end plates, leading to reduced motor coordination and endurance[46–50]. The endurance of rats exposed to MPT was tested using the rotarod experiment. Ten SD rats (10 weeks) were trained on a rotarod for 4 days (Fig. 5a), and during the training, all animals showed similar Lf, latency to fall (Lf = time to fall from rotating rod with 2–20 rpm, Methods). The observed Lf on day 4 was considered as 100%. Simultaneously, during these 4 days, the same animals were trained to walk through an alley to measure SFI, as shown in Fig. 4a, b. The SFI values on day 4 are considered as unexposed controls. On day 4, animals were randomly divided into two groups ($n = 5$ in each group), and exposed to MPT (150 mg/kg) through a dermal route in the presence of either normal fabric or Oxime-fabric (Fig. 5a). Animals that received MPT through normal fabric showed a significant drop in latency to fall from day 5 to 7. At the same time, Oxime-fabric completely prevented such decrease (Fig. 5b). Similarly, post MPT exposure from day 5 to 7, for animals in normal fabric group SFI reduced significantly, while Oxime-fabric prevented a drop in SFI values (Fig. 5c). Cumulatively, these results suggest that Oxime-fabric could deactivate MPT, and prevents insecticide-induced reduction in endurance and neuronal dysfunction.

Oxime-fabric prevents repeated insecticide exposure-induced mortality in vivo

As farmers in the field repeatedly get exposed to multiple doses of insecticides, which could cause adverse health effects[51–53], we investigated the robustness of Oxime-fabric to prevent ethyl paraoxon (EPx, an activated OP insecticide)-induced mortality in rats. In survival experiments, to partly mimic the field scenario of multiple exposures, 18 SD rats were randomized into three groups ($n = 6$ per group), and all animals in three groups received EPx through the dermal route (50 mg/kg/day on day 0, and 25 mg/kg/day on days 1–5) once a day until >50% mortality was observed in any two of the groups (Fig. 6a). In case of animals received EPx through either normal fabric or Oxime-fabric, the same fabric was used for all days to test the robust nature of the Oxime-fabric. Animals that received EPx either directly or through normal fabric exhibited the characteristic of OP poisoning symptoms[54], such as muscular fibrillation, salivation, lacrimation, diarrhea, gasping, respiratory distress, and tremors. On the other hand, the animals that received EPx repeatedly through Oxime-fabric did not show signs of toxicity. All animals directly exposed to the EPx group died within 24 h, while all the animals that received EPx through
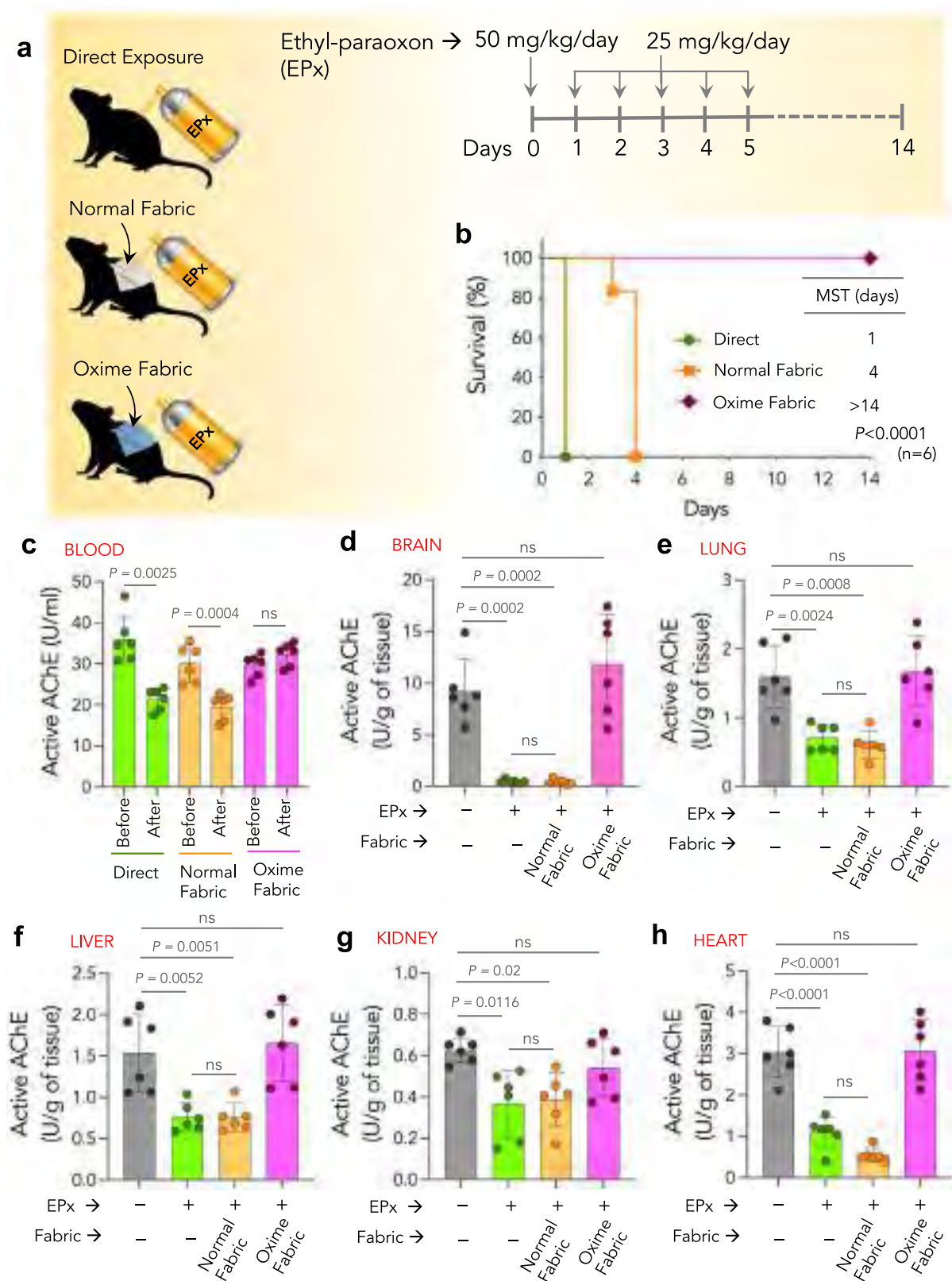
normal fabric died within 4 days, with a median survival time (MST) of 1 and 4 days, respectively. On the contrary, all animals that received EPx through Oxime-fabric survived (Fig. 6b). A remarkable 100% survival rate was observed in the presence of Oxime-fabric ($n = 6$; $P = 0.0001$, Mantel-Cox test). From all the animals, the blood was collected before exposure to EPx (day 0) and at the terminal stage (on day 1 for directly exposed animals, and days 4 and 14 for animals that received EPx through normal fabric and Oxime-fabric, respectively). Animals that received EPx through Oxime-fabric were tested for any delayed signs of insecticide toxicity for 14 days, and the study was terminated on day 14. Notably, no visible delayed signs of toxicity, such as muscular fibrillation, salivation, lacrimation, diarrhea, gasping, and respiratory distress, were observed. Quantification of active AChE in the blood before and after exposure to EPx revealed that when EPx was exposed

Fig. 6 | Oxime-fabric prevented mortality during repeated exposure of ethyl-paraoxon (EPx), in vivo. a Sprague-Dawley rats (10 weeks, males) were randomized in three groups (*n* = 6 rats per group); (i) direct exposure of EPx, (ii) normal fabric + EPx, and (iii) Oxime-fabric + EPx. On day 0, 50 mg/kg/day of EPx and 25 mg/kg/day of EPx were applied dermally for five days. **b** Median survival time (MST) for direct exposure of EPx and EPx received through the normal fabric was 1 and 4 days, respectively, while the Oxime-fabric group did not show mortality (*P* < 0.0001; Mantel-Cox test). **c–h** Active AChE in blood and organs was quantified using a modified Ellman's assay. Blood AChE activity dropped significantly in direct EPx and normal fabric groups, while inhibition of AChE was prevented in Oxime-fabric group animals (**c**). Organs were collected either immediately after mortality (for

group i and ii animals) or on day 14 (group iii animals), and the amount of active AChE was quantified using Ellman's assay in brain (**d**), lung (**e**), liver (**f**), kidney (**g**), and heart (**h**). Dermal exposure of EPx directly or through normal fabric significantly reduced the active AChE in tissues. On the contrary, Oxime-fabric has deactivated EPx and prevented EPx-induced inhibition of AChE. Data are mean ± s.d. (*n* = 6 rats per group). **b** *P* values were determined by Mantel-Cox test, and for **c** by two-tailed Student's *t* test with Welch's correction, and for **d–h**, by ordinary one-way ANOVA with Tukey's post hoc analysis by GraphPad PRISM 9, and exact *P* values are indicated. ns not significant. Source data are provided as a Source Data file.

either directly or through normal fabric, it showed a significant decrease in active AChE (Fig. 6c). At the same time, Oxime-fabric prevented the inhibition of AChE activity (Fig. 6c). Additionally, the tissues were collected from animals that received EPx either directly or through normal fabric immediately after they died. Since 100% survival was observed in the Oxime-fabric group, those animals were sacrificed on day 14, and their tissues were collected. The active AChE in the brain, lung, liver, kidney, and heart was quantified. Data shown in Fig. 6d–h suggest that dermal exposure of EPx either directly or through normal fabric caused a significant decrease in active AChE levels in tissue. However, on the contrary, repeated EPx exposure through Oxime-fabric did not decrease the active AChE levels. It is noteworthy that tissue AChE levels were tested at the terminal point (day 14) for Oxime-fabric group, which might be possible that some of the AChE might have been recovered by day 14. Therefore, these results suggest that Oxime-fabric deactivates OP insecticides in a truly catalytic manner to prevent insecticide-induced toxicity and mortality. Since Oxime-fabric can be washed and reused, as shown in Fig. 2, and it effectively prevents repeated exposure (Fig. 6), we propose that these properties of Oxime-fabric could be beneficial to develop protective suits for farmers who repeatedly get exposed to high doses of insecticides.

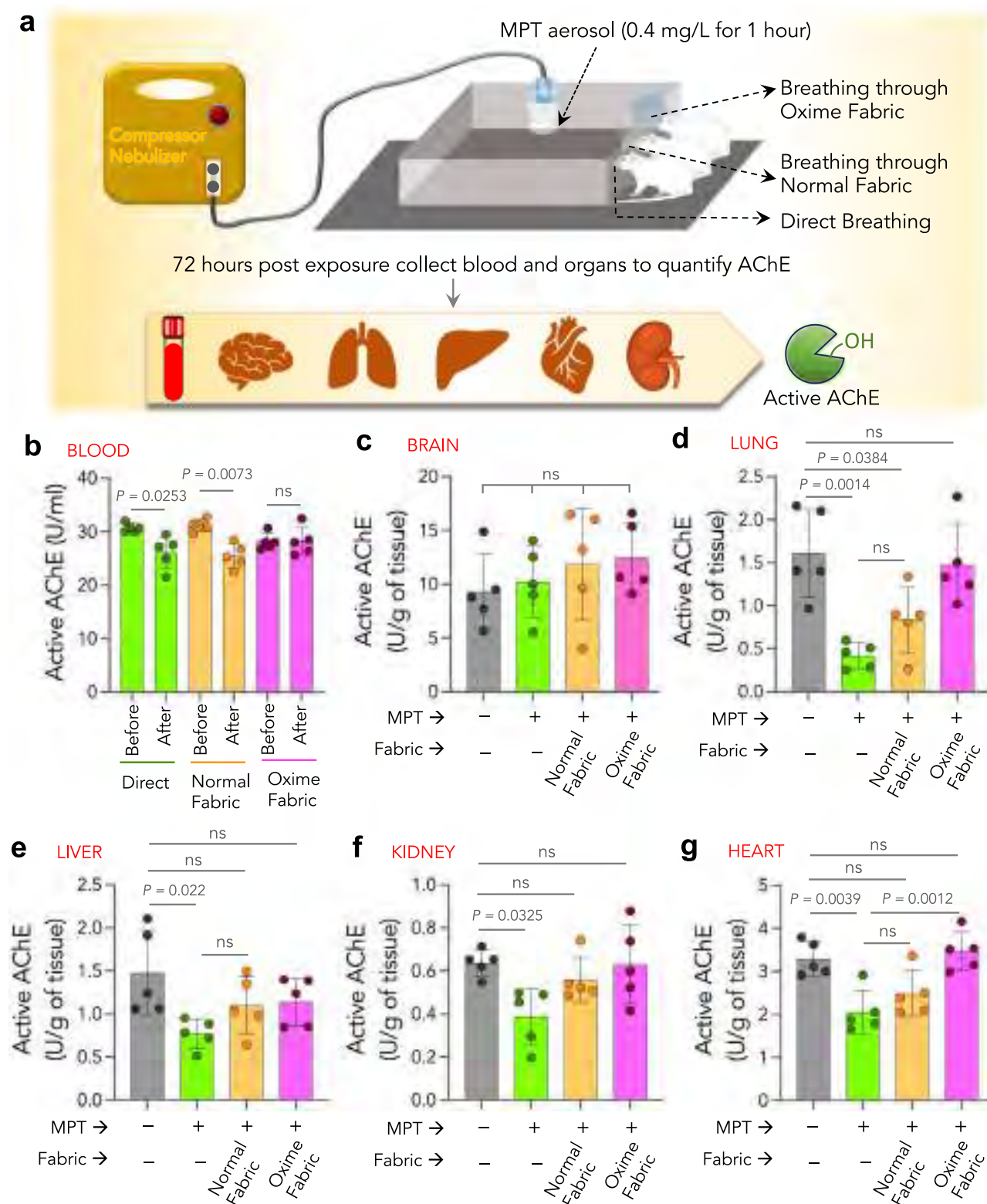### Oxime-fabric prevents insecticide exposure through inhalation route, in vivo

Although dermal exposure accounts for major insecticide toxicity, agriculture workers are also exposed to insecticides through inhalation of air-borne vapors and aerosol/particulate matter. Typically, inhalation exposure nearly accounts for less than 10% of overall exposure[55]. However, inhalation exposure assumes importance, especially for highly volatile insecticides. Therefore, we tested the ability of Oxime-fabric to prevent insecticide exposure through the inhalation route. To test that, we built a chamber where insecticide aerosol can be filled, and restrained animals can inhale aerosols either directly or through the fabric, mimicking the facemask (Fig. 7a and Methods). See the Methods for generating MPT insecticide aerosols. Fifteen SD rats (10-12 weeks) were randomized into three groups (*n* = 5 per group), and they were made to inhale MPT aerosols for 1 h either directly or through normal fabric or Oxime-fabric (Fig. 7a). The blood was collected from animals before exposure and post-exposure 3 days. The quantification of active AChE in the blood at pre and post-inhalation exposure revealed that when animals inhaled MPT aerosols either directly or through normal fabric, active AChE levels in the blood significantly decreased (Fig. 7b). However, no such decrease was observed when animals inhaled MPT aerosols through Oxime-fabric (Fig. 7b). Additionally, three days post-exposure animals were sacrificed, and tissues such as brain, lung, liver, kidney, and heart were isolated and active AChE was quantified and compared with the active AChE in tissues collected from unexposed naive rats (Fig. 7c–g). The data has shown an interesting trend. In brain tissue, there is no significant difference in active AChE levels in animals that were exposed to aerosol MPT either directly or through normal/Oxime fabrics compared to unexposed animals

(Fig. 7c). On the contrary, the active AChE levels in lung tissue of animals that were exposed to MPT aerosols either directly or through normal fabric significantly decreased compared to unexposed animals, whereas Oxime-fabric prevented such decrease in active AChE levels (Fig. 7d). Active AChE levels in liver, kidney and heart tissue of directly exposed animals were significantly decreased compared to unexposed animals (Fig. 7e–g), however, in the presence of either normal fabric or Oxime-fabric has significantly prevented the reduction in active AChE level in these tissues (Fig. 7e–g). Cumulatively, these results suggest that insecticide exposure through the inhalation route is moderate, and Oxime-fabric can prevent insecticide exposure through the inhalation route.

Discussion

With the growing demand to increase agriculture productivity to match the food needs of the world's population, the use of OP insecticides has continuously increased over the last six decades[56–58]. Due to low economic strata, agriculture farmers from developing countries manually spray insecticides, whereas, in developing countries, insecticides are usually sprayed using automation. Therefore, the lack of protective gear during spraying is causing direct exposure to insecticides through dermal and nasal routes. OP and carbamate insecticide-induced inhibition of AChE leads to severe acute toxicity, including muscle dysfunction, neuronal dysfunction, respiratory arrest, and cardiac arrest. Additionally, muscle weakness due to acute insecticide exposure contributes significantly to morbidity and consumes healthcare resources such as hospital beds because of prolonged hospitalization[59]. The costs of hospitalization for OP insecticide poisoning have been reported in Sri Lankan and Bangladeshi studies[60–62]. The long-term exposure to insecticides is known to lead several adverse health effects, including risk of metabolic disorders, loss of neuromuscular function[63], neuropsychological performance[64], and neuropsychological dysfunction[13]. The usual protective headgear, facemasks, gloves, and suits are infrequently used due to high cost and discomfort under tropical conditions. Efforts have been made by other groups to develop metal nanoparticle-based active barrier creams[23,24]. However, those systems are not adopted for commercial use due to their potential to cause dermal toxicity. Alternatively, we have developed a *poly*-Oxime-based dermal gel that can efficiently deactivate insecticides to prevent dermal exposure[25]. Although the *poly*-Oxime dermal gel system is efficient, it has two limitations: (i) it cannot prevent exposure through the inhalation route, and (ii) potential non-compliance from agriculture workers as it must be applied all over the body each time they spray insecticides. Additionally, farmers' regular cotton fabric cloths do not prevent insecticide exposure. Earlier attempts to develop protective clothing relied on an adsorptive polyurethane layer impregnated with activated carbon for OPs adsorption[65]. However, such clothes cannot deactivate OPs and must be carefully handled and disposed-off to ensure safety. Cumulatively, the currently available solutions are not adequate to prevent insecticide exposure. Therefore, this critical unmet need encouraged us to develop a nucleophile-attached Oxime-fabric that catalytically hydrolyzes various insecticides upon contact.

a MPT aerosol (0.4 mg/L for 1 hour) — Breathing through Oxime Fabric / Breathing through Normal Fabric / Direct Breathing

72 hours post exposure collect blood and organs to quantify AChE

Active AChE

b BLOOD — Active AChE (U/ml); $P = 0.0253$; $P = 0.0073$; ns; Before/After Direct, Before/After Normal Fabric, Before/After Oxime Fabric

c BRAIN — Active AChE (U/g of tissue); ns; MPT → − + + +; Fabric → − − Normal Fabric Oxime Fabric

d LUNG — Active AChE (U/g of tissue); ns; $P = 0.0384$; $P = 0.0014$; ns; MPT → − + + +; Fabric → − − Normal Fabric Oxime Fabric

e LIVER — Active AChE (U/g of tissue); ns; ns; $P = 0.022$; ns; MPT → − + + +; Fabric → − − Normal Fabric Oxime Fabric

f KIDNEY — Active AChE (U/g of tissue); ns; ns; $P = 0.0325$; MPT → − + + +; Fabric → − − Normal Fabric Oxime Fabric

g HEART — Active AChE (U/g of tissue); ns; ns; $P = 0.0039$; $P = 0.0012$; ns; MPT → − + + +; Fabric → − − Normal Fabric Oxime Fabric

We have optimized a curing process to covalently attach silyl-pralidoxime to the cellulose of fabric to generate Oxime-fabric. The curing process was optimized in a way that the textile industry can adopt the same process using existing machinery to scale up manufacturing of Oxime-fabric in the future, without the need for huge upfront investment to build new infrastructure. Our data suggest that Oxime-fabric can chemically hydrolyze OPs and prevent insecticide-induced AChE inhibition in rat blood, ex vivo. Subsequently, even after 50 rounds of detergent washes, silyl-oxime did not leach from the fabric, and retained its activity to hydrolyze insecticides, suggesting the reusability of Oxime-fabric, which makes Oxime-fabric an economically viable option for agriculture workers. Oxime-fabric can hydrolytically deactivate carbamates and a wide range of commercially available OP formulations, including Macacid-50, Aalphos, Raise-505 and Profex Super. The activity of Oxime-fabric against a wide range of insecticides shows its robustness. Our data suggest that Oxime-fabric, when used as a bodysuit, can hydrolyze OP before it reaches the skin, thus preventing AChE inhibition in blood and internal organs,

Fig. 7 | Oxime-fabric prevents methyl parathion (MPT) exposure through inhalation route, in vivo. a Schematic of experimental design: MPT aerosols (0.4 mg/L for 1 h) were generated through a nebulizer that was connected to a closed chamber, where three groups of animals were restrained and inhaled MPT aerosols for 1 h. Fifteen Sprague-Dawley rats were randomly divided into three groups. Group 1 animals inhaled aerosols directly, while group 2 and 3 animals inhaled aerosols through normal and Oxime-fabric, respectively. **b** Active AChE was quantified before and after 72 h of post-exposure, and data showed that MPT aerosol exposure either directly or through normal fabric did not prevent MPT-induced AChE inhibition, while Oxime-fabric prevented inhibition of AChE.

c–g Three days post-exposure to MPT aerosols, animals were sacrificed, tissues were collected, and the amount of active AChE was quantified in brain (**c**), lung (**d**), liver (**e**), kidney (**f**), and heart (**g**). Nasal exposure of MPT directly or through normal fabric significantly reduced the active AChE in tissues. On the contrary, Oxime-fabric has deactivated the aerosol form of MPT and prevented MPT-induced inhibition of AChE. Data are mean ± s.d. ($n = 5$ rats per group). **b** P values were determined by two-tailed Student's t-test with Welch's correction, and for **c–g** by ordinary one-way ANOVA with Tukey's post hoc analysis by GraphPad PRISM 9, and exact P values are indicated. ns = not significant. Source data are provided as a Source Data file.

including the brain, lung, liver, kidney, and heart. Thus far, there are no examples of fabric-mediated insecticide hydrolysis and prevention of AChE inhibition in vivo. We have done a detailed cost-analysis of Oxime-fabric for commercial use. A comparison analysis between potential price of Oxime-fabric PPE and cost of various commercially available physical barrier PPEs to reduce chemical exposure suggest that Oxime-fabric PPE is cost-effective and affordable (see Supplementary Table S1 and analysis).

Exposure to insecticides causes muscle weakness and loss of endurance[48,59]. As farming demands intense physical activity from agriculture workers, insecticide-induced muscle weakness and loss of endurance can prevent farmers from working at their total capacity, hence, a drop in their productivity. In our preclinical models, a significant loss of endurance and neuromuscular coordination was observed when rats were exposed to insecticides directly or through the normal fabric. On the contrary, Oxime-fabric could deactivate insecticides and quantitatively prevent the loss of endurance, suggesting its potential use to protect agriculture workers from losing their productivity. Furthermore, through Gait analysis, we have demonstrated that Oxime-fabric can prevent insecticide-induced sciatic nerve damage and prevent perturbation of neuromuscular signaling at neuromuscular junctions, hence, can protect neuromuscular junctions. Due to frequent spraying, farmers repeatedly get exposed to insecticides, which causes chronic toxicity and severe adverse health effects[13,63,64]. When rats were repeatedly exposed to ethyl paraoxon directly, or through the normal fabric, all animals died within four days. In contrast, the same doses of repeated exposure through Oxime-fabric could not cause any mortality, and a 100% survival has been observed. Therefore, these results demonstrate the robustness and true catalytic nature of Oxime-fabric to hydrolyze insecticides.

Dermal absorption and respiratory inhalation are the primary routes of exposure to insecticides[66,67]. While applying volatile insecticide products, respiratory exposure occurs. However, for non-volatile insecticides, respiratory inhalation also occurs when insecticides are sprayed in an inhalable aerosol form[55]. Typically, in agriculture farming, approximately 10% of total insecticide exposure occurs through the nasal route, with the rest via dermal absorption[55]. Therefore, we have demonstrated that rats, when inhaling aerosol forms of OPs either directly or through a normal fabric mask, have shown insecticide-induced AChE inhibition. In contrast, the Oxime-fabric mask has prevented the entry of aerosol forms of insecticides and, hence, prevented the inhibition of AChE. The data suggest that Oxime-fabric can prevent insecticide exposure through the respiratory route.

In conclusion, we have developed an Oxime-fabric that hydrolyzes insecticides upon contact and significantly prevents OP and carbamate insecticide-induced AChE inhibition, thereby preventing insecticide exposure-caused muscle dysfunction, neuronal dysfunction, perturbed neuromuscular signaling, and mortality. Oxime-fabric-based bodysuits and facemasks can prevent insecticide exposure through dermal and inhalation routes. Oxime-fabric is highly scalable, washable, reusable, and affordable; therefore, it may increase compliance from agriculture workers and significantly improve their quality of life.

Methods

All the preclinical experiments presented in this study were performed in compliance with extant regulatory guidelines. All animal studies strictly adhered to institutional and national guidelines for humane animal use. The experimental protocols were approved by the Institutional Animal Ethics Committee (IAEC) at the Institute for Stem Cell Science and Regenerative Medicine (INS-IAS-2020/15(R1)). For all experiments, Sprague-Dawley albino rats at 10 to 14 weeks of age were used. Animals were provided by the animal house at the National Centre for Biological Sciences, Bengaluru. Animals were caged maximum 4 per cage before the experiment and individually after starting the experiment. Food and water were offered *ad libitum*.

Materials

Bromophenol blue sodium salt (BPB), Pralidoxime, (3-Chloropropyl) triethoxysilane (TCI), methyl parathion, ethyl paraoxon, cypermethrin, Sodium bicarbonate, Ethylene glycol, snake-skin dialysis membrane (MWCO-3500 Da, Thermo Fisher Scientific), Isoflurane (Isotroy), Triton X-100, Sodium dodecyl sulfate (SDS), 5,5'-dithiobis (2-nitrobenzoic acid) (DTNB), Acetylthiocholine iodide (AsChI), Ketamine, and Xylazine were used. Commercial formulations were purchased from local vendors. Macacid-50 (Methyl parathion 50%, Insecticides (India) Ltd., Chopanki, Rajasthan, India, Aalphos (Monocrotophos 36%, Agastya Agro Ltd., Muraharipally, Telangana, India), Raise-505 (Chlorpyrifos 50% + Cypermethrin 5% EC, Agastya Agro Ltd., Muraharipally, Telangana, India), and Profex Super (Profenofos 40% + Cypermethrin 4% EC, Nagarjuna Agrichem Ltd., Punjagutta, Hyderabad, India). Unless mentioned otherwise, all the chemicals were purchased from Sigma-Aldrich.

Synthesis of Silyl-oxime

A mixture of pralidoxime (16.38 mmol, 2 g, 1eq), (3-chloropropyl)triethoxysilane (16.38 mmol, 3.94 g, 1eq) and KI (8.19 mmol, 1.36 g, 0.5eq) were taken in 50ml acetone. The reaction mixture was refluxed at 55 °C with stirring for 48 h under an inert nitrogen atmosphere. Once the reaction was complete, the product precipitated upon cooling, and the solid precipitate was separated via filtration and subsequently washed with an excess of ice-cold acetone to eliminate any unreacted starting materials. After drying under vacuum conditions, 0.595 g (yielding 8%) of pure Silyl-Oxime was obtained as a white solid. ^1H-NMR (*DMSO-D6*, 800 MHz): δ: 13.17–13.16 (1H, *s*), 8.99–8.97 (1H, *d*), 8.77–8.76 (1H, *s*), 8.58–8.54 (1H, *t*), 8.45–8.42 (1H, *d*), 8.12–8.09 (1H, *t*), 4.73–4.67 (2H, *m*), 3.46–3.42 (6H, *q*), 1.90–1.84 (2H, *m*), 1.07–1.04 (9H, *t*). ^{13}C-NMR (*D2O, 150 MHz*): δ: 150.45, 149.14, 138.31, 125.19, 122.34, 59.37, 47.63, 25.38, 17.122, 6.67. Mass: m/z: 326.17.

Covalent functionalization of silyl-oxime on cellulose fabric

A 100 cm² of cotton fabric weighing 2 grams, with a density of 200 grams per square meter (GSM), was immersed in a 100 ml solution containing 1% sodium bicarbonate. The fabric was then heated to 100 °C for 1 h. Following this treatment, the fabric was thoroughly rinsed with an excess of water and allowed to air dry at room temperature Subsequently, 0.2 gram of silyl-oxime (10%, wt/wt w.r.t. fabric weight)

was dissolved in a 100 ml mixture of water and ethylene glycol (in a 60:40 ratio), and fabric was soaked in this solution for 3 h. After this soaking period, fabric was removed and allowed to air dry for 1 h. Following, it was subjected to a curing process at 70 °C for 30 min followed by an additional curing step at 120 °C for 20 min. Any unconjugated silyl-oxime was removed by washing the fabric with water. The amount of silyl-oxime covalently attached to the fabric was estimated using bromophenol blue assay. Additional characterization has been done using CP/MAS ^{13}C-NMR studies on a 400 MHz Jeol solid-state spectrometer.

Bromophenol blue assay
A Bromophenol Blue (BPB) assay was carried with a slightly modified version of known method[36,37]. A fabric sample with a known area of 9 cm^2, which had been functionalized, was soaked in 2 ml of BPB solution (10 mM). After soaking for 20 min, fabric was removed and thoroughly washed with regular water to ensure that there was no further leaching of BPB, and it was dried using tissue paper. Subsequently, 1.5 ml of a 1% SDS solution was employed to extract the dye from the fabric, resulting in a solution of dissolved dye. This solution was subjected to UV analysis to measure the absorption at 591 nm, allowing for the determination of the BPB concentration. Using a calibration curve, the concentration of BPB was calculated, which is equivalent to the concentration of silyl-oxime present on the fabric.

Detergent washing of Oxime-fabric
The Oxime-fabric (silyl-oxime attached fabric) was subjected to a delicate washing cycle which is widely available in commonly used washing machines. In delicate cycle setting, Oxime-fabric was washed for 7 mins with a mild non-ionic detergent (0.1%), which has slow washing and spinning. Between each cycle of washing, the fabric was rinsed with normal cold water and dried for 10 mins. Using this process, Oxime-fabric was washed for 10, 25, and 50 cycles, and subsequently, the amount of silyl-oxime on fabric and its activity to hydrolyze insecticide were tested using Franz diffusion assay after 10, 25, and 50 wash cycles.

Ex vivo efficacy of Oxime-fabric to prevent insecticide-induced AChE inhibition (Franz diffusion assay)
The dialysis membrane (MWCO 3500 Da) was hydrated overnight in the deionized water at room temperature. Subsequently, it was placed between the donor and acceptor compartments of the Franz diffusion cells (DBK Diffusion apparatus) and clamped to avoid any leakage. The experiment was carried out in three groups (membrane, normal fabric, and Oxime-fabric) comprising four diffusion cells in each set. Between two chambers, 10 cm^2 of either normal fabric or Oxime-fabric was placed on the dialysis membrane. Subsequently, the acceptor chamber was filled with 1000× diluted rat blood, and 1 ml of 2.5 μM MPT in phosphate buffer (pH 8) was added into the donor chamber. The temperature of acceptor chamber was maintained at 37 °C. Samples were collected at after 3 h and analyzed using modified Ellman's method[33] (as mentioned elsewhere) for AChE activity as a proxy for MPT exposure. Similarly, prior to MPT exposure, AChE activity was measure, which was considered as unexposed control. In Ellman's assay, we used 5,5′-Dithiobis(2-nitrobenzoic acid)(DTNB), and acetylthiocholine iodide (ASChI) which is specific for AChE. For the colorimetric assay, according to Ellman's method, reaction mixtures were made up of 0.1 mM phosphate buffer (pH 7.4) containing 0.5 mM DTNB and ASChI at a final concentration of 20 mM. The reaction was performed at 25 °C and monitored at 405 nm.

In vitro efficacy of Oxime-fabric to reduce permeation by hydrolyzing insecticide
Franz diffusion chamber was setup as descried in previous assay. In this assay, acceptor compartment was filled with Phosphate-Buffered Saline (PBS, pH 7.4) instead of rat blood. The experiment was carried out three groups (insecticide exposure through normal fabric or Hazmat suit fabric or Oxime-fabric) comprising four diffusion cells in each set. Between two chambers, 10 cm^2 of either normal fabric or Oxime-fabric was placed on the dialysis membrane. 1 μg of MPT was added in the donor chamber. The temperature of acceptor chamber was maintained at 37 ± 0.5 °C using a thermostatic water bath under constant stirring. Samples were withdrawn from acceptor (1 ml) and donor chamber (20 μl) at 1 and 180 mins, and an equal amount of phosphate buffer (pH 7.4) was replaced. The amount of MPT permeated through the membrane, and amount of *para*-nitrophenol formed at each time interval was analyzed by UFLC (Shimadzu, PDA: SPD-M20A, C18 reverse phase column: LC-20AD Prominence Chromatograph). MPT was detected using 60% Acetonitrile in double distilled water (DDW) as mobile phase at 1 ml/min, with a retention time of 5.5 min at 280 nm while maintaining the column at 40 °C. For detection of *para*-nitrophenol, we used 22% acetonitrile, % tri-ethylamine, and 1% tri-fluoro acetic acid in DDW as mobile phase at 0.5 ml/min flow rate through column maintained at 40 °C with a retention time of 3.6 min.

Protection from a single dose acute dermal exposure to methyl parathion (MPT), in vivo
SD rats (10 weeks) were randomized to three groups ($n = 5$ in each group): (i) direct exposure (MPT 150 mg/kg), (ii) normal fabric (10 × 8 cm, MPT 150 mg/kg), Oxime-fabric (10 × 8 cm, MPT 150 mg/kg). To maximize the contact of the fabric, the dorsal coat was clipped using a hair clipper under mild anesthesia (2.5% Isoflurane) 24 hrs prior to insecticide application taking care not to damage the integrity of the skin. Unless specified otherwise, the total area of 10 cm^2 was marked and used for dermal exposure experiments. Before the exposure, 2 μl of blood was collected for the initial active blood AChE quantification. The exposure was performed under mild anesthesia (2.5% isoflurane) for 90 min. After 72 h of post-exposure, animals were sacrificed, and blood and organs such as the brain, lungs, liver, kidney, and heart were collected for AChE quantification. Organ tissue was homogenized (Polytrion PTMR 2100, 1500 rpm) in nine volumes of solution D [1 M NaCl, 1% Triton X-100, 0.01 M Tris-HCl, 0.01 M EDTA (pH 7.4)] and incubated on ice for 1 h, followed by centrifugation at 1888 × g for 45 min. The supernatant was used to quantify the active AChE. The whole blood was diluted 1000× in phosphate buffer for the AChE quantification. The active AChE in blood and organs was quantified by modified Ellman's assay[36]. The active AChE in organs that were collected from the rats that were unexposed to MPT was considered an unexposed control.

Survival and AChE inhibition study in rats exposed to multiple dermal doses of Ethyl-paraoxon (EPx), in vivo
SD rats (11 weeks) were randomized to three groups ($n = 6$ rats per group): (i) direct exposure (no cloth), (ii) normal fabric (8 × 6 cm), Oxime-fabric (8 × 6 cm), and shaved dorsal hair before the experiment to maximize contact with fabric. In direct exposure group, on day 0, EPx (50 mg/kg/day) was given directly on the skin, and all animals died within 24 h. In normal fabric group, on day 0, 50 mg/kg/day of EPx was given on the top of fabric, and subsequently, from day 1 to 4, 25 mg/kg/day dose of EPx was given. All animals in group died before day 5. In Oxime-fabric group, on day 0, 50 mg/kg/day of EPx was given, and from day 1 to 5, 25 mg/kg/day dose of EPx was given, and animals in this group survived till the termination of the study (day 14). In all animals prior to exposure, 2 μl of blood was collected to quantify initial active blood AChE as an internal control. The insecticide exposure was performed under mild anesthesia (2.5% isoflurane) for 20 min. Immediately after mortality (group 1 and 2) or on the day 14 (group 3), animals were sacrificed, and their organs were collected to quantify AChE level as described above.

AChE inhibition study in rats exposed to aerosol form of MPT, in vivo

A custom-made polycarbonate and acrylic sheet chamber (40 cm width × 40 cm length × 10 cm height) was designed where the insecticide aerosols can be filled using a nebulizer, and restrained animals can inhale aerosols either directly or through the fabric, mimicking the facemask (Fig. 7a). The chamber was designed to expose 16 animals at once breathing the same aerosol to avoid any experimental differences. SD rats (10 weeks) were randomized into three groups ($n = 5$ rats per group): (i) direct inhalation (no mask) (ii) normal fabric mask, (iii) Oxime-fabric mask and connected to an aerosol chamber with only nose inside the chamber through a 3 cm diameter aperture (with or without fabric mask). MPT (0.4 mg/L) aerosols were generated through flow rate of 6.8 L/min, nebulization rate of 0.3 ml/min using a nebulizer (Model: CNB69011). The exposure was performed under anesthesia (Ketamine 91 mg/kg and Xylazine 9.1 mg/kg were administered intraperitoneally) for 1 h. After 72 h of post-exposure, animals were sacrificed, and their organs and blood were collected to quantify AChE level as described above.

Gait analysis and electromyogram

Gait analysis was performed on 15 male rats (10 weeks) to evaluate their walking pattern. To get footprints, four paws were colored with different non-toxic watercolors, and the animal was trained to walk through an ally (8 cm width, 120 cm length, and 10 cm height) leading to its home cage. After training, animals were divided randomly into three groups, (i) direct exposure, (ii) normal fabric, and (iii) Oxime-fabric. Footprints were analyzed manually, and Sciatic functional index (SFI) was calculated using following formula[44,45].

$$SFI = \left[\left(\frac{ETOF - NTOF}{NTOF} \right) + \left(\frac{NPL - EPL}{EPL} \right) + \left(\frac{ETS - NTS}{NTS} \right) + \left(\frac{EIT - NIT}{NIT} \right) \right] \frac{220}{4}$$

Where, N indicates normal/before exposure and E indicates after exposure, TOF: distance to opposite foot; PL: distance from the heel to the third toe, the print length; TS: distance from the first to the fifth toe, the toe spread; IT: distance from the second to the fourth toe, the intermediate toe spread. SFI values were calculated before and 72 h post MPT exposure.

EMG of animals from these three groups and unexposed animals was recorded using a Muscle-Spiker box (Backyard Brains®). Skin surface electrodes were used with adhesive pads and conductive gel to facilitate the recordings. To track the muscle spasms, we recorded EMG between *spinotrapezius* and *Gluteus maximus* when the animal was awake.

Rotarod test

Total 10 male SD rats (10 weeks) were used to study loss of endurance in MPT-exposed animals and ability of Oxime-fabric to prevent the same. Animals were placed on a Rotarod treadmill (Columbus Instruments; Rotamex-5 1.4, lane width: 9.3 cm, diameter of rod: 7 cm, fall distance: 48.3 cm) and were subjected to a uniform increase in acceleration between 0 to 20 rpm and were allowed to run at 20 rpm as till the animal got tired and fell off the rod, and time of fall was recorded. Rats were trained for 4 days before the exposure where animals were randomly grouped into two groups (i) normal fabric, and (ii) Oxime-fabric. On day 4, in both groups animals were exposed to MPT (150 mg/kg) either through normal fabric or Oxime-fabric. Subsequently, latency to fall was calculated as a time taken to fall on any day with respect to day 4 (before exposure) and was converted to percentage. Simultaneously, Gait analysis was performed on the same 10 animals on day 4 (prior to MPT exposure) and measured SFI as described above. Post MPT exposure, every 24 h SFI was calculated for 72 h.

Statistical analyses and reproducibility

In experiments with multiple groups, ordinary one-way ANOVA with Tukey's post hoc test was used. In experiments with multiple groups, which are time-course studies, repeated measures of one-way ANOVA were used. The two-tailed Student's t test with Welch's corrections was used to compare two experimental groups. In survival experiments, Mantel–Cox test was used. The probability value (P) < 0.05 was considered as a statistically significant difference. Statistical analysis and graphing were performed with GraphPad PRISM 9. Data presented in this manuscript is reproducible, data collected from at least $n = 4$, from three independent experiments.

Reporting summary

Further information on research design is available in the Nature Portfolio Reporting Summary linked to this article.

Data availability

All data generated or analyzed during this study are included in this published article and its supplementary information files or are available from the corresponding author upon request. Source Data is provided as a FigShare repository. Source data are provided with this paper.

References

1. Eddleston, M., Buckley, N. A., Eyer, P. & Dawson, A. H. Medical management of acute organophosphorus pesticide poisoning. *Lancet* **371**, 597–607 (2008).
2. Mew, E. J. et al. The global burden of fatal self-poisoning with pesticides 2006-15: systematic review. *J. Affect. Disord.* **219**, 93–104 (2017).
3. Boedeker, W., Watts, M., Clausing, P. & Marquez, E. The global distribution of acute unintentional pesticide poisoning: estimations based on a systematic review. *BMC Public Health* **20**, 1875 (2020).
4. Koelle, G. B. The histochemical localization of cholinesterases in the central nervous system of the rat. *J. Comp. Neurol.* **100**, 211–235 (1954).
5. Brightman, M. W. & Albers, R. W. Species differences in the distribution of extraneuronal cholinesterases within the vertebrate central nervous system. *J. Neurochem.* **4**, 244–250 (1959).
6. Speed, H. E. et al. Delayed reduction of hippocampal synaptic transmission and spines following exposure to repeated subclinical doses of organophosphorus pesticide in adult mice. *Toxicol. Sci.* **125**, 196–208 (2012).
7. Campos, E., dos Santos Pinto da Silva, V., Sarpa Campos de Mello, M. & Barros Otero, U. Exposure to pesticides and mental disorders in a rural population of Southern Brazil. *Neurotoxicology* **56**, 7–16 (2016).
8. Damalas, C. A. & Koutroubas, S. D. Farmers' exposure to pesticides: toxicity types and ways of prevention. *Toxics* **4**, 1 (2016).
9. Jørs, E., Neupane, D. & London, L. Pesticide poisonings in low- and middle-income countries. *Environ. Health Insights* **12**, 1–3 (2018).
10. Mancini, F., Van Bruggen, A. H., Jiggins, J. L., Ambatipudi, A. C. & Murphy, H. Acute pesticide poisoning among female and male cotton growers in India. *Int. J. Occup. Environ. Health* **11**, 221–232 (2005).
11. Tomenson, J. A. & Matthews, G. A. Causes and types of health effects during the use of crop protection chemicals: data from a survey of over 6,300 smallholder applicators in 24 different countries. *Int. Arch. Occup. Environ. Health* **82**, 935–949 (2009).
12. Burchfiel, J. L. & Duffy, F. H. Organophosphate neurotoxicity: chronic effects of sarin on the electroencephalogram of monkey and man. *Neurobehav. Toxicol. Teratol.* **4**, 767–778 (1982).
13. Rosenstock, L., Keifer, M., Daniell, W. E., McConnell, R. & Claypoole, K. Chronic central nervous system effects of acute

organophosphate pesticide intoxication. The pesticide health effects study group. *Lancet* **338**, 223–227 (1991).

14. Jokanovic, M., Oleksak, P. & Kuca, K. Multiple neurological effects associated with exposure to organophosphorus pesticides in man. *Toxicology* **484**, 153407 (2023).

15. González-Alzaga, B. et al. Pre- and postnatal exposures to pesticides and neurodevelopmental effects in children living in agricultural communities from South-Eastern Spain. *Environ. Int.* **85**, 229–237 (2015).

16. Bouchard, M. F. et al. Prenatal exposure to organophosphate pesticides and IQ in 7-year-old children. *Environ. Health Perspect.* **119**, 1189–1195 (2011).

17. Chang, F. K., Chen, M. L., Cheng, S. F., Shih, T. S. & Mao, I. F. Field protection effectiveness of chemical protective suits and gloves evaluated by biomonitoring. *Occup. Environ. Med.* **64**, 759–762 (2007).

18. Singh, B. & Gupta, M. K. Pattern of use of personal protective equipments and measures during application of pesticides by agricultural workers in a rural area of Ahmednagar district, India. *Indian J. Occup. Environ. Med.* **13**, 127–130 (2009).

19. MacFarlane, E., Carey, R., Keegel, T., El-Zaemay, S. & Fritschi, L. Dermal exposure associated with occupational end use of pesticides and the role of protective measures. *Saf. Health Work* **4**, 136–141 (2013).

20. Chilcott, R. P. et al. Evaluation of a barrier cream against the chemical warfare agent VX using the domestic white pig. *Basic Clin. Pharmacol. Toxicol.* **97**, 35–38 (2005).

21. Millerioux, J. et al. In vitro selection and efficacy of topical skin protectants against the nerve agent VX. *Toxicol. In Vitro* **23**, 539–545 (2009).

22. Bignon, C., Amigoni, S., Devers, T. & Guittard, F. Barrier cream based on CeO2 nanoparticles grafted polymer as an active compound against the penetration of organophosphates. *Chem. Biol. Interact.* **267**, 17–24 (2017).

23. Salerno, A. et al. In vitro skin decontamination of the organophosphorus pesticide paraoxon with nanometric cerium oxide CeO2. *Chem. Biol. Interact.* **267**, 57–66 (2017).

24. Zenerino, A. et al. New CeO2 nanoparticles-based topical formulations for the skin protection against organophosphates. *Toxicol. Rep.* **2**, 1007–1013 (2015).

25. Thorat, K. et al. Prevention of pesticide-induced neuronal dysfunction and mortality with nucleophilic poly-Oxime topical gel. *Sci. Adv.* **4**, eaau1780 (2018).

26. Auffan, M. et al. CeO2 nanoparticles induce DNA damage towards human dermal fibroblasts in vitro. *Nanotoxicology* **3**, 161–171 (2009).

27. Benameur, L. et al. DNA damage and oxidative stress induced by CeO2 nanoparticles in human dermal fibroblasts: Evidence of a clastogenic effect as a mechanism of genotoxicity. *Nanotoxicology* **9**, 696–705 (2015).

28. Eyer, P. The role of oximes in the management of organophosphorus pesticide poisoning. *Toxicol. Rev.* **22**, 165–190 (2003).

29. Aktar, Md, W., Sengupta, D. & Chowdhury, A. Impact of pesticide use in agriculture: their benefits and hazards. *Interdiscip. Toxicol.* **2**, 1–12 (2009).

30. Agnihotri, N. P. Pesticides consumption in agriculture in India – un update. *Pestic. Res. J.* **12**, 150–155 (2000).

31. Yang, Y. C., Szafraniec, L. L., Beaudry, W. T. & Bunton, C. A. Perhydrolysis of nerve agent VX. *J. Org. Chem.* **58**, 6964–6965 (1993).

32. Toullec, J. & Moukawim, M. Cetyltrimethylammonium hydroperoxide: an efficient reagent for promoting phosphate ester hydrolysis. *Chem. Commun.* **2**, 221–222 (1996).

33. Bhattacharya, S. & Kumar, V. P. Evidence of enhanced reactivity of DAAP nucleophiles toward dephosphorylation and deacylation reactions in cationic Gemini micellar media. *J. Org. Chem.* **69**, 559–562 (2004).

34. Bhattacharya, S. & Kumar, V. P. Ester cleavage properties of synthetic hydroxybenzotriazoles in cationic monovalent and gemini surfactant micelles. *Langmuir* **21**, 71–78 (2005).

35. Kumar, V. P., Ganguly, B. & Bhattacharya, S. Computational study on hydroxybenzotriazoles as reagents for ester hydrolysis. *J. Org. Chem.* **69**, 8634–8642 (2004).

36. Yamamoto, K. Sensitive determination of quaternary ammonium salts by extraction-spectrophotometry of ion associates with bromophenol blue anion and coextraction. *Anal. Chem. Acta* **302**, 75–79 (1995).

37. Burel, C., Direur, G., Rivas, C. & Purevdorj-Gage, L. Colorimetric detection of residual quaternary ammonium compounds on dry surfaces and prediction of antimicrobial activity using bromophenol blue. *Lett. Appl. Microbiol.* **72**, 358–365 (2021).

38. Nam, D. C., Ha, Y. M., Park, M. K. & Cho, S. K. The rs662 polymorphism of paraoxonase 1 affects the difference in the inhibition of butyrylcholinesterase activity by organophosphorus pesticides in human blood. *Int. J. Clin. Pharmacol. Ther.* **54**, 622–627 (2016).

39. Worek, F., Eyer, P. & Thiermann, H. Determination of acetylcholinesterase activity by the Ellman assay: a versatile tool for in vitro research on medical countermeasures against organophosphate poisoning. *Drug Test. Anal.* **4**, 282–291 (2012).

40. Dawson, A. H. et al. Acute human lethal toxicity of agricultural pesticides: a prospective cohort study. *PLOS Med.* **7**, e1000357 (2010).

41. World Health Organization. *The WHO recommended classification of pesticides by hazard and guidelines to classification 2009*, 1–60 (World Health Organization, 2010).

42. Walker, J. L., Evans, J. M., Meade, P., Resig, P. & Sisken, B. F. Gait-stance duration as a measure of injury and recovery in the rat sciatic nerve model. *J. Neurosci. Methods* **52**, 47–52 (1994).

43. Baptista, A. F. et al. A new approach to assess function after siatic nerve lesion in the mouse – adaptation of the sciatic static index. *J. Neurosci. Methods* **161**, 259–264 (2007).

44. deMedinaceli, L., Freed, W. J. & Wyatt, R. J. An index of the functional condition of rat sciatic nerve based on measurements made from walking tracks. *Exp. Neurol.* **77**, 634–643 (1982).

45. Sarikcioglu, L., Demirel, B. M. & Utuk, A. Walking track analysis: an assessment method for functional recovery after sciatic nerve injury in the rat. *Folia Morphol.* **68**, 1–7 (2009).

46. Spyker, J. M. & Avery, D. L. Neurobehavioral effects of prenatal exposure to the organophosphate Diazinon in mice. *J. Toxicol. Environ. Health* **3**, 989–1002 (1977).

47. Stamper, C. R., Balduini, W., Murphy, S. D. & Costa, L. G. Behavioral and biochemical effects of postnatal parathion exposure in the rat. *Neurotoxicol. Teratol.* **10**, 261–266 (1998).

48. Karalliedde, L. & Henry, J. A. Effects of organophosphates on skeletal muscle. *Hum. Exp. Toxicol.* **12**, 289–296 (1993).

49. Buttemer, W. A., Story, P. G., Fildes, K. J., Baudinette, R. V. & Astheimer, L. B. Fenitrothion, an organophosphate, affects running endurance but not aerobic capacity in fat-tailed dunnarts (*Sminthopsis crassicaudata*). *Chemosphere* **72**, 1315–1320 (2008).

50. Zhu, H., Rockhold, R. W., Baker, R. C., Kramer, R. E. & Ho, I. K. Effects of single or repeated dermal exposure to methyl parathion on behavior and blood cholinesterase activity in rats. *J. Biomed. Sci.* **8**, 467–474 (2001).

51. Maroni, M., Fait, A. & Colosio, C. Risk assessment and management of occupational exposure to pesticides. *Toxicol. Lett.* **107**, 145–153 (1999).

52. Woodruff, T. J., Kyle, A. D. & Bois, F. Y. Evaluating health risks from occupational exposure of pesticides and the regulatory response. *Environ. Health Perspect.* **102**, 1088–1096 (1994).

53. Maroni, M., Fanetti, A. C. & Metruccio, F. Risk assessment and management of occupational exposure to pesticides in agriculture. *Med. Lav.* **97**, 430–437 (2006).

54. Edson, E. F. & Noakes, D. N. The comparative toxicity of six organophosphorus insecticides in the rat. *Toxicol. Appl. Pharmacol.* **2**, 523–539 (1960).

55. Dowling, K. C. & Seiber, J. N. Importance of respiratory exposure to pesticides among agricultural populations. *Int. J. Toxicol.* **21**, 371–381 (2002).

56. Igbedioh, S. O. Effects of agricultural pesticides on humans, animals and higher plants in developing countries. *Arch. Environ. Health Int. J.* **46**, 218–224 (1991).

57. Gunnell, D., Eddleston, M., Phillips, M. R. & Konradsen, F. The global distribution of fatal pesticides self-poisoning: Systematic review. *BMC Public Health* **7**, 357 (2007).

58. Patel, V. et al. Suicide mortality in India: a nationally representative survey. *Lancet* **379**, 2343–2351 (2012).

59. Jayawardane, P. et al. The spectrum of intermediate syndrome following acute organophosphate poisoning: a prospective cohort study from Sri Lanka. *PLoS Med.* **5**, e147 (2008).

60. Wickramasinghe, K. et al. Cost to government health-care services of treating acute self-poisonings in a rural district in Sri Lanka. *Bull. World Health Organ.* **87**, 180–185 (2009).

61. Verma, V., Paul, S., Ghose, A., Eddleston, M. & Konradsen, F. Treatment of self-poisoning at a tertiary-level hospital in Bangladesh: cost to patients and government. *Trop. Med. Int. Health* **22**, 1551–1560 (2017).

62. Ahrensberg, H. et al. Estimating the government health-care cost of treating pesticide poisoned and pesticide self-poisoned patients in Sri Lanka. *Glob. Health Action.* **12**, 1692616 (2019).

63. Peiris-John, R. J., Ruberu, D. K., Wickremasinghe, A. R., Smit, L. A. M. & van der Hoek, W. Effects of occupational exposure to organophosphate pesticides on nerve and neuromuscular function. *J. Occup. Environ. Med.* **44**, 352–357 (2002).

64. Fiedler, N., Kipen, H., Kelly-McNeil, K. & Fenske, R. Long-term use of organophosphates and neuropsychological performance. *Am. J. Ind. Med.* **32**, 487–496 (1997).

65. Crawford, D. M. & Escarsega, J. A. Dynamic mechanical analysis of novel polyurethane coating for military applications. *Thermocim. Acta* **357–358**, 161–168 (2000).

66. Damalas, C. A. & Eleftherohorinos, I. G. Pesticide exposure, safety issues, and risk assessment indicators. *Int. J. Environ. Res. Public Health* **8**, 1402–1419 (2011).

67. Maestrelli, P., Boschetto, P., Fabbri, L. M. & Mapp, C. E. Mechanisms of occupational asthma. *J. Allergy Clin. Immunol.* **123**, 531–544 (2009).

Acknowledgements

Author contributions

P.K.V. conceived and designed the experiments. M.K.M., K.T., T.P.P., O.S., S.C., V.R., R.K., A.S., H.M. designed, performed the experiments, and analyzed the data. M.K.M., T.P.P., S.C., V.R., H.M., R.K. synthesized compounds and functionalized fabric. M.K.M., K.T., O.S., V.R., R.K., A.S. performed in vitro and in vivo experiments. P.K.V. wrote the manuscript, and all authors discussed the results and revised the manuscript. P.K.V. supervised the project.

Competing interests

P.K.V., K.T., and S.C. hold patents related to this technology: "Composition, materials, and methods for deactivating toxic agents" (Granted Indian patent: 201841006678 and granted Sri Lankan Patent # 20419). All compositions and methods of use described in this manuscript were covered in the patent applications. P.K.V., K.T., and S.C. are inventors of patents that were licensed to Sepio Health, a company that has licensed IP generated by P.K.V., K.T., and S.C., that may benefit financially if the IP is further validated. The interests of P.K.V. were reviewed and are subject to a management plan overseen by his institution in accordance with its conflict of interest policies. P.K.V. and O.S. are equity holders in Sepio Health. The remaining authors declare no competing interests.

Additional information

Supplementary information The online version contains supplementary material available at https://doi.org/10.1038/s41467-024-49167-3.

Correspondence and requests for materials should be addressed to Praveen Kumar Vemula.

Peer review information *Nature Communications* thanks Michael Eddleston, and the other, anonymous, reviewer(s) for their contribution to the peer review of this work. A peer review file is available.

Reprints and permissions information is available at http://www.nature.com/reprints

Publisher's note Springer Nature remains neutral with regard to jurisdictional claims in published maps and institutional affiliations.

Prevention of pesticide-induced neuronal dysfunction and mortality with nucleophilic poly-Oxime topical gel

Ketan Thorat[1,2], Subhashini Pandey[1,3], Sandeep Chandrashekharappa[1], Nikitha Vavilthota[1], Ankita A. Hiwale[1], Purna Shah[1], Sneha Sreekumar[1], Shubhangi Upadhyay[1], Tenzin Phuntsok[1], Manohar Mahato[1], Kiran K. Mudnakudu-Nagaraju[1], Omprakash Sunnapu[1], Praveen K. Vemula[1,4]*

Organophosphate-based pesticides inhibit acetylcholinesterase (AChE), which plays a pivotal role in neuromuscular function. While spraying in the field, farmworkers get exposed to pesticides through the dermal route. Internalized pesticide inhibits AChE, which leads to neurotoxicity, cardiotoxicity, cognitive dysfunction, loss of endurance, and death in severe cases. Here, we present a nucleophilic pyridine-2-aldoxime–functionalized chitosan-based topical gel (*poly*-Oxime gel) that rapidly deactivates organophosphates, methyl parathion (MPT), on the skin of rats, which leads to reduced AChE inhibition in the blood and tissues. Testing the robustness of *poly*-Oxime gel, we report reduction in AChE inhibition following repeated dermal administration of MPT in the presence of *poly*-Oxime gel. Furthermore, *poly*-Oxime gel prevented MPT-induced neuromuscular dysfunction, loss of endurance, and locomotor coordination. We observe a 100% survival in rats following topical MPT administration in the presence of *poly*-Oxime gel. This prophylactic gel may therefore help farmworkers by limiting pesticide-induced toxicity and mortality.

INTRODUCTION

Acetylcholinesterase (AChE) is abundant in both central and peripheral nervous system (*1, 2*). In addition to chemical warfare agents (CWAs), organophosphate pesticides [such as methyl parathion (MPT), malathion, paraoxon, and chlorpyrifos] are AChE inhibitors. Inhibition of AChE leads to the accumulation of the neurotransmitter acetylcholine, resulting in neurological disorders, suffocation, paralysis, and death in severe cases (*3, 4*). India is one of the prime countries in pesticide usage in the world, with a vast majority of agricultural workers being repeatedly exposed to pesticides in the field (*5, 6*). In addition to neurotoxic effects, AChE inhibition leads to cardiotoxicity, reduced immunity, infertility, and delayed sexual maturation (*7*). Cohort studies reveal that pre- and postnatal exposures to pesticides impede neurodevelopment in children living in agricultural communities and increase susceptibility to neuropsychiatric disorders (*8, 9*).

According to the World Health Organization (WHO) Recommended Classification of Pesticides by Hazard, organophosphate pesticides oxydemeton-methyl and methamedophos belong to class I (extremely/highly hazardous); dimethoate, fenthion, quinalphos, chlorpyrifos, prothiofos, and diazinon belong to class II (moderately hazardous); and malathion and pirimifos-methyl belong to class III (slightly hazardous) (*10, 11*). It is clear that systemic exposure to pesticides through the dermal route is a health hazard. Preventive strategies to eliminate or minimize dermal exposure to reduce pesticide-induced toxicity are a less attended clinical need. Although the personal protective equipment (PPE) such as suits, gloves, face masks, headgear, and boots are available, they are scarcely used, mainly because of high cost and discomfort under tropical conditions (*12–14*). The most effective way to prevent pesticide exposure is chemical deactivation of pesticides, and existing PPE lack this ability. There have been attempts to formulate physical barrier creams in the past to attenuate exposure to pesticides or CWAs (*15–17*). This design comes with an inherent limitation of expo-sure, as the pesticide that is arrested on the surface can still enter the system through the oral or ocular route via hand contact. In addition, each pesticide brand has different additive formulations, and these formulations have variable penetrance through physical barrier creams. The noncatalytic nature of this approach also limits the amount of pesticide the barrier creams can arrest. Therefore, physical barrier creams are not effective in preventing exposure. The metal nanoparticles, like CeO_2, are studied as potential chemical deactivators of pesticides/CWAs (*18, 19*). However, CeO_2 nanoparticles are known to cause DNA damage in dermal fibroblasts, an effect that necessarily limits their use in dermal protectants (*20, 21*).

To understand the awareness of agricultural workers about the pesticide-induced toxicity, we interacted with several farmers and their families in the field. All of them were aware of pesticide-induced toxicity, as they experience pain right after they spray pesticides in the field. However, because of the lack of any protective technologies, they suffer, and they expressed their willingness to adopt any topical technologies that can prevent pesticide exposure. Because of the low purchasing power of this sector, the affordable cost would be a key differentiating factor to have compliance to adopt these technologies by the end user—the farmer. This unmet need inspired us to develop prophylactic technologies to prevent pesticide exposure during spraying in the field. An ideal user-compliant solution would be a low-cost, easy-to-use, nonobstructive biocompatible material, which could inactivate pesticides on the skin and prevent their penetration. A topical gel with catalytic activity to cleave/hydrolyze pesticides before entering into the skin may serve as a prophylactic strategy to reduce chronic exposure (Fig. 1A). The aim/objective of this study was to determine whether a nucleophilic pyridine-2-aldoxime–functionalized chitosan-based topical gel (*poly*-Oxime gel) could be used as a prophylactic gel to deactivate pesticides on the skin before they enter the body. However, multiple technical hurdles exist in designing this catalytically robust prophylactic topical gel. The first is the identification of a reactive nucleophile that can act by rapidly hydrolyzing organophosphate ester on the skin before it enters. Also, it should catalytically, not stoichiometrically, cleave organophosphates. Second, the topical gel should be chemically active in different climate conditions to be effective in tropical and cold countries.

[1]Institute for Stem Cell Biology and Regenerative Medicine (inStem), GKVK Campus, Bellary Road, Bangalore, 560065 Karnataka, India. [2]Manipal Academy of Higher Education, Manipal, 576104 Karnataka, India. [3]The University of Trans-Disciplinary Health Sciences and Technology, Attur (post), Yelahanka, Bangalore, 560064 Karnataka, India. [4]Ramalingaswami Re-entry Fellow, Department of Biotechnology, New Delhi, India.
*Corresponding author. Email: praveenv@instem.res.in
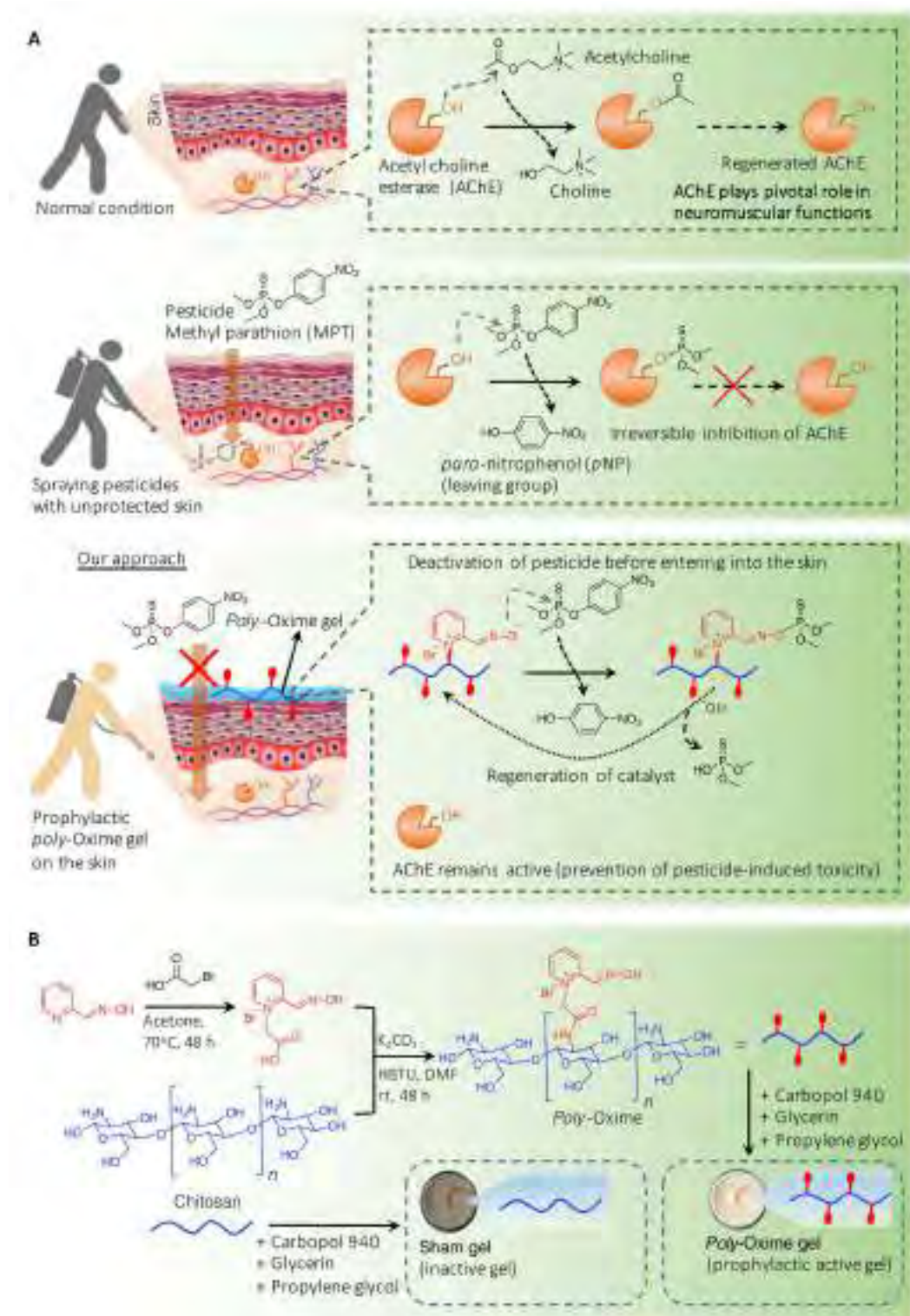
Fig. 1. Nucleophilic *poly*-Oxime gel to deactivate pesticides to limit toxicity. (**A**) Dermal penetration of pesticide (MPT) leads to the inhibition of AChE, which plays a pivotal role in biological functions including neuronal signaling and neuromuscular coordination (NMC). MPT-mediated inhibition of AChE leads to severe toxicity including neuromuscular dysfunction, loss of endurance, and locomotor function. In our approach, the presence of α-nucleophile (an oxime) attached polymer (*poly*-Oxime) formulated as a topical gel could deactivate organophosphorus ester, MPT, through hydrolysis. This limits MPT penetration into the skin, which leads to the reduction of pesticide-induced toxicity. (**B**) Synthesis of *poly*-Oxime using pyridine-2-aldoxime connected to chitosan through acetamide linker. With humectants like glycerin, propylene glycol, and carbopol 940, topical gel was prepared. Two types of topical gels, *poly*-Oxime–containing active gel and, as a control, unfunctionalized chitosan–containing inactive sham gel, were prepared. rt, room temperature; DMF, N,N′-dimethylformamide.

Here, we present a nucleophilic topical gel (*poly*-Oxime) that is capable of catalytically deactivating organophosphates efficiently on the skin, thereby reducing inhibition of AChE quantitatively and limiting pesticide-induced toxicity and mortality. The *N*-hydroxy α-nucleophile–containing *poly*-Oxime was converted into a gel by addition of excipients like carbopol 940, glycerin, and propylene glycol (Fig. 1B). This α-nucleophile–based topical gel solves the aforementioned challenges. A direct dermal exposure of a widely used pesticide, MPT, in rats significantly inhibited the activity of AChE in blood, brain, lung, liver, and heart. A single-dose dermal exposure of MPT (150 mg/kg) in rats dampened the locomotor coordination function, altered neuromuscular signaling, and led to death with a median survival time of 4 days. The same dose of MPT in the presence of *poly*-Oxime topical gel did not induce any adverse effects, and a 100% survival was observed.

RESULTS

Synthesis of *poly*-Oxime gel and deactivation of pesticides in vitro and ex vivo

Most pesticides are organophosphate esters. Thus, a nucleophile-mediated ester hydrolysis is an efficient way to deactivate pesticides. α-Nucleophiles are known as efficient groups for hydrolytic cleavage of organophosphates (*22–24*). Oxime (*N*-hydroxy compound) is a potent α-effect *O*-nucleophile (*25, 26*). Therefore, we reasoned that pyridine-2-aldoxime would be a powerful α-nucleophile, which can be functionalized on a biopolymer, chitosan (Fig. 1B). Chitosan, a biocompatible polymer, has been extensively used to develop a wide range of biomaterials (*27, 28*). Conjugation of pyridine-2-aldoxime to chitosan through an acetamide linker in solution phase generated *poly*-Oxime (Fig. 1B and Supplementary Methods). The degree of functionalization was 40%. A detailed characterization of *poly*-Oxime is given in the Supplementary Materials. The kinetics of MPT hydrolysis was obtained by monitoring the appearance of *p*-nitrophenoxide spectrophotometrically at 400 nm (Fig. 1A and see Materials and Methods). The soluble *poly*-Oxime polymer was used to study the catalytic activity toward decontamination of different pesticides. The observed pseudo–first-order (k_{obs}) values for the cleavage of MPT, paraoxon, and chlorpyrifos were 4.59×10^{-4}, 2.28×10^{-4}, and 5.55×10^{-4} s^{-1}, respectively. Data in table S1 show that *poly*-Oxime is an effective catalyst for the hydrolytical deactivation of multiple organophosphates, in that they afford more than two orders of magnitude rate enhancement over the background reaction. *Poly*-Oxime also showed activity at different temperatures (at 20°C, $k_{obs} = 3.37 \times 10^{-4}$ s^{-1}; at 30°C, $k_{obs} = 7.18 \times 10^{-4}$ s^{-1}; at 40°C, $k_{obs} = 17.57 \times 10^{-4}$ s^{-1}).

To evaluate the ability of *poly*-Oxime gel to prevent pesticide penetration into the skin, we formulated the *poly*-Oxime (2%, w/w) into a topical gel using the following additives: glycerin (6.8%, w/w), propylene glycol (3.74%, w/w), and carbopol 940 (1.8%, w/w; see Materials and Methods). Sham gel, as a control, was prepared using the same composition, with unmodified chitosan replacing the *poly*-Oxime. Both gels have shown standard gel-like behavior in rheology studies (fig. S1) and could be applied to the skin. A temperature-dependent rheology studies at 25°, 35°, and 45°C with *poly*-Oxime gel revealed that at higher temperatures, it maintains its gel-like behavior but becomes softer as seen in the reduction in G' values (fig. S1, C to E). The fact that, in linear viscoelastic range, all the gels showed $G' > G''$ suggests that they behave like viscoelastic solids or gels. Carbopol 940 is a hydrophilic colloidal gum that offers a high thickening gel property due to water absorption,

leading to the formation of macroscopic swollen particles. This formation is attributed to hydrogen bonding between carboxylic groups of the polymer and water molecules. The observed softening of gel upon addition of the *poly*-Oxime polymer could be explained because of charges in quaternary *N* and deprotonated oxime groups that promote electrostatic interaction with solvent, rather than hydrogen bonding. This might result in reduced solvent interaction in terms of hydrogen bonding and thus formation of softer gels. Franz diffusion apparatus was used to mimic the transdermal penetration (Fig. 2A). The uncoated dialysis membrane [molecular weight cutoff (MWCO), 3.5 kDa] or the membrane coated with a thin layer of sham gel or *poly*-Oxime gel was placed between donor and acceptor chambers. Subsequently, MPT was added into the donor chamber and the acceptor chamber was filled with phosphate-buffered saline (PBS). The chamber's temperature was maintained at 37°C. At different time points (0, 0.25, 0.5, 1, 2, 3, 4, and 5 hours), the concentration of MPT and its hydrolytically degraded product *p*-nitrophenol (*p*NP) was quantified in both donor and acceptor chambers using ultrafast liquid chromatography (UFLC; Fig. 2, B to E). In the presence of the uncoated membrane or sham gel–coated membrane, MPT was quantitatively penetrated into the acceptor chamber within 3 hours, whereas *poly*-Oxime gel prevented MPT penetration (Fig. 2, B and C). It suggests that sham gel does not act as a physical barrier and MPT can easily pass through the gel. Data in Fig. 2 (D and E) show that *poly*-Oxime gel was able to degrade MPT into *p*NP, which was quantified in both donor and acceptor chambers. After 3 hours, the deactivation was nearly complete and the *p*NP that formed in the donor compartment started to diffuse into the acceptor compartment. *p*NP was not generated in any of those chambers in the absence of *poly*-Oxime gel. These results suggest that *poly*-Oxime gel prevents the penetration of MPT, not as a physical barrier but through chemically hydrolyzing MPT.

Organophosphates are known to inhibit AChE in blood (*29*). An ex vivo assay was carried out using rat blood in Franz diffusion cell to evaluate the ability of *poly*-Oxime gel to limit MPT-induced AChE inhibition (Fig. 2F). Akin to the previous experiment, three groups were taken (uncoated, sham gel, and *poly*-Oxime gel–coated membranes between both chambers) along with the no MPT group, 1000× diluted rat blood was taken in the acceptor chamber, and the percentage of the AChE activity was quantified using modified colorimetric Ellman's assay (see Materials and Methods) (*30*). In the absence of MPT, no change was observed in the activity of AChE after 3 hours (Fig. 2G). The addition of MPT (1 μM) in the donor chamber led to a significant inhibition of AChE activity in blood. The presence of native membrane or sham gel–coated membrane did not limit MPT-mediated AChE inhibition (Fig. 2G). On the contrary, *poly*-Oxime gel deactivated MPT before entering into the acceptor chamber, thereby completely reducing MPT-induced inhibition of blood AChE activity. *Poly*-Oxime gel could hydrolytically cleave a wide range of commercial organophosphate formulations (fig. S2). Under similar reaction conditions, sham gel, which was made with native chitosan without oxime groups, did not deactivate pesticides, suggesting that *poly*-Oxime α-nucleophile is essential for the reactivity (fig. S2). These results suggest that *poly*-Oxime gel could limit pesticide-induced AChE inhibition by chemically deactivating organophosphates.

To validate the role of the oxime group in imparting the ability to limit pesticide exposure, we blocked the active oxime group with methyl ether. *O*-methoxy pyridine-2-aldoxime (methoxyOxime) was covalently attached to chitosan (*poly*-methoxyOxime) using the same process that was used for the *poly*-Oxime polymer (a detailed synthesis protocol
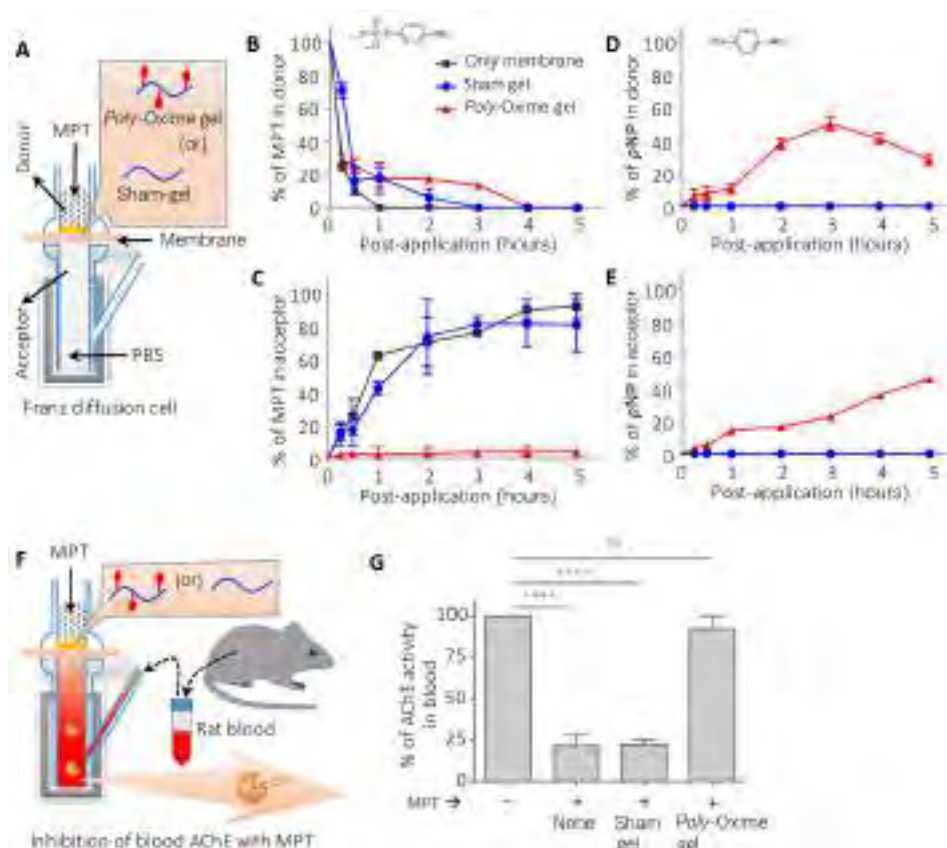
Fig. 2. *Poly*-Oxime gel deactivates MPT to limit MPT-mediated AChE inhibition ex vivo. (**A**) Schematic of Franz diffusion cell: A thin layer of either *poly*-Oxime gel or sham gel was applied on a dialysis membrane, which was placed between donor and acceptor chambers. (**B** to **E**) Concentration of MPT and *p*NP (hydrolytic degradation product of MPT) in donor and acceptor chambers was measured using UFLC. The presence of sham gel did not prevent the diffusion of MPT into the acceptor chamber and could not hydrolyze MPT to generate *p*NP, whereas *poly*-Oxime actively hydrolyzed to limit the penetration of toxic MPT into the acceptor chamber. (**F** and **G**) An ex vivo assay to demonstrate the ability of *poly*-Oxime to limit MPT-induced assay AChE inhibition using rat blood. AChE containing rat blood was placed in the acceptor chamber, and MPT was added in the donor chamber in the presence of either *poly*-Oxime or sham gel. Active AChE was measured in the blood before and 3 hours after addition of MPT. In the absence of *poly*-Oxime gel, MPT diffused into an acceptor chamber and significantly inhibited AChE activity. However, *poly*-Oxime gel could hydrolyze MPT before diffusion, therefore limiting the MPT-induced inhibition of AChE. Data are means ± SD (*n* = 3, performed at least twice); *P* values were determined by one-way analysis of variance (ANOVA). ****P < 0.0001. ns, not significant.

and characterization is given in Supplementary Methods). Akin to *poly*-Oxime gel, the *poly*-methoxyOxime gel was prepared and its ability to reduce MPT-induced AChE inhibition in the blood was evaluated using Franz diffusion cell ex vivo. While *poly*-Oxime gel completely decreased the MPT-induced AChE inhibition, blocking of oxime nucleophile with methoxy ether (*poly*-methoxyOxime gel) led to the loss of its activity (fig. S3). The inability of *poly*-methoxyOxime gel to prevent AChE inhibition validates the importance of oxime nucleophile to deactivate MPT.

Poly-Oxime gel prevents pesticide-induced AChE inhibition in blood and tissue in vivo

To evaluate the ability of *poly*-Oxime gel to prevent MPT-induced AChE inhibition, 18 Sprague-Dawley rats (10 to 13 weeks) were randomly divided into three groups (*n* = 6 per group). The dorsal coat was clipped, and the 10-cm^2 area was exposed to MPT directly or in the presence of the sham gel or *poly*-Oxime gel layer (see Materials and Methods). According to the WHO, pesticides that have LD$_{50}$ (median lethal dose) of 10 to 100 mg/kg of body weights in rats (dermal exposure) are considered as "highly hazardous" (class Ib) (*10*, *11*). To test the robustness of *poly*-Oxime gel, we dermally exposed all groups to

MPT (150 mg/kg) (Fig. 3A). Quantification of active AChE in the blood at pre-exposure (0 hours) and post-exposure (96 hours) revealed that dermal exposure of MPT alone or in the presence of sham gel significantly decreased the active AChE, whereas in the presence of *poly*-Oxime gel no such decrease was seen (Fig. 3B). Animals that were exposed to MPT alone or in the presence of sham gel lost ~20% of their initial body weight by day 4, while animals that were exposed to MPT in the presence of *poly*-Oxime gel did not lose their weight and showed normal weight gain (fig. S4). In addition, on day 4, animals were sacrificed, and tissues like brain, heart, liver, and lung were isolated and quantified for active AChE in comparison with the naïve rat tissues. Data in Fig. 3 (C to F) suggest that the MPT exposure leads to a decrease in active AChE levels, while sham gel could not protect from the MPT exposure. On the contrary, the presence of *poly*-Oxime gel limited the reduction of active AChE. These results demonstrate that *poly*-Oxime gel does not act like a typical barrier gel, but it hydrolytically deactivates organophosphate, leading to limiting AChE inhibition.

Poly-Oxime gel prevents pesticide-induced mortality in vivo

As multiple exposures of MPT could cause mortality, we investigated the ability of *poly*-Oxime gel to prevent MPT-induced mortality in rats.
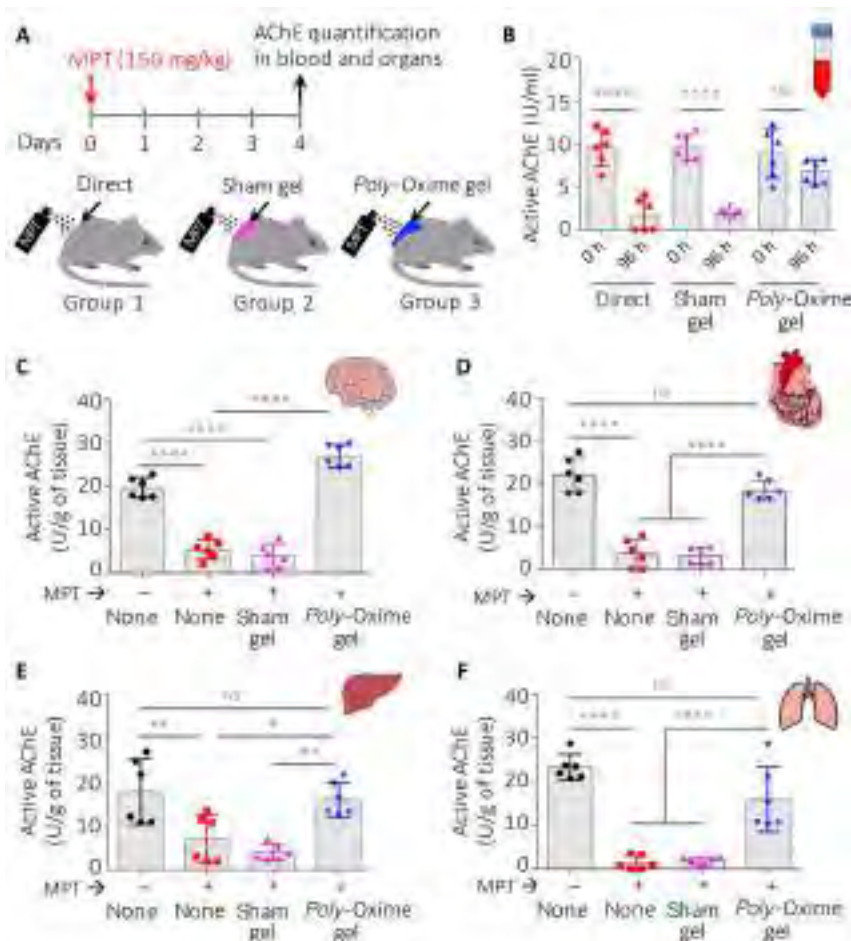
Fig. 3. *Poly*-Oxime gel limits AChE inhibition after exposure to a lethal dose of MPT in vivo. (**A**) Coat on the dorsal side of rats was clipped 1 day before the exposure. A dose of MPT (150 mg/kg) was applied on the skin either directly or in the presence of the sham gel (220 mg per animal) or *poly*-Oxime gel (220 mg per animal) layer. (**B**) Active AChE in the blood was quantified using Ellman's assay. Direct exposure of MPT significantly reduced the active AChE in the blood. Sham gel could not limit MPT-induced AChE inhibition, while *poly*-Oxime gel deactivated MPT before entering into the skin, therefore reducing the MPT-induced AChE inhibition. (**C** to **F**) On day 5, rats were sacrificed, tissue was collected, and the amount of active AChE was quantified. Dermal exposure of MPT either directly on the skin or in the presence of sham gel led to the decrease in the active AChE in all tissues such as brain, heart, liver, and lung, while *poly*-Oxime gel significantly reduced this MPT-mediated deactivation of AChE. Data in (B) to (F) are means ± SD ($n = 6$ rats per group); P values were determined by one-way ANOVA with Tukey post hoc test. *$P < 0.05$, **$P < 0.01$, ****$P < 0.0001$.

A single dose of 150 mg/kg leads to 100% mortality in a direct exposure group with a mean survival time (MST) of 4 days. Therefore, for survival experiments, the dose was brought down to 100 mg/kg to understand response to multiple exposures and thus partly mimic the field scenario of multiple exposures. First, 18 Sprague-Dawley rats were randomized into three groups ($n = 6$), and all groups received MPT (100 mg/kg per day) once a day until >50% mortality was observed in one of the groups. Group 1 animals received MPT without any gel, sham gel was applied daily on group 2 animals, and *poly*-Oxime gel was applied daily on group 3 animals, 30 min before the MPT exposure (Fig. 4A). Animals in groups 1 and 2 showed the characteristics of organophosphate pesticide poisoning in the rats (*31*); symptoms include salivation, muscular fibrillation, diarrhea, lacrimation, respiratory distress, gasping, decreased body temperature, and tremors. On the contrary, group 3 animals that received MPT after the application of prophylactic *poly*-Oxime gel did not show any signs of toxicity. All animals directly exposed to the MPT group died in 5 days, while all the animals in the sham gel group died within 7 days, with an MST of 4 and 6 days, re-

spectively, and all animals that received MPT after the *poly*-Oxime gel application survived (Fig. 4B). A 100% survival rate was observed in the presence of *poly*-Oxime gel ($n = 6$; $P = 0.0001$, Mantel-Cox test). The blood was collected before exposing to MPT (day 0) and at the terminal stage (on day 3 for groups 1 and 2 and on day 30 for group 3). Animals in group 3 were tested for any delayed signs of toxicity for 30 days, and the study was terminated on day 30. No visible delayed signs of toxicity like muscular fibrillation, diarrhea, lacrimation, and respiratory distress were observed. Quantification of active AChE in the blood revealed that direct exposure of MPT and the sham gel group showed a decrease in active AChE, while *poly*-Oxime gel limited the inhibition of AChE activity (Fig. 4C). In addition, brain tissue was collected from group 1 and 2 animals immediately after they died. Because not even a single animal died in group 3, they were sacrificed on day 30 and their brain tissue was harvested. The active AChE in tissues was quantified. Exposure of MPT either directly or in the presence of sham gel significantly decreased the active AChE, while *poly*-Oxime gel prevented reduction of active AChE in the brain (fig. S5A). In addition, while animals in groups 1 and 2 that
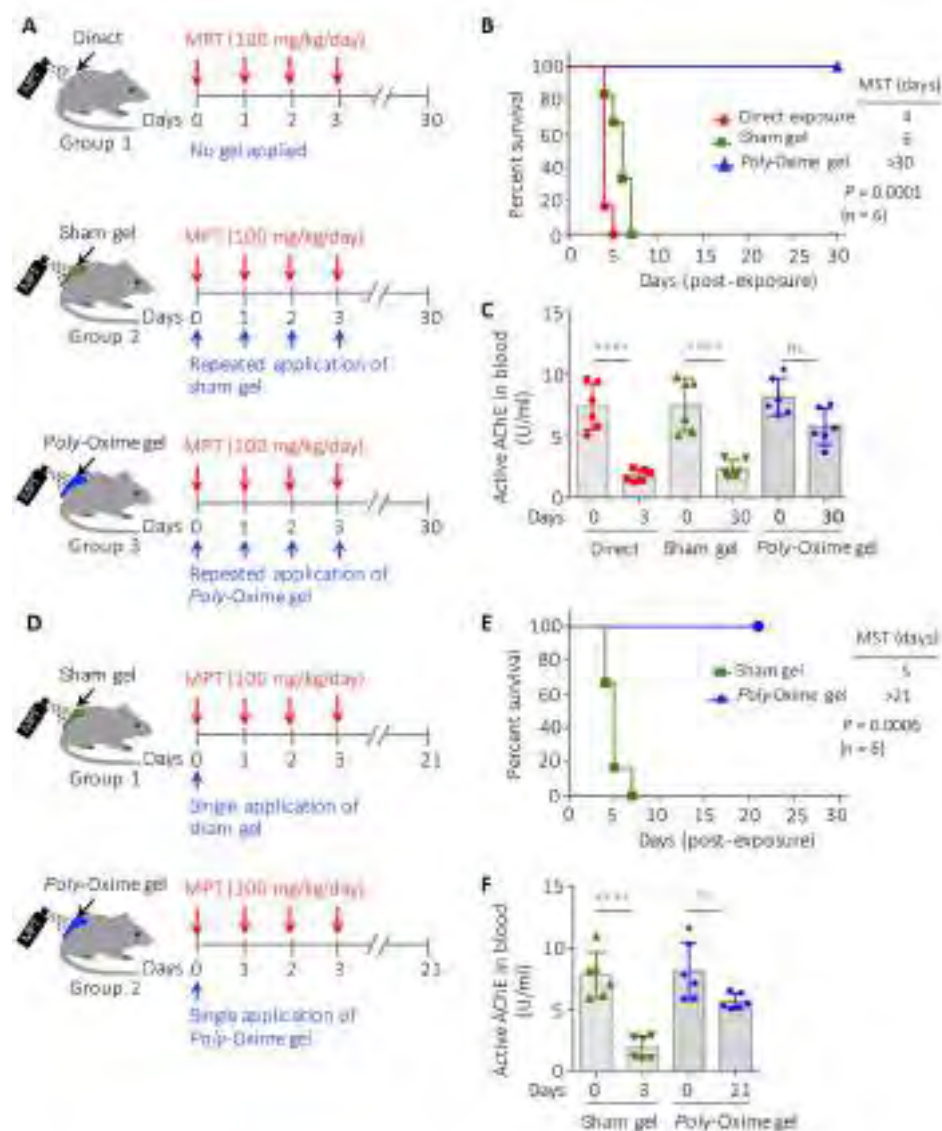
Fig. 4. Either daily or a single application of *poly*-Oxime gel prevented mortality during repeated exposure of MPT in vivo. (**A**) Sprague-Dawley rats (10 weeks, males) were randomized in three groups (*n* = 6 rats per group): (i) direct exposure of MPT, (ii) sham gel + MPT, and (iii) *poly*-Oxime gel + MPT. Either sham gel or *poly*-Oxime gel (220 mg per rat per day) was applied every day before the MPT exposure (100 mg/kg per day for 4 days). Organs were collected either immediately after mortality or on day 30. AChE activity in blood and organs was quantified using modified Ellman's assay. (**B**) MST for direct exposure of MPT and MPT received in the presence of sham gel was 4 and 6 days, respectively, while *poly*-Oxime gel–applied group did not show mortality. (**C**) Blood AChE activity dropped markedly in direct MPT and sham gel groups, while inhibition was reduced in *poly*-Oxime gel–applied animals. (**D**) Rats were divided into two groups (*n* = 6 rats per group). On day 0, 220 mg of sham gel and *poly*-Oxime gel was applied dermally on group 1 and 2 animals, respectively. Without further applying any gel, MPT (100 mg/kg per day) was given daily for 4 days. Organs were collected either immediately after mortality or on day 21. (**E**) MST for sham gel was 5 days, while *poly*-Oxime gel–applied group did not show mortality. (**F**) Blood AChE activity dropped markedly in group 1, while the inhibition was reduced in group 2. *P* values were determined by Mantel-Cox test (B and E) and one-way ANOVA with Tukey post hoc test (C and F). **$P < 0.01$, ****$P < 0.0001$.

received MPT lost their body weight, group 3 animals that were exposed to MPT in the presence of *poly*-Oxime gel continue to gain weight normally until the end of the study (fig. S5B).

An oxime could hydrolyze multiple organophosphate molecules in a truly catalytic manner. After cleaving one molecule of organophosphate, an oxime nucleophile could regenerate and cleave more organophosphate molecules (Fig. 1A). To test the robust nature of *poly*-Oxime gel in vivo, we randomized 12 Sprague-Dawley rats into two groups

(*n* = 6). On day 0, we applied 220 mg of sham gel or *poly*-Oxime gel on group 1 and 2 animals, respectively. In one-time post-application of the gel, both groups received MPT (100 mg/kg per day) for 4 days (Fig. 4D). All the animals in the sham gel group died within 7 days with an MST of 5 days, whereas a 100% survival was observed in one-time *poly*-Oxime gel–treated group (*n* = 6; *P* = 0.0006, Mantel-Cox test; Fig. 4E). Analysis of active AChE in the blood revealed that sham gel could not reduce MPT-mediated inhibition of AChE in the blood and

brain tissue compared to the presence of prophylactic *poly*-Oxime gel (Fig. 4F and fig. S6A). In addition, animals in the *poly*-Oxime gel group did not lose their body weight compared to the sham gel group (fig. S6B). When *poly*-Oxime gel was applied before the MPT exposure, in addition to providing 100% survival, there were no visible signs such as shivering and stress-induced porphyrin discharge, which are hallmarks of pesticide-induced toxicity and stress. Cumulatively, these results suggest that *poly*-Oxime gel can deactivate organophosphate pesticides in a robust manner to prevent pesticide-induced toxicity and mortality. We propose that this property of *poly*-Oxime gel could be protective for farmers and workers who are exposed to high doses of pesticides repeatedly.

Poly-Oxime gel prevents pesticide-induced loss of motor coordination and altered neuromuscular signaling

Organophosphate pesticides bind and subsequently inhibit the AChE in synaptic clefts of the neuromuscular junction (*32–34*). Lethal effects are cardiovascular collapse and respiratory failure. Signaling at motor end plate gets impaired because of AChE inhibition. Therefore, pesticide exposure leads to the reduction in motor coordination and altered neuromuscular signaling (*35–37*). Pesticide-induced stress reduces the endurance (*38, 39*). The endurance and motor coordination of rats exposed to MPT with and without *poly*-Oxime gel were tested using the rotarod experiment. Three groups of male Sprague-Dawley rats (*n* = 4 in each group) were trained on a rotarod for 4 days (Fig. 5A), and while training, animals in all the groups showed similar latency to fall (L_f, time to fall from rotating rod with 2 to 20 rpm). L_f on day 4 was considered as 100%. After recording L_f on day 4, group 1 animals were left unexposed, group 2 animals were directly exposed to MPT, and group 3 animals received MPT in the presence of *poly*-Oxime gel. After the MPT exposure, group 2 animals showed a significant drop in the latency to fall, thus indicating an MPT-induced reduction in endurance (Fig. 5B). On the contrary, group 3 animals that received MPT in the presence of prophylactic *poly*-Oxime gel did not show a reduction in latency to fall and continued improvement in the performance like unexposed group 1, which suggests that *poly*-Oxime gel prevents the pesticide-induced reduction in endurance. We used acceleration in rotation speed from 2 to 60 rpm, with a step size of 4 rpm to study the neuromuscular coordination (NMC) of rats under constant need to readjust the muscle recruitment. After training for 6 days, animals were similarly divided into three groups (*n* = 5 per group) and tested for NMC. Animals in group 2 showed a significant drop in NMC, while *poly*-Oxime gel could prevent this drop of NMC and showed performance similar to that of unexposed animals (Fig. 5C).

Gait analysis is a conventionally used noninvasive method to study sciatic nerve injury and recovery. The pattern of walking is decided by the posture of the foot, angle formed with the ground, and the force exerted. These things combined will establish a particular print length, toe spread, and intertoe spread of an animal, and it gets affected if there is any impairment of nerve function (Fig. 5D) (*40, 41*). When analyzed for sciatic functional index (SFI), which is an empirically derived formula to evaluate nerve function (see Materials and Methods), the direct exposure group showed values decreasing to −30 to −60, which indicates partial impairment of sciatic nerve function. However, the *poly*-Oxime gel–protected animals showed no significant reduction in SFI, suggesting complete prevention of nerve function impairment (Fig. 5E).

Visible muscular spasms were observed in the animals directly exposed to MPT. We recorded electromyogram (EMG) for biceps femoris of the left hind limb under 2.5% isoflurane anesthesia and between

spinotrapezius and gluteus maximus when the animal was awake. In either case, EMG showed frequent muscle activity. This involuntary muscle activity was completely absent in the animals protected with *poly*-Oxime gel before the application of MPT (Fig. 5, F and G).

DISCUSSION

Increasing resistance in pest is forcing agriculture farmers to use a cocktail of potent organophosphates in the field. However, the lack of any protective measure during spraying in the field is causing a direct exposure to pesticides. High dermal penetration of pesticides leads to acute toxicity, including neural dysfunction, muscle dysfunction, and respiratory arrest. Currently, adverse toxic effects of pesticides are a major concern for farmworkers. Although the use of PPE could be an alternative route, the lack of compliance due to uncomforted use in developing countries is a major hurdle. In developing countries, the manual spray of pesticides is still the primary practice, as compared to developed countries where the machine spray or aerial spray is being practiced. A manual spray of pesticides leads to direct dermal exposure. Human studies reveal that pre- and postnatal exposure to pesticides delays neuronal development in children who are living in agricultural communities. In addition, it increases susceptibility to neuropsychiatric disorders (*8, 9*). Therefore, a few attempts were made to develop physical barrier creams (*15, 16*). Because of the high skin penetration of pesticides, commercial physical barrier creams were not sufficient to prevent pesticide entry into the body (fig. S7). This prompted us to devise a new strategy, which is a chemical deactivation of pesticides on the skin to prevent their entry into the body. We have designed a polymeric super-nucleophile (α-nucleophile)–mediated hydrolysis of pesticides on the skin.

Poly-Oxime could be formulated into the dermal gel using excipients. Our data suggest that a thin layer of *poly*-Oxime gel can hydrolyze organophosphates on the skin; therefore, it can prevent AChE inhibition quantitatively in blood and in all internal organs such as brain, lung, liver, and heart. Previously, there were no examples that demonstrated prevention of AChE inhibition in vivo. Our data demonstrate that *poly*-Oxime gel does not act as a physical barrier. Instead, it hydrolyzes organophosphate ester, MPT, into nonharmful hydrolytic products such as dimethyl phosphate and *p*NP, which cannot inhibit AChE. *Poly*-Oxime gel can hydrolytically cleave a wide range of pesticides, including commercial organophosphate formulations such as chlorpyriphos, prophenophos, and monocrotophos, and therefore can prevent pesticide-induced AChE inhibition. The activity of *poly*-Oxime gel against a broader range of pesticides shows its robustness. As farmers spray pesticides in all seasons including cold winters and hot summers, the prophylactic gel should be active at a wide range of temperature. The fact that the *poly*-Oxime showed an efficient catalytic activity at temperatures ranging from 20° to 40°C and retained its activity even after prolonged exposure to ultraviolet (UV) light shows stability and ability to function in varying weather conditions (fig. S8).

Farming in developing countries is labor-intensive and demands strenuous physical activity from agriculture workers. As pesticide exposure is known to affect endurance and NMC, farmers lose their ability to work with full capacity. In rat models, we recapitulated the loss of endurance and NMC due to pesticide exposure. Our data demonstrate that the presence of *poly*-Oxime gel completely prevented pesticide-induced loss of endurance and NMC. In addition, pesticide exposure can severely damage nerves such as the sciatic nerve. Using Gait analysis, we demonstrated that direct exposure to pesticide significantly
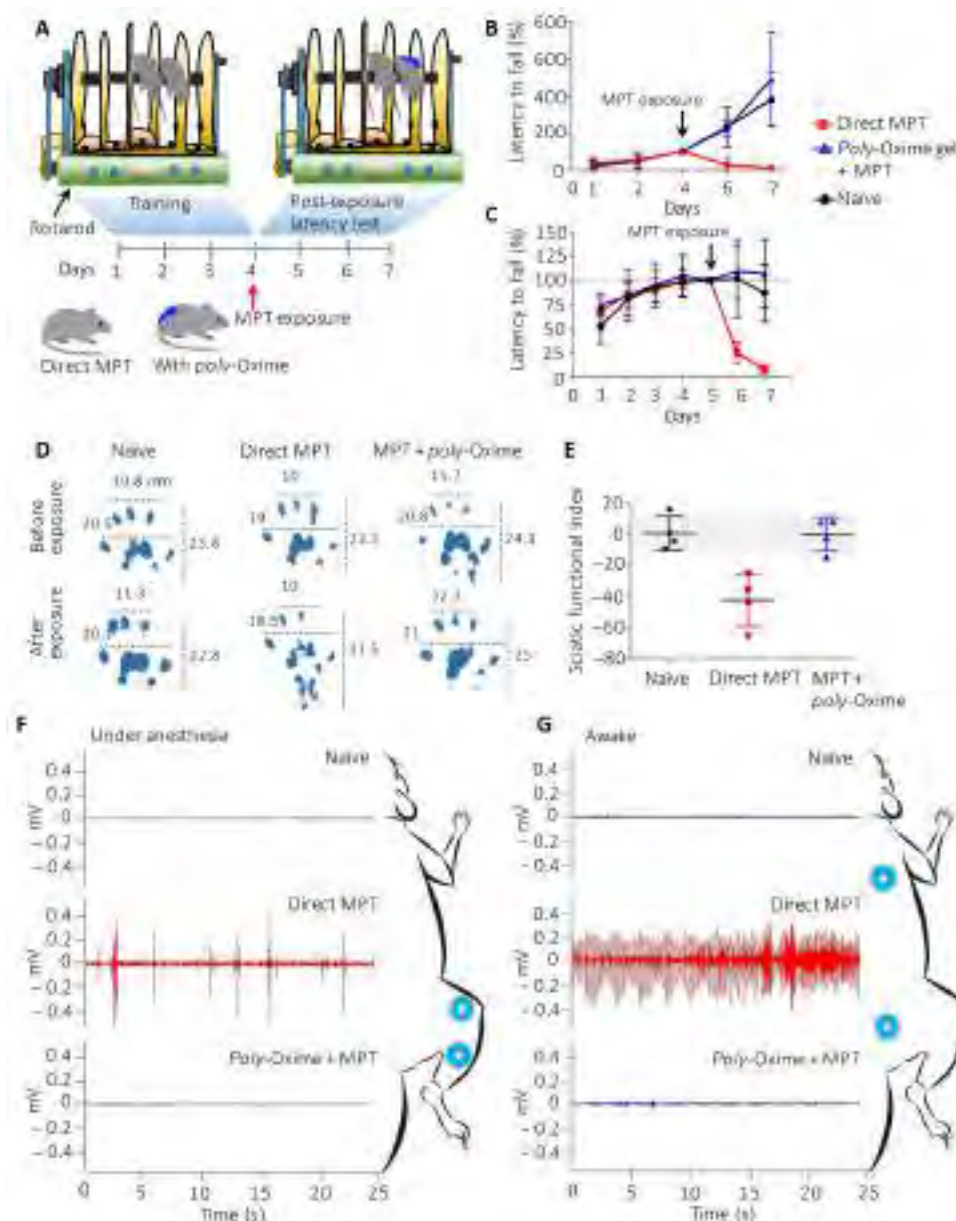
Fig. 5. *Poly*-Oxime gel prevented loss of endurance, NMC, nerve function impairment, and uncontrolled muscle activity in vivo. (**A**) Rotarod was used to study endurance and NMC in MPT animals either directly or in the presence of *poly*-Oxime gel. (**B**) Latency to fall was measured by measuring the time the animal stayed on rotarod at a constant speed of 20 rpm, and it was normalized to the day of exposure. Directly exposed MPT animals showed significant reduction endurance that was prevented by *poly*-Oxime cream. (**C**) When animals were subjected to increasing speed from 2 to 60 rpm, the rpm reached before falling was taken as a measurement to assign NMC score, and data were normalized to the day of exposure. *Poly*-Oxime cream showed complete rescue of loss of NMC, which was observed with direct exposure MPT animals. (**D** and **E**) Paw prints of animals were exposed either directly or in the presence of *poly*-Oxime gel before and after exposure. Prints were used to calculate SFI. Direct exposure animals showed greatly reduced SFI that represents impairment of sciatic nerve function, which was again rescued by *poly*-Oxime cream. (**F**) EMGs were recorded under 2.5% isoflurane anesthesia and (**G**) when animals were awake. *Poly*-Oxime cream showed complete prevention of muscle spasm.

damaged the sciatic nerve, while the presence of *poly*-Oxime gel prevented this damage.

To demonstrate the efficiency of *poly*-Oxime gel to prevent pesticide-induced mortality, we used two sets of experiments. In the first set, rats were repeatedly exposed to a pesticide, while every day a thin layer of *poly*-Oxime gel was applied before pesticide exposure. While rats died in the absence of *poly*-Oxime gel (MST, 4 days), the presence

of *poly*-Oxime gel prevented mortality and a 100% survival was observed. In the second set, *poly*-Oxime gel was applied only once on day 0 and repeatedly exposed to pesticide for 4 days. Even a single application of *poly*-Oxime gel completely prevented mortality with a 100% survival. A daily or single application of sham gel led to 100% mortality with an MST of 7 and 6 days, respectively. This demonstrates the stability, robustness, and true catalytic nature of *poly*-Oxime gel.

In conclusion, we have developed a prophylactic topical gel (*poly*-Oxime) that can limit pesticide-induced systemic AChE inhibition and therefore can prevent loss of motor coordination, loss of endurance, altered neuromuscular function, and mortality. Thus, in addition to bringing awareness to agriculture workers, this technology may offer a great promise for farmers and workers who use pesticides. The ability of *poly*-Oxime gel to deactivate organophosphate in a catalytic manner also has a potential to be used for protection against organophosphate-based CWAs.

MATERIALS AND METHODS
Study design
The goal of this study was to design a nucleophilic topical gel to chemically deactivate pesticides on the skin to prevent pesticide-induced neuronal dysfunction and mortality. We hypothesized that nucleophile-mediated hydrolysis of pesticides into nonharmful products could prevent systemic AChE inhibition.
In vitro
We initially examined the hydrolytic cleavage of pesticides using a nucleophilic topical gel, thereby preventing inhibition of AChE using Franz diffusion cells.
In vivo
A series of experiments were designed to recapitulate pesticide-induced systemic AChE inhibition, loss of endurance, loss of NMC, sciatic nerve damage, and lethality in rats upon dermal exposure of pesticide, MPT. We tested the hypothesis of the presence of nucleophilic *poly*-Oxime gel that can deactivate pesticides on the skin and prevent pesticide-induced toxicity and mortality.

Rats
For all experiments, 10- to 14-week-old Sprague-Dawley albino rats were used for experiments. Animals were provided by the animal house at the National Centre for Biological Sciences, Bengaluru. Animals were caged (maximum, four per cage) before the experiment and individually after starting the experiment. Food and water were offered ad libitum. All rat studies were performed according to institutional and national guidelines for humane animal use. Experimental protocols were approved by the Institute Animal Ethical Committee at the Institute for Stem Cell Biology and Regenerative Medicine (INS-IAE-2016/09).

Materials
Pyridine-2-aldoxime, bromoacetic acid, chitosan (medium molecular weight), dimethyl formamide, potassium carbonate, *O*-(benzotriazol-1-yl)-*N*,*N*,*N*′,*N*′-tetramethyluronium hexafluorophosphate (HBTU), parathion methyl (PESTANAL), methyl paraoxon (PESTANAL), chlorpyrifos (PESTANAL), carbopol 940, glycerin, propylene glycol, triethanolamine (TEA; S. D. Fine-Chem Limited, Bangalore), snake skin dialysis membrane (MWCO, 3.5 kDa; Thermo Fisher Scientific), trifluoroacetic acid, *p*NP (Alfa Aesar), isoflurane (Isotroy), Triton X-100, EDTA (Thermo Fisher Scientific), 5,5′-dithiobis(2-nitrobenzoic acid) (DTNB), acetylthiocholine iodide (ASChI), and deionized water were used. Unless mentioned otherwise, all chemicals were procured from Sigma-Aldrich.

Synthesis of *poly*-Oxime and *poly*-methoxyOxime
A detailed stepwise synthesis procedure and a detailed characterization of intermediate compounds and final polymers are described in Supplementary Methods.

Catalytic efficiency of *poly*-Oxime
A solution of *poly*-Oxime (2 mg/ml) in 1% acetic acid was used to study its catalytic ability to cleave pesticides. The reactions were studied spectrophotometrically by monitoring the hydrolysis of pesticides (MPT, methyl paraoxon, or chlorpyrifos) at $25 \pm 0.1°C$ and pH 8.2 by measuring the absorbance at 400 nm as a function of time. Pseudo–first-order rate constants were obtained by using an excess of nucleophile (2.5×10^{-4} M) over the substrate (2.5×10^{-5} M). For all the kinetic runs, the absorbance/time result fits very well to the first-order rate equation. To study temperature stability, the same reactions were carried out at 20°, 30°, and 40°C.

Preparation of *poly*-Oxime gel
The dermal gel was formulated by using carbopol 940 (1.8%), glycerin (6.81%), propylene glycol (3.74%), and *poly*-Oxime polymer (2%) mixed in water (85.6%). The pH of the gel was maintained at 8 by TEA. For sham gel, the unfunctionalized chitosan polymer, instead of the *poly*-Oxime polymer, was used, serving as a control gel with all ingredients but no catalytic activity.

In vitro and ex vivo efficacy of *poly*-Oxime dermal gel to reduce permeation of pesticide
The dialysis membrane (MWCO, 3.5 kDa) was hydrated overnight in the deionized water at room temperature. It was then placed between the donor and acceptor compartments of the Franz diffusion cells (DBK Diffusion apparatus) and clamped to avoid any leakage. The acceptor compartment was filled with PBS (pH 7.4), making uniform contact with a dialysis membrane. The experiment was performed in three groups (only membrane, sham gel, and *poly*-Oxime gel) comprising three diffusion cells in each set. *Poly*-Oxime or sham gel (220 mg) was applied uniformly on 10-cm^2 area on the donor compartment side of the dialysis membrane. On the gel, 1 μg of MPT was added in 500 μl of PBS, and in the direct exposure, MPT was added directly on the dialysis membrane. The temperature of the acceptor chamber was maintained at $37 \pm 0.5°C$ using a thermostatic water bath under constant stirring. Samples were withdrawn from acceptor (1 ml) and donor chambers (20 μl) at a regular interval of 1 hour, and an equal amount of phosphate buffer (pH 7.4) was replaced. The amount of MPT that permeated through the membrane and the amount of *p*NP that formed at each time interval were analyzed using UFLC (photodiode array: SPD-M20A, C18 reverse-phase column: LC-20AD Prominence Chromatograph, Shimadzu). MPT was detected using 60% acetonitrile in double-distilled water (DDW) as mobile phase at 1 ml/min, with a retention time of 5.5 min at 280 nm while maintaining the column at 40°C. For detection of *p*NP, we used 22% acetonitrile, 0.5% triethylamine, and 1% trifluoroacetic acid in DDW as mobile phase at a flow rate of 0.5 ml/min through a column maintained at 40°C with a retention time of 3.6 min.

Similarly, in another set of experiment, we replaced the solution in the acceptor chamber with rat blood 1000× diluted in phosphate buffer (pH 8.0). The entire diffusion apparatus was maintained at 5°C to maintain the blood AChE activity. Samples were collected at regular intervals and analyzed using Ellman's method (as mentioned elsewhere) for AChE activity as a proxy for the MPT exposure.

Protection from acute exposure to MPT
Rats were randomized to one of four experimental groups ($n = 6$ in each group): (i) no exposure (no MPT was given), (ii) direct exposure (MPT, 150 mg/kg), (iii) sham gel (220 mg of gel; MPT, 150 mg/kg), and (iv) *poly*-Oxime gel (220 mg of gel; MPT, 150 mg/kg). Polymer concentration

in the gel was 2% (w/w). The dorsal coat was clipped using a hair clipper under mild anesthesia (2.5% isoflurane) 24 hours before the dermal pesticide application, taking care not to damage the integrity of the skin. Unless specified otherwise, the total area of 10 cm^2 was marked and used for dermal exposure experiments. In gel treatment groups, 220 mg of gel was uniformly applied 1 hour before the pesticide exposure (Fig. 3). Before exposure, 200 µl of blood was collected using retro-orbital puncture and evaluated for various parameters as an internal control. After 96 hours of post-exposure, blood was collected using cardiac puncture under anesthesia. After sacrificing the animals, organs such as brain, heart, lungs, and liver were harvested. Organ tissue was homogenized (Polytron PT-MR 2100, 15,000 rpm) in nine volumes of solution D [1 M NaCl, 1% Triton X-100, 0.01 M tris-HCl, 0.01 M EDTA (pH 7.4)] and incubated on ice for 1 hour, followed by centrifugation at 13,300 rpm for 45 min. The supernatant was used to quantitate active AChE. Whole blood diluted 1:1000 in phosphate buffer was used for AChE quantification. The activity of AChE in blood and organs was quantified by modified Ellman's assay. In this assay, we used DTNB and ASChI, which is specific for AChE. For the colorimetric assay, according to Ellman's method, reaction mixtures were made up in 0.1 mM phosphate buffer (pH 7.4) containing 0.5 mM DTNB and ASChI at a final concentration of 20 mM. The reaction was performed at 25°C and monitored at 405 nm.

Survival and AChE inhibition study in rats exposed to MPT multiple times

Rats were randomized to three groups (n = 6 rats per group): (i) direct exposure (no gel, MPT given dermally, 100 mg/kg per day for 4 days), (ii) sham gel (220 mg of sham gel applied daily dermally 30 min before the MPT exposure), and (iii) poly-Oxime gel [220 mg of gel applied daily dermally before applying MPT (100 mg/kg per day) daily for 4 days] (Fig. 4A). In all animals before exposure, 200 µl of blood was collected using retro-orbital puncture and evaluated for AChE activity as an internal control. Immediately after mortality or on day 30, animals were sacrificed, and their organs were collected to quantify the AChE level as described above. Similarly, another set of a single application of gel experiments was performed (n = 6 rats per group). In this experiment, 220 mg of sham gel or poly-Oxime gel was applied only once, i.e., on day 0, and on the same gels, these animals received MPT (100 mg/kg per day) for 4 days (Fig. 4D).

Rotarod test

A total of 12 male Sprague-Dawley rats (10 weeks) were used to study the loss of endurance in MPT-exposed animals and the ability of poly-Oxime gel to prevent the same. Animals were placed on a Rotarod treadmill (Rotamex-5 1.4, Columbus Instruments; lane width, 9.3 cm; diameter of rod, 7 cm; fall distance, 48.3 cm), subjected to a uniform increase in acceleration between 0 and 20 rpm, and allowed to run at 20 rpm until the animal got tired and fell off the rod, and the time of fall was recorded. Rats were trained for 3 days before the exposure, where animals were randomly grouped into three groups: (i) direct exposure, (ii) poly-Oxime gel–treated, and (iii) control. On day 4, animals of the direct exposure group were exposed to a dosage of 150 mg/kg, and the animals of treatment group were given poly-Oxime gel and then exposed to the same dosage of MPT. Latency to fall was calculated as the time taken to fall on any day with respect to day 4 (before exposure) and was converted to percentage.

Similarly, to study NMC, 15 animals were trained on an increasing rotarod acceleration between 2 and 60 rpm, with an acceleration step of 4 rpm every 8 s. On day 5 of training, animals were divided into three groups: (i) direct exposure, (ii) poly-Oxime gel–treated, and (iii) naïve control. On day 5, animals of the direct exposure group were exposed to a dosage of 150 mg/kg, and the animals of treatment group were given poly-Oxime gel and then exposed to the same dosage of MPT. Animals were given a score of +1 for each step up in the acceleration (increase by 4 rpm) before the fall, and the percentage of NMC was calculated with respect to day 5 (before exposure).

Gait analysis and EMG

Gait analysis was performed on 15 male rats (10 weeks old) to evaluate their walking pattern. To obtain footprints, four paws were colored with different nontoxic water colors and animal was trained to walk through an ally (width, 8 cm; length, 120 cm; height, 10 cm), leading to its home cage. After training, animals were divided randomly into three groups: (i) direct exposure, (ii) poly-Oxime gel–treated, and (iii) naïve control. Footprints were analyzed manually, and SFI was calculated using following formula (40, 41)

$$SFI = \left[\left(\frac{E_{TOF} - N_{TOF}}{N_{TOF}} \right) + \left(\frac{N_{PL} - E_{PL}}{E_{PL}} \right) + \left(\frac{E_{TS} - N_{TS}}{N_{TS}} \right) + \left(\frac{E_{IT} - N_{IT}}{N_{IT}} \right) \right] \frac{220}{4}$$

where N indicates normal/before exposure, E indicates after exposure, TOF is the distance to the opposite foot, PL is the distance from the heel to the third toe (the print length), TS is the distance from the first toe to the fifth toe (the toe spread), and IT is the distance from the second toe to the fourth toe (the intermediate toe spread).

EMG of animals from these three groups was recorded using Muscle SpikerBox (Backyard Brains). Skin surface electrodes were used with adhesive pads and conductive gel to facilitate the recordings. To track the muscle spasms under anesthesia (2.5% isoflurane in carbogen), EMG from biceps femoris of left hind limb was recorded. To avoid animal from disturbing the electrodes, we recorded EMG between spinotrapezius and gluteus maximus when the animal was awake.

Statistical analysis

The two-tailed Student's t test was used to compare differences between two experimental groups. In experiments with multiple groups, one-way ANOVA with Tukey post hoc test was used. In survival experiments, Mantel-Cox test was used. $P < 0.05$ was considered as a statistically significant difference. Statistical analysis and graphing were performed with Prism 6 (GraphPad Software).

Fig. S7. Ex vivo Franz diffusion assay with various barrier creams to measure AChE inhibition.
Fig. S8. Ex vivo Franz diffusion assay with poly-Oxime gel before and after exposure to UV light.
Table S1. Pseudo–first-order rate constants for hydrolysis of organophosphates by poly-Oxime polymer.
Supplementary Methods

REFERENCES AND NOTES

1. M. W. Brightman, R. W. Albers, Species differences in the distribution of extraneuronal cholinesterases within the vertebrate central nervous system. *J. Neurochem.* **4**, 244–250 (1959).
2. G. B. Koelle, The histochemical localization of cholinesterases in the central nervous system of the rat. *J. Comp. Neurol.* **100**, 211–235 (1954).
3. H. E. Speed, C. A. Blaiss, A. Kim, M. E. Haws, N. R. Melvin, M. Jennings, A. J. Eisch, C. M. Powell, Delayed reduction of hippocampal synaptic transmission and spines following exposure to repeated subclinical doses of organophosphorus pesticide in adult mice. *Toxicol. Sci.* **125**, 196–208 (2012).
4. A. Watson, D. Opresko, R. Young, V. Hauschild, J. King, K. Bakshi, Organophosphate nerve agents, in *Handbook of Toxicology of Chemical Warfare Agents*, R. C. Gupta, Ed. (Academic Press, 2009), pp. 43–67.
5. P. C. Abhilash, N. Singh, Pesticide use and application: An Indian scenario. *J. Hazard. Mater.* **165**, 1–12 (2009).
6. S. Narayan, J. S. Sinsheimer, K. C. Paul, Z. Liew, M. Cockburn, J. M. Bronstein, B. Ritz, Genetic variability in *ABCB1*, occupational pesticide exposure, and Parkinson's disease. *Environ. Res.* **143**, 98–106 (2015).
7. J. Bajgar, Organophosphates/nerve agent poisoning: Mechanism of action, diagnosis, prophylaxis, and treatment. *Adv. Clin. Chem.* **38**, 151–216 (2004).
8. M. F. Bouchard, J. Chevrier, K. G. Harley, K. Kogut, M. Vedar, N. Calderon, C. Trujillo, C. Johnson, A. Bradman, D. B. Barr, B. Eskenazi, Prenatal exposure to organophosphate pesticides and IQ in 7-year-old children. *Environ. Health Perspect.* **119**, 1189–1195 (2011).
9. B. González-Alzaga, A. F. Hernández, M. Rodríguez-Barranco, I. Gómez, C. Aguilar-Garduño, I. López-Flores, T. Parrón, M. Lacasaña, Pre- and postnatal exposures to pesticides and neurodevelopmental effects in children living in agricultural communities from South-Eastern Spain. *Environ. Int.* **85**, 229–237 (2015).
10. World Health Organization, *The WHO Recommended Classification of Pesticides by Hazard and Guidelines to Classification 2009* (World Health Organization, 2010), pp. 1–60.
11. A. H. Dawson, M. Eddleston, L. Senarathna, F. Mohamed, I. Gawarammana, S. J. Bowe, G. Manuweera, N. A. Buckley, Acute human lethal toxicity of agricultural pesticides: A prospective cohort study. *PLOS Med.* **7**, e1000357 (2010).
12. B. Singh, M. K. Gupta, Pattern of use of personal protective equipments and measures during application of pesticides by agricultural workers in a rural area of Ahmednagar district, India. *Indian J. Occup. Environ. Med.* **13**, 127–130 (2009).
13. E. MacFarlane, R. Carey, T. Keegel, S. El-Zaemay, L. Fritschi, Dermal exposure associated with occupational end use of pesticides and the role of protective measures. *Saf. Health Work* **4**, 136–141 (2013).
14. F. K. Chang, M. L. Chen, S. F. Cheng, T. S. Shih, I. F. Mao, Field protection effectiveness of chemical protective suits and gloves evaluated by biomonitoring. *Occup. Environ. Med.* **64**, 759–762 (2007).
15. C. Bignon, S. Amigoni, T. Devers, F. Guittard, Barrier cream based on CeO₂ nanoparticles grafted polymer as an active compound against the penetration of organophosphates. *Chem. Biol. Interact.* **267**, 17–24 (2017).
16. R. P. Chilcott, C. H. Dalton, I. Hill, C. M. Davison, K. L. Blohm, E. D. Clarkson, M. G. Hamilton, Evaluation of a barrier cream against the chemical warfare agent VX using the domestic white pig. *Basic Clin. Pharmacol. Toxicol.* **97**, 35–38 (2005).
17. J. Millerioux, C. Cruz, A. Bazire, G. Lallement, L. Lefeuvre, D. Josse, In vitro selection and efficacy of topical skin protectants against the nerve agent VX. *Toxicol. In Vitro* **23**, 539–545 (2009).
18. A. Zenerino, T. Boutard, C. Bignon, S. Amigoni, D. Josse, T. Devers, F. Guittard, New CeO₂ nanoparticles-based topical formulations for the skin protection against organophosphates. *Toxicol. Rep.* **2**, 1007–1013 (2015).
19. A. Salerno, T. Devers, M.-A. Bolzinger, J. Pelletier, D. Josse, S. Briançon, In vitro skin decontamination of the organophosphorus pesticide paraoxon with nanometric cerium oxide CeO₂. *Chem. Biol. Interact.* **267**, 57–66 (2017).
20. L. Benameur, M. Auffan, M. Cassien, W. Liu, M. Culcasi, H. Rahmouni, P. Stocker, V. Tassistro, J.-Y. Bottero, J. Rose, A. Botta, S. Pietri, DNA damage and oxidative stress induced by CeO₂ nanoparticles in human dermal fibroblasts: Evidence of a clastogenic effect as a mechanism of genotoxicity. *Nanotoxicology* **9**, 696–705 (2015).
21. M. Auffan, J. Rose, T. Orsiere, M. De Meo, A. Thill, O. Zeyons, O. Proux, A. Masion, P. Chaurand, O. Spalla, A. Botta, M. R. Wiesner, J.-Y. Bottero, CeO₂ nanoparticles induce DNA damage towards human dermal fibroblasts in vitro. *Nanotoxicology* **3**, 161–171 (2009).
22. S. Bhattacharya, V. P. Kumar, Evidence of enhanced reactivity of DAAP nucleophiles toward dephosphorylation and deacylation reactions in cationic Gemini micellar media. *J. Org. Chem.* **69**, 559–562 (2004).
23. J. Toullec, M. Moukawim, Cetyltrimethylammonium hydroperoxide: An efficient reagent for promoting phosphate ester hydrolysis. *Chem. Commun.* **0**, 221–222 (1996).
24. Y. C. Yang, L. L. Szafraniec, W. T. Beaudry, C. A. Bunton, Perhydrolysis of nerve agent VX. *J. Org. Chem.* **58**, 6964–6965 (1993).
25. V. P. Kumar, B. Ganguly, S. Bhattacharya, Computational study on hydroxybenzotriazoles as reagents for ester hydrolysis. *J. Org. Chem.* **69**, 8634–8642 (2004).
26. S. Bhattacharya, V. P. Kumar, Ester cleavage properties of synthetic hydroxybenzotriazoles in cationic monovalent and gemini surfactant micelles. *Langmuir* **21**, 71–78 (2005).
27. M. Shin, S.-G. Park, B.-C. Oh, K. Kim, S. Jo, M. S. Lee, S. S. Oh, S.-H. Hong, E.-C. Shin, K.-S. Kim, S.-W. Kang, H. Lee, Complete prevention of blood loss with self-sealing haemostatic needles. *Nat. Mater.* **16**, 147–152 (2017).
28. P. K. Dutta, J. Dutta, V. S. Tripathi, Chitin and chitosan: Chemistry, properties and applications. *J. Sci. Ind. Res.* **63**, 20–31 (2004).
29. D. C. Nam, Y. M. Ha, M. K. Park, S. K. Cho, The rs662 polymorphism of paraoxonase 1 affects the difference in the inhibition of butyrylcholinesterase activity by organophosphorus pesticides in human blood. *Int. J. Clin. Pharmacol. Ther.* **54**, 622–627 (2016).
30. F. Worek, P. Eyer, H. Thiermann, Determination of acetylcholinesterase activity by the Ellman assay: A versatile tool for in vitro research on medical countermeasures against organophosphate poisoning. *Drug Test. Anal.* **4**, 282–291 (2012).
31. E. F. Edson, D. N. Noakes, The comparative toxicity of six organophosphorus insecticides in the rat. *Toxicol. Appl. Pharmacol.* **2**, 523–539 (1960).
32. B. Ballantyne, T. C. Marrs, Overview of the biological and clinical aspects of organophosphates and carbamates, in *Clinical and Experimental Toxicology of Organophosphates and Carbamates* (Butterworth-Heinemann, 1992), pp. 3–14.
33. Y. Masuda, Cardiac effect of cholinesterase inhibitors used in Alzheimer's disease—From basic research to bedside. *Curr. Alzheimer Res.* **1**, 315–321 (2004).
34. A. M. Saadeh, N. A. Farsakh, M. K. al-Ali, Cardiac manifestations of acute carbamate and organophosphate poisoning. *Heart* **77**, 461–464 (1997).
35. L. Karalliedde, J. A. Henry, Effects of organophosphates on skeletal muscle. *Hum. Exp. Toxicol.* **12**, 289–296 (1993).
36. C. R. Stamper, W. Balduini, S. D. Murphy, L. G. Costa, Behavioral and biochemical effects of postnatal parathion exposure in the rat. *Neurotoxicol. Teratol.* **10**, 261–266 (1998).
37. J. M. Spyker, D. L. Avery, Neurobehavioral effects of prenatal exposure to the organophosphate Diazinon in mice. *J. Toxicol. Environ. Health* **3**, 989–1002 (1977).
38. H. Zhu, R. W. Rockhold, R. C. Baker, R. E. Kramer, I. K. Ho, Effects of single or repeated dermal exposure to methyl parathion on behavior and blood cholinesterase activity in rats. *J. Biomed. Sci.* **8**, 467–474 (2001).
39. W. A. Buttemer, P. G. Story, K. J. Fildes, R. V. Baudinette, L. B. Astheimer, Fenitrothion, an organophosphate, affects running endurance but not aerobic capacity in fat-tailed dunnarts (*Sminthopsis crassicaudata*). *Chemosphere* **72**, 1315–1320 (2008).
40. L. Sarikcioglu, B. M. Demirel, A. Utuk, Walking track analysis: An assessment method for functional recovery after sciatic nerve injury in the rat. *Folia Morphol.* **68**, 1–7 (2009).
41. L. de Medinaceli, W. J. Freed, R. J. Wyatt, An index of the functional condition of rat sciatic nerve based on measurements made from walking tracks. *Exp. Neurol.* **77**, 634–643 (1982).

Citation: K. Thorat, S. Pandey, S. Chandrashekharappa, N. Vavilthota, A. A. Hiwale, P. Shah, S. Sreekumar, S. Upadhyay, T. Phuntsok, M. Mahato, K. K. Mudnakudu-Nagaraju, O. Sunnapu, P. K. Vemula, Prevention of pesticide-induced neuronal dysfunction and mortality with nucleophilic poly-Oxime topical gel. *Sci. Adv.* **4**, eaau1780 (2018).

Science Advances

Prevention of pesticide-induced neuronal dysfunction and mortality with nucleophilic poly-Oxime topical gel

Ketan Thorat, Subhashini Pandey, Sandeep Chandrashekharappa, Nikitha Vavilthota, Ankita A. Hiwale, Purna Shah, Sneha Sreekumar, Shubhangi Upadhyay, Tenzin Phuntsok, Manohar Mahato, Kiran K. Mudnakudu-Nagaraju, Omprakash Sunnapu and Praveen K. Vemula

ARTICLE TOOLS	http://advances.sciencemag.org/content/4/10/eaau1780
SUPPLEMENTARY MATERIALS	http://advances.sciencemag.org/content/suppl/2018/10/15/4.10.eaau1780.DC1
REFERENCES	This article cites 38 articles, 2 of which you can access for free http://advances.sciencemag.org/content/4/10/eaau1780#BIBL
PERMISSIONS	http://www.sciencemag.org/help/reprints-and-permissions

Use of this article is subject to the Terms of Service